INFORMATION TO USERS

This manuscript has been reproduced from the microfilm master. UMI films the text directly from the original or copy submitted. Thus, some thesis and dissertation copies are in typewriter face, while others may be from any type of computer printer.

The quality of this reproduction is dependent upon the quality of the copy submitted. Broken or indistinct print, colored or poor quality illustrations and photographs, print bleedthrough, substandard margins, and improper alignment can adversely affect reproduction.

In the unlikely event that the author did not send UMI a complete manuscript and there are missing pages, these will be noted. Also, if unauthorized copyright material had to be removed, a note will indicate the deletion.

Oversize materials (e.g., maps, drawings, charts) are reproduced by sectioning the original, beginning at the upper left-hand corner and continuing from left to right in equal sections with small overlaps.

ProQuest Information and Learning
300 North Zeeb Road, Ann Arbor, MI 48106-1346 USA
800-521-0600

POLY(4-VINYLPYRIDINE)-FILLED MICROPOROUS MEMBRANES: FACTORS AFFECTING TRANSPORT AND SELECTIVITY

By

DAVID STACHERA, B.Sc.

A Thesis

Submitted to the School of Graduate Studies

in Partial Fulfilment of the Requirements

for the Degree

Doctor of Philosophy

McMaster University

POLY(4-VINYLPYRIDINE)-FILLED MICROPOROUS MEMBRANES: FACTORS AFFECTING TRANSPORT AND SELECTIVITY

DOCTOR OF PHILOSOPHY (2000)
Department of Chemistry

McMaster University
Hamilton, Ontario

TITLE: Poly(4-Vinylpyridine)-Filled Microporous Membranes: Factors Affecting Transport and Selectivity

AUTHOR: David Stachera, B.Sc. (McMaster University)

SUPERVISOR: Professor Ronald F. Childs

NUMBER OF PAGES: xx, 246

ABSTRACT

Pore-filled anion exchange membranes containing poly(4-vinylpyridinium) have been prepared by photochemically initiated free radical polymerization of 4-vinylpyridine and divinylbenzene in the pores of a polypropylene microporous membrane followed by alkylation or protonation of the incorporated poly(4-vinylpyridine).

The mass increase of poly(4-vinylpyridine) incorporated in the polypropylene substrate can be controlled from 0 to 200%. Scanning electron microscope images show that the poly(4-vinylpyridine) is distributed evenly throughout the membrane. Membrane water contents range from 25% to 65%. The membranes have ion exchange capacities up to 4.8 meq/g of dry membrane and fixed charge concentrations up to 7.2 eq/kg of membrane water.

The effects of mass gain, divinylbenzene content and the size of the quaternizing alkyl group on the rate of acid transport through the membranes and the selectivity of acid transport relative to salt transport have been determined. Activation energies as well as entropy terms for the diffusion of acid through the membranes have been determined which provide information regarding the mechanism of acid transport in the membranes. The mobility of the membrane water was determined by Pulsed-Gradient Spin-Echo NMR experiments which, combined with Differential Scanning Calorimetry experiments, provides information about the structure of the water in the membranes.

An increase in divinylbenzene content or an increase in the length of the quaternizing alkyl group resulted in a decrease in acid transport and a dramatic increase in selectivity of acid over salt transport. The improved performance resulting from alkylation of the pyridine nitrogen atom compared to protonation was determined to be a result of an increase in water structure and resulting decrease in the mobility of the membrane water.

It has been proposed that the structure of the water in a given membrane is of one type only and not found in the form of "bound" and "free" portions. The nature of the membrane water changes depending on the substituent on the pyridine nitrogen atom but is not present in more than one state in any given membrane.

The work conducted in this thesis extends the understanding of acid transport through anion exchange membranes and the factors affecting acid/salt selectivity. It has been determined that acid transport is largely dependent on membrane water content and independent of the degree of structure of the membrane water. The acid/salt selectivity of the membranes was found to be a result of Donnan exclusion while the increased selectivity of the alkylated membranes compared to the protonated membranes was determined to be a result of the increase in membrane water structure in the former.

ACKNOWLEDGEMENTS

I would like to extent my sincere gratitude to my supervisor, Dr. R.F. Childs, for his help throughout the years spent producing the work in this thesis. His positive attitude and insightful comments have been a tremendous assistance.

Thanks to my supervisory committee members, Drs. B.E. McCarry and A.D. Bain for their support. I would also like to thank Dr. Alicja Mika for her valuable suggestions and comments over the years. Thanks to Dr. P.M. Macdonald for the use of his NMR facilities for the PGSE experiments, Frank Gibbs for his help with the DSC experiments and Dr. T. Petric for the use of his impedance spectrometer.

Thanks also to the members of the research group: Marcus, Chris, Brad, Ashok, Richard. They made working in the lab an enjoyable time. I have the benefit of good friendships and have many good memories of my time spent at McMaster.

I would like to thank NSERC, OGS and McMaster University for financial support and 3M Canada for providing the membrane substrates.

Finally, I would especially like to thank my wife Tracy for her love and support and my daughters Emily and Erin for the joy they bring to my life.

TABLE OF CONTENTS

LIST OF FIGURES

LIST OF TABLES

LIST OF SCHEMES

LIST OF ABBREVIATIONS

D_{app}	Apparent Diffusion Coefficient
D_i	Diffusion Coefficient of i
DMPA	2,2-dimethoxy-2-phenylacetophenone
DSC	Differential Scanning Calorimetry
DVB	Divinylbenzene
E	Electrical Potential
E_a	Activation Energy
F	Faraday Constant
IEC	Ion Exchange Capacity
MO	Mesityl Oxide
PGSE	Pulsed Gradient Spin Echo
PP	Polypropylene
R	Gas Constant
U	Apparent Dialysis Coefficient
u_i	Chemical Potential of i
z_i	Charge of i

CHAPTER ONE

INTRODUCTION

The European Society of Membrane Science and Technology has defined a membrane as "an intervening phase separating two phases and/or acting as an active or passive barrier to the transport of matter between phases" [1]. Another definition states "A membrane is a separator between two fluids of different composition which enforces selectivity in the transport of species (solvent, solutes or ions) between them" [2]. More generally, a membrane is a thin film composed of organic polymer, a ceramic or other inorganic material, or, in some cases, a thin film of liquid. Membranes may be natural or synthetic. The natural membranes in plants and animals play vital roles in these biological systems.

Synthetic membranes have been developed for use in such areas as water purification, the recovery of valuable components from waste streams, the separation of alcohol from water-alcohol mixtures, oil refining processes, fuel cells and others. Separation is a key component in many chemical processes, indeed, the separation step is the single most expensive step in many industrial chemical processes. Much research has been devoted to increasing the efficiency of separations, leading to the development of new materials and technologies, including the membrane based separation systems.

Membrane processes may be divided into three categories according to the driving force for the transport process. These three driving forces are pressure differential, concentration differential and an electrical potential field. Microfiltration, ultrafiltration, reverse osmosis, gas separation, vapour permeation and pervaporation are examples that use a pressure differential across the membrane as a driving force. A difference in concentration across the membrane is the driving force for dialysis while the driving force for electrolysis and electrodialysis is a potential field applied across the membrane.

The efficiency of a membrane based separation is judged in terms of two parameters: the rate of the transport process and selectivity of the transport process. Ideally the goal is to achieve a very high rate of transport, or flux, of the desired component and no transport of any undesirable component. In reality, an acceptable balance must be found between flux and selectivity because these two parameters generally oppose one another. An increase in flux usually results in a loss in selectivity.

The focus of this thesis is on membranes designed for use in acid recovery from waste solutions as might be found in the metal finishing industries. These membranes use a difference in concentration as a driving force for separation by diffusion dialysis but may also be used in electrodialysis applications where the driving force is an electric field. Another potential application of these membranes is in fuel cell technology. Ion exchange membranes can be used as ionic conductors separating the anodic and cathodic compartments of some fuel cells [3-5].

1.1. Treatment of Spent Pickling Liquors

An important operation in the production of certain metal products is the removal of the oxide scale from their surfaces [6]. The removal of the scale is usually performed by immersing the metal in an acid bath for a brief period. The type of acid, or acids, used depends on the metal. Some of the acids that are used industrially and the metals that are treated are listed in Table 1.1.

Table 1.1. Acids Recovered by Diffusion Dialysis

Acid	Used For:
H_2SO_4	Steel plate and wire pickling
H_2SO_4	Aluminum anodizing
HCl	Aluminum etching
HNO_3/HF	Stainless steel pickling

With use, the acid concentration of a bath is gradually reduced as the acid reacts with the metal oxides and with some base metal, resulting in an aqueous solution of acid and metal salt which is no longer as effective in treating the metals. This spent liquor constitutes a major disposal problem, which has been addressed in a number of different ways.

1.1.1. Disposal Without Treatment

A number of methods have been used or proposed in the past for disposing of spent liquors without treatment. Examples of such procedures are discharge into deep wells, fissures in cavernous limestone, abandoned mines, exhausted oil and gas sands, artificial lagoons, gravel sumps near large bodies of water and sewers terminating in rivers, lakes or tidewater [6].

Wells and limestone fissures eventually refuse to accept any more spent liquor through sealing of the openings by deposition of reaction products. Pollution of ground water from seepage of the spent liquor is a distinct possibility.

Artificial lagoons, which depend on a combination of bottom seepage and solar evaporation, have been used but they usually require a larger ground area than is available.

Direct discharge into large bodies of water or rivers has been used as a means of disposal, which doesn't involve excessive cost. Oxidation of the ferrous iron colours the water brown in localized areas and its appearance becomes objectionable.

These methods are typically no longer available as options for disposal of spent pickling liquor due to increased environmental concerns.

1.1.2. Neutralization

The treatment of waste acid baths, such as those from the steel industry, with an alkaline agent affords a simple process either for neutralization of the acid alone or for

complete precipitation of the iron, although neutralization is more expensive than disposal without treatment.

Soda ash has been used to neutralize the free acid and the spent liquor is then disposed of into municipal sewerage, where permitted. In some cases, lime has been used to neutralize the free acid and the resulting suspension is pumped to lagoons where the ferrous iron gradually oxidizes and precipitates as hydrated ferric oxide.

The most common treatment in the past has been the addition of sufficient lime slurry for complete precipitation of the iron. The mixture is then discharged to a lagoon where evaporation and bottom seepage occurs. From time to time the accumulated sludge must be removed from the lagoon and disposed of [6].

1.1.3. Recovery of By-products

As a result of the high cost of disposal of spent liquors by neutralization and the elimination of the option of disposal without treatment by increased environmental controls, the recovery of acids and other by-products from the spent solutions has become the preferred method of dealing with the acid baths. A large number of processes have been patented; few of them, however, have ever been used commercially. The recovery processes have generated such products as iron salts, sulfuric acid (and other acids), electrolytic iron, building materials and ammonium sulfate. Although recovery products other than acid are obtained, the focus of this thesis is on the recovery of acids.

1.1.3.1. Recovery of Acid From Spent Liquor

A number of different processes for acid recovery have been developed, ranging from acid sorption in a resin unit [7] to electrodialysis of spent liquor [8-12]. Another process that has seen some success industrially is acid recovery by diffusion dialysis [6]. One advantage of diffusion dialysis is the low energy requirements.

1.1.3.1.1 Acid Recovery by Diffusion Dialysis

While electrodialysis requires substantial electrical energy, diffusion dialysis relies on the difference in chemical potential of species on either side of a membrane and external power is only required to circulate the solutions. The separation of acid from salts is achieved by using an anion exchange membrane. The membrane allows the selective transport of anions across the membrane, while ideally remaining impermeable to cations other than protons. The ability for protons to leak across anion exchange membranes is well known [12]. The migration of protons can occur both by diffusion as well as by transfer from one water molecule to another, the Grotthus mechanism [13,14]. Diffusion dialysis was first applied industrially in the late 1950s and has been used to extract acids from solutions containing metal salts [6,13,15-32].

1.2. Ion Exchange Membranes

Unlike pressure driven membrane applications, which do not necessarily require charged membranes, recovery of acid from solutions containing other salts requires the

use of a membrane with a fixed positive charge. A membrane with a fixed charge, either positive or negative, is called an ion exchange membrane [2]. Its properties include pronounced differences in permeability for counter ions (ions of the opposite charge to the membrane fixed charges), co-ions (ions of the same charge as the membrane fixed charges) and neutral species as well as high ionic conductivity [33]. An illustration of an anion exchange membrane (a membrane with fixed positive charges) is shown in Fig. 1.1.

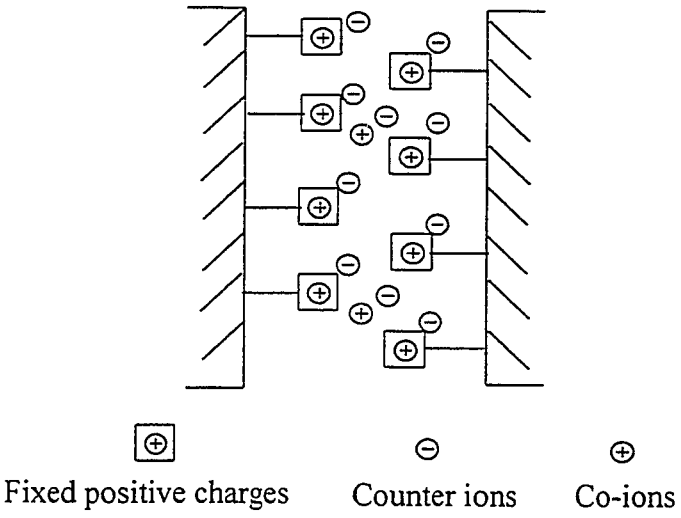

Fig. 1.1. Illustration of an anion exchange membrane pore.

The fixed charges are the ion exchange groups covalently bonded to the polymer membrane. For anion exchange membranes they are commonly quaternized amine groups and for cation exchange membranes they are usually either sulfonate or carboxylate. The counter ions are of opposite charge to the fixed ionic groups and must be present for charge balance. Co-ions are ions of the same charge as the fixed ionic groups. Thicknesses of commercial ion exchange membranes are usually in the range of 0.1 mm to 1 mm.

When in contact with electrolyte solutions of low concentrations, the membrane contains a large number of counter ions but relatively few co-ions. This is an effect of Donnan exclusion, a concept that will be discussed shortly. Counter ions are admitted into the membrane and have little difficulty in passing through while co-ions, on the other hand, are excluded from the membrane. This leads to the permselectivity of the ion exchange membrane for counter ions.

The amount of fixed charge present in an ion exchange membrane may be expressed in two ways: either as milliequivalents of fixed ions per gram of dry membrane (meq/g), a parameter frequently found in the academic and manufacturers literature, or as equivalents of fixed ions per kilogram of water in the membrane (eq/kg). As ions are transported through the aqueous regions of a membrane it is frequently more useful to use the latter definition of fixed charge concentration when attempting to understand membrane transport properties.

This permselectivity for counter ions is the basis for the diffusion dialysis recovery of acid from a mixed acid and salt solution. The metal co-ions are rejected from the membrane and therefore are not transported across the membrane. The acid protons, however, have the ability to transport through the membrane by the Grotthus mechanism. This mechanism is assumed, in this thesis, to be the mode of proton migration and will be discussed later. The resulting permeate solution is rich in acid and diminished in metal salts.

1.2.1. Donnan Exclusion

An ion exchange membrane in contact with an ionic solution will freely exchange ions with a charge opposite to that of the fixed charge within the membrane (counter ions). However, ions with the same charge as the fixed ions in the membrane (co-ions) are excluded and ideally cannot pass through the membrane. This exclusion, as a result of electrostatic repulsion, is called Donnan exclusion, named for F.G. Donnan who first reported the phenomenon [2,33,34]. Fig 1.2. is an illustration of this feature.

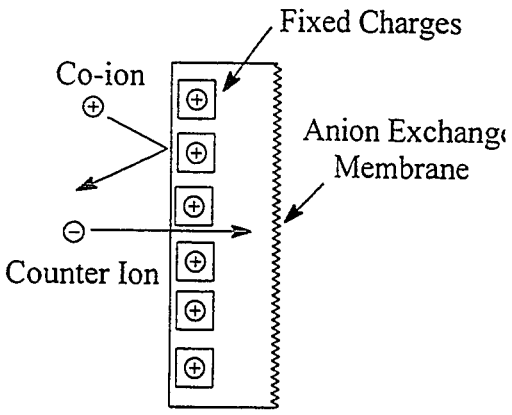

Fig. 1.2. Donnan Exclusion in an anion exchange membrane.

Co-ion uptake and electrolyte sorption are equivalent because of the electroneutrality requirement, hence the electrolyte is excluded from the ion exchange membrane. The efficiency with which co-ions are rejected by Donnan exclusion depends upon the concentration of the solutions in contact with the membrane as well as upon the concentration of fixed ionic groups in the hydrated membrane [2]. When the membranes are in contact with dilute solutions, Donnan exclusion is quite effective. As the

concentration of the solution increases, however, Donnan exclusion becomes less efficient. This decrease in Donnan exclusion is a result of a decrease in the Donnan potential of the membrane when in contact with more concentrated electrolyte solutions.

1.2.2 Donnan Potential

The exclusion of co-ions from the membrane results from the electrical repulsion between the fixed ionic groups and the co-ions which have the same charge sign. Therefore the efficiency with which co-ions are excluded from the membrane depends largely upon the proximity of the ions of like charge [2]. The selectivity will thus be improved by increasing the fixed charge concentration within the membrane.

When an ion exchange membrane is in contact with a dilute electrolyte solution, the concentration of counter ions in the membrane is much higher than the concentration of counter ions in solution. The counter ions try to reduce this concentration difference by diffusing out of the membrane into the solution, but this results in a charge imbalance in both the membrane and the solution. Since the electroneutrality requirements are no longer met, an electrical potential, the Donnan potential, is generated at the membrane surface that tries to pull the counter ions back into the membrane. As a result, counter ions accumulate in solution at the membrane-solution interface. This counter ion accumulation and the resulting Donnan potential are illustrated in Fig. 1.3. for an anion exchange membrane.

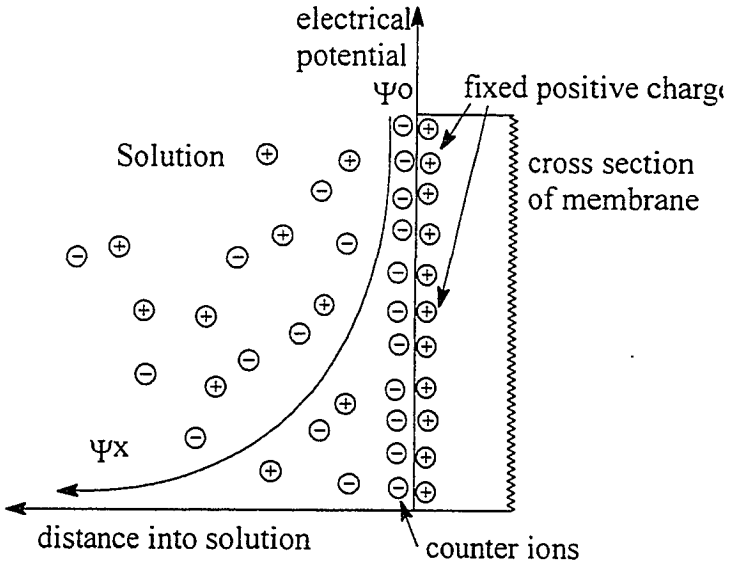

Fig. 1.3. Diagram of the distribution of ions and the electrical potential in the vicinity of the membrane-solution interface for an anion exchange membrane. ψ^o and ψ^x are the electrical potentials of the counter ion in solution at the membrane-solution interface and at a distance x from the membrane, respectively.

The Donnan potential can be calculated in the following manner. When an ion exchange membrane is contacted with an electrolyte solution and equilibrium is reached, the chemical potential of the ionic component in the two phases can be calculated by the following equations. In the solution:

$$\mu_i = \mu_i^0 + RT\ln a_i + z_i F\varphi \qquad (1.1)$$

In the membrane

$$\mu_i^m = \mu_i^{0\,m} + RT\ln a_i^m + z_i F\varphi^m \qquad (1.2)$$

where μ_i is the chemical potential of the ion i, μ_i^0 is the standard chemical potential of the ion i, a_i is the activity of ion i, z_i is the charge of ion i, φ is the potential of the phase, R is

the gas constant, T is the absolute temperature and F is the Faraday constant. The superscript m denotes the membrane phase.

At equilibrium, the chemical potentials in both phases are equal, $\mu_i = \mu_i^m$, thus equations 1.1 and 1.2 may be equated. If the standard states for both phases are assumed to be equal, $\mu_i^0 = \mu_i^{0m}$, the following equation is obtained which allows calculation of the Donnan potential, the potential difference between the membrane and solution phases:

$$E_{Donnan} = \varphi^m - \varphi = RT/z_iF \ln(a_i/a_i^m)$$

As an example, for a given monovalent ionic solute with an activity ratio (a_i/a_i^m) of 1:10, the equilibrium Donnan potential at 25°C is -59 mV.

1.2.3. Proton Transport Through Anion Exchange Membranes

Table 1.2. lists some ions and their diffusion coefficients in water at 25°C [35]. As can be seen, the proton diffusion coefficient is substantially greater than all other ions.

Table 1.2. Ionic Diffusion Coefficients, D_i, in Water at Infinite Dilution at 25°C (10^{-9} m^2/sec)

$Cation_i$	D_i	$Anion_i$	D_i
H^+	9.31	OH^-	5.28
Li^+	1.03	F^-	1.47
Na^+	1.33	Cl^-	2.03
K^+	1.96	Br^-	2.08
Mg^{2+}	0.71	SO_4^{2-}	1.06

Protons have the ability to migrate by two different processes. The first process is migration by simple diffusion. In this case, the hydrated proton moves by random Brownian motion in solution. This is similar to the migration of any ion in solution. The free solution diffusion coefficient of a proton is 2.30×10^{-9} m^2/s [36]. The second process is known as transport by the Grotthus mechanism [13,14]. This mechanism involves proton exchange between water molecules. Hydrogen bonds are formed and broken along a series of water molecules leading to the transport of protons at a much greater diffusion rate than would be expected by simple diffusion. This mechanism was advanced to explain the anomalously high diffusion coefficient of protons in water, which is 9.31×10^{-9} m^2/s as seen in Table 1.2. The diffusion coefficient includes both the Grotthus and free solution diffusion processes.

The Grotthus mechanism is illustrated in Fig. 1.4. A proton is transferred from an H_3O^+ molecule to a neighbouring H_2O molecule which, in turn, transfers a proton to another neighbouring H_2O molecule. This process occurs over the network of hydrogen bonded water molecules and the net result is the rapid transport of a proton at a rate much faster than could be accomplished by simple diffusion alone.

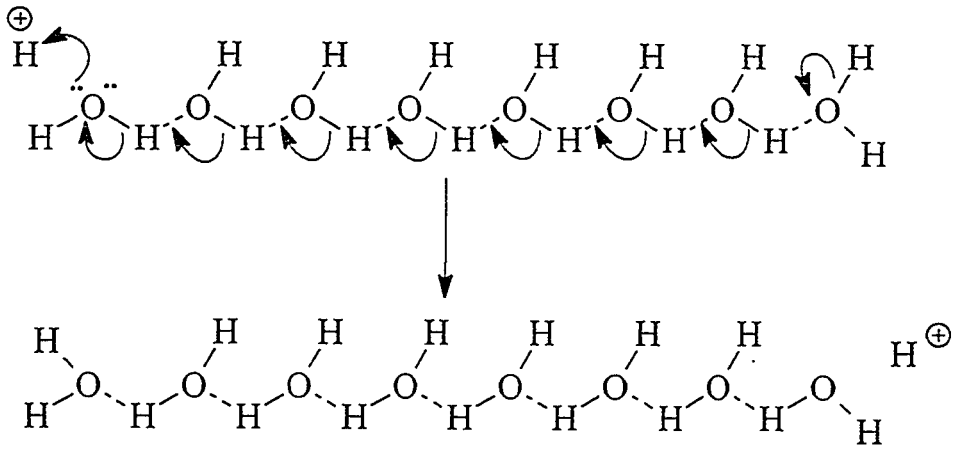

Fig. 1.4. Proton Transport by the Grotthus Mechanism

Referring to Fig. 1.4, a proton is transported from the left to the right in the figure but the proton that appears on the right is not the same proton that was initially present on the left. If the series of hydrogen bonded water molecules was extended from the solution on one side of the membrane, through the membrane to the solution on the other side, a proton could be transported across the membrane without ever introducing a proton into the membrane. In this manner, the exclusion of cations by an anion exchange membrane would have no effect on the transport of protons since, in principle, a proton need not actually be present in the membrane at any time. The transport of HCl across an anion exchange membrane can be readily accomplished by proton transport via the Grotthus mechanism accompanied by simple diffusion of the chloride ion, which is free to exchange in the membrane. This ability for protons to "leak" across anion exchange membranes can be exploited in diffusion dialysis recovery of acid but in fact poses a problem for concentration of acids by electrodialysis [11,13]. Metal co-ion transport

across the anion exchange membranes is ideally prevented by the Donnan exclusion mechanism, but, in practice, some metal ion leakage does occur.

1.2.4. Preparation of Ion Exchange Membranes

There are two general approaches to introducing the ion exchange groups into the membrane. The first approach involves copolymerization of an unsubstituted alkene or crosslinking agent with a functionalized alkene bearing the ionic group or a precursor to the ionic group. The second involves the polymerization of an alkene with subsequent introduction of ion exchange groups into the polymer.

1.2.4.1 Perfluorinated Membranes

One of the earliest classes of ion exchange membranes introduced into the market place were the perfluorinated Nafion™ membranes developed by Dupont in the 1970s. These membranes were used mainly in the chlor-alkali industry where their chemical stability was a main advantage. Copolymerization of tetrafluoroethylene with a substituted monomer was carried out by radical initiated polymerization in either aqueous or nonaqueous media. The substituted monomers have the general structure shown in Fig. 1.5.

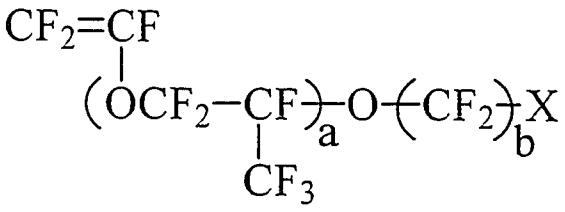

Fig. 1.5. Perfluorinated Functionalized Alkene. X = SO_3^-, COO^- : a = 0-2 : b = 1-4

The cation ion exchange polymers are then formed into membranes by conventional molding and extrusion techniques. Cation exchange membranes are typically based on sulfonate or carboxylate functionalities. Anion exchange membranes have been produced using the perfluorinated monomers by reaction of a sulfonyl fluoride polymer with a diamine followed by reaction with an alkyl halide to give a quaternary ammonium centre, Scheme 1.1.

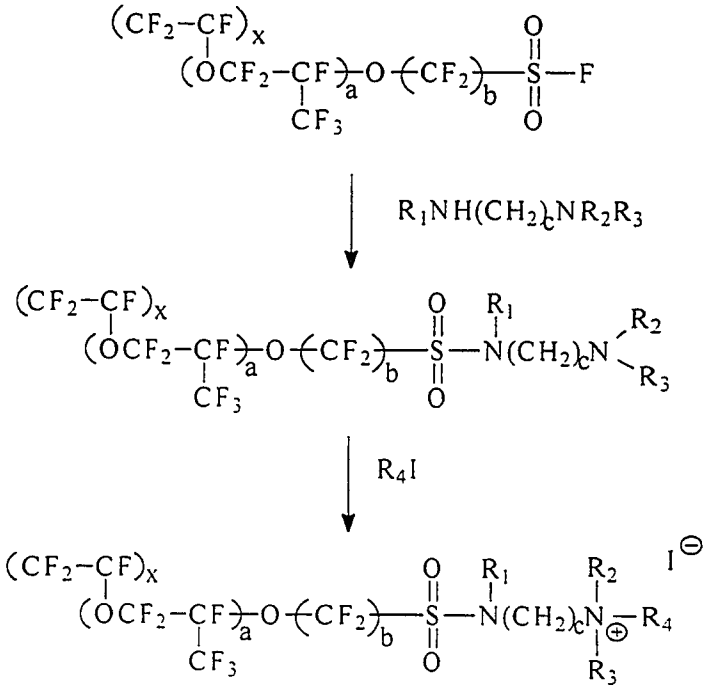

Scheme 1.1. Formation of Perfluorinated Anion Exchange Membrane

1.2.4.2. Hydrocarbon Membranes

Hydrocarbon ion exchange membranes are commonly based on a copolymer of styrene or vinylpyridine and divinyl benzene in which the fixed ionic charges are introduced after polymerization. The term "hydrocarbon" refers to the hydrocarbon backbone of the polymers, as opposed to the perfluorinated polymers described in the previous section. Acrylic acid can be used to form cation exchange membranes. Some representative monomers are shown in Fig. 1.6.

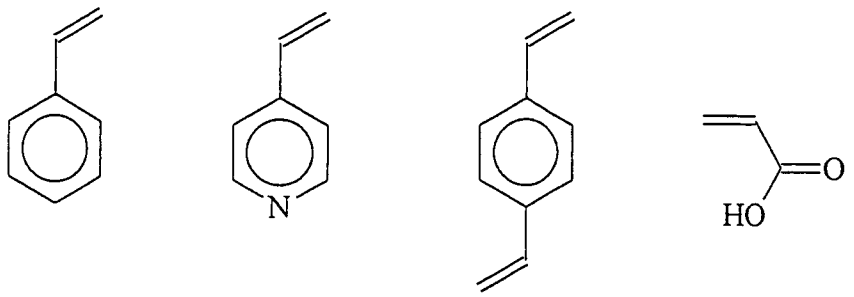

Styrene 4-Vinylpyridine 1,4-Divinylbenzene Acrylic Acid

Fig. 1.6. Some Monomers Used for Hydrocarbon Ion Exchange Membranes

The ratio of styrene, vinylpyridine or acrylic acid to divinylbenzene controls the extent of crosslinking, critical to the properties of the polymers as ion exchange membranes, in particular the water content of the membranes. The polymerization is carried out using a radical initiator and the kinetics of the chain extension reactions are probably close to mass transport controlled and therefore is not very sensitive to the structure of the olefin. As a result, the polymer formed has a composition similar to the composition of the initial monomer solution.

To generate cation exchange membranes, the fixed ionic groups are generally sulfonate or carboxylate, the former produced by sulfonation of the styrene groups using concentrated sulfuric acid or chlorosulfonic acid and the latter by use of acrylic acid as the functionalized monomer.

Most anion exchange membranes are based on quaternary ammonium ion exchange sites. These groups can be introduced by chloromethylation of the styrene groups followed by reaction with a tertiary amine to yield the anion exchange site. Alternatively, vinylbenzylchloride can be used as the functionalized monomer which is then reacted with a tertiary amine. One other route to anion exchange membranes is to replace the styrene monomer with vinylpyridine which contains a nitrogen centre which may be quaternized by reaction with alkyl halides to form the positively charged site.

The formation of these hydrocarbon based ion exchange polymers into membranes has presented some challenges [2]. Despite the ability to vary the extent of crosslinking, and hence the swelling of the polymer, membranes made from these polymers alone are always too brittle and lacked the mechanical stability essential for commercial use. As a result, other polymers were employed to improve the membrane strength. Common techniques use a hydrophobic polymer in combination with the ion exchange polymer. The styrene and divinylbenzene can be prepared in a solution including a hydrophobic polymer, which gives added strength to the final polymer. An example of this approach is the paste method, developed by the Tokuyama Corporation [37,38]. This procedure involves mixing a fine powder of poly(vinylchloride) with the

liquid monomers for the ion exchange polymer, initiator and a plasticizer. The paste is spread on a fine reinforcing mesh and clamped between two sheets of protective polymer. During the polymerization the poly(vinylchloride) powder fuses into a continuous film.

1.2.4.3. Bipolar Membranes

The concept of a bipolar membrane is to fabricate a membrane composed of two layers, an anion exchange layer and a cation exchange layer. In the presence of an electric field, water at the interface of the two polymer films will dissociate and the H^+ and OH^- ions formed will then migrate in opposite directions to produce acid and base on opposite sides of the bipolar membrane. This technique has been used for purification of acids and bases [39]. The principle of a bipolar membrane is illustrated in Fig. 1.7.

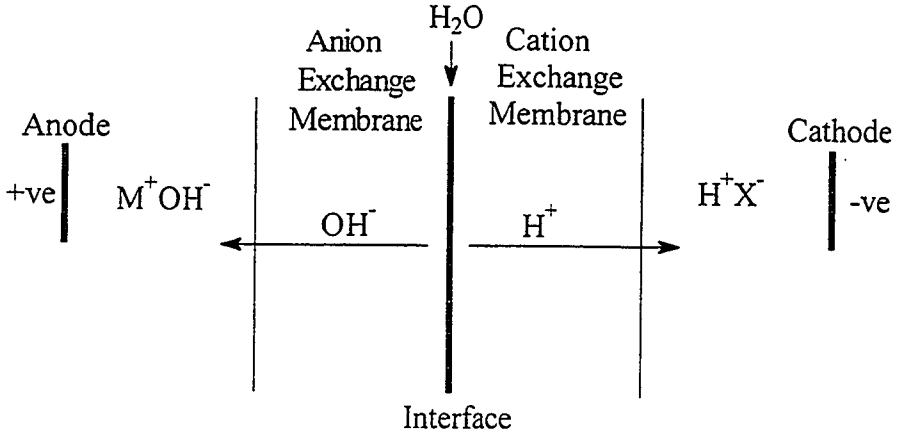

Fig. 1.7. Water Splitting Using a Bipolar Membrane

Bipolar membranes have been made by clamping an anion exchange membrane and a cation exchange membrane together but this method allowed for a gap to develop between the membranes and resulted in an increase in the local resistance, thus reducing

efficiency. Thermoplastic membranes have been heated and pressed together and ion-conducting adhesives have been used to join the two layers.

Another approach to ion exchange membrane fabrication in general that was used to produce a bipolar membrane is the simple casting of a polyelectrolyte solution onto a removable support. The first layer was formed from a solution of anion exchange polymer cast onto the support. Following solvent evaporation, the second layer containing a solution of cation exchange polymer was cast overtop of the first and the laminate was then heated in an oven.

1.2.5. Morphology of Ion Exchange Membranes

1.2.5.1 Perfluorinated Membranes

It is generally accepted that fluorocarbon polymers undergo phase separation when swollen by water [2,40-42]. The swollen polymer has hydrophobic zones composed of the perfluorinated chains and hydrophilic zones created by the clustering of the fixed charge sites. The ionic groups hydrate and form water filled pores or channels through which ions migrate. There is evidence for phase separation that comes from several different sources.

The aqueous pores have been visualized by transmission electron microscopy following the deposition of silver from aqueous solutions of Ag^+ within the membrane

using a reducing agent such as Sn^{2+} [2]. The silver deposits non-uniformly as a series of patches with sizes of 3 - 10 nm.

Wide angle x-ray diffraction has been used to study the hydrophobic zones and the results show that for all ionic forms of the sulfonic acid polymer, as well as the carboxylate polymers, the membranes have significant domains which are crystalline and close in structure to poly(tetrafluoroethylene) [41]. Small angle x-ray diffraction studies have been done to probe the aqueous phase of the membranes. Scattering maxima are seen to be a function of the water content of the membranes. The peak attributed to the aqueous clusters increases in intensity as the water content is increased [2,41].

A cluster network model has been proposed by Gierke [40] whereby the aqueous domains of the membrane are thought to consist of uniform spherical clusters of fixed ionic groups, in the range of 4 nm in diameter, interconnected by narrow channels, approximately 1 nm long and 1 nm in diameter. The narrow channels between the clusters were introduced to explain the very high ionic selectivity achieved by Nafion and other similar membranes.

The two phases in fluorocarbon membranes have important roles in determining the membrane properties and performance. The hydrophobic fluorocarbon domain provides mechanical and physical strength while the aqueous domains provide the ionic conductivity and selectivity of ionic transport.

1.2.5.2. Hydrocarbon Membranes

Unlike the perfluorinated membranes, hydrocarbon membranes do not phase separate into hydrophobic and hydrophilic domains [2]. The structure of the majority of hydrocarbon membranes consists of the fixed ionic groups being attached to the hydrocarbon backbone by relatively short and rigid sidechains, typically a single aromatic ring, in a highly crosslinked network. The short sidechains and extensive crosslinking greatly restricts the mobility of the polymer chains and inhibits any reorganization into hydrophobic and aqueous regions.

There is generally a high concentration of fixed charge sites, regularly spaced throughout the membrane, leading to a uniform structure. When the membranes are swollen with water, they have a structure that resembles a concentrated electrolyte solution [2].

1.2.6. Pore-Filled Membranes

Ion exchange polymers which lack sufficient mechanical strength to be used as membrane materials on their own can be anchored into a suitable host substrate that is mechanically stable. Such membranes can be referred to as "pore-filled".

A pore-filled membrane receives its mechanical strength from the host substrate which is both physically and chemically stable and of sufficient porosity to accept an adequate amount of ion exchange polymer. The pore filling material serves as the

separation media, possessing the chemical and physical properties required for the specific separation process.

Various materials have been introduced into porous substrates including organic complexing agents [43] and polyelectrolytes [44]. One of the key issues in fabrication of pore-filled membranes is the manner in which the material is incorporated into the porous substrate. There are a variety of methods that have been used to introduce pore-filling materials into support membranes and are reviewed in the following sections.

1.2.6.1. Physical Adsorption

Perhaps the simplest method of introducing materials into host supports is by physical adsorption. A solution containing the material to be introduced is brought into contact with the support membrane and the material then enters the pores of the membrane. The pore-filling material is held within the pores of the host membrane by van der Waals forces, dipole interactions or, if both the material to be incorporated and the host membrane are charged, electrostatic interactions.

Imato and coworkers [43] impregnated a microporous poly(propylene) film with a solution of tri-n-octylamine in 1-decanol to form a supported liquid membrane. The amine was used as a mobile carrier for the diffusion dialysis transport of organic and inorganic anions in acid solution. In general, supported liquid membranes are not stable due to desorption of the pore-filling material during use.

Anderson and Kim prepared pore-filled membranes by adsorbing aqueous solutions of poly(styrenesulfonate) into porous mica sheets [44]. The membranes were used to study the effects of adsorbed polymer layers on dextran transport through microporous membranes under pressure driven applications. The use of high molecular weight polymers as adsorbed pore-filling agents creates a more stable membrane than simple supported liquid membranes but long term stability is still a problem.

In order to more securely anchor the pore-filling material, alternative processes were developed.

1.2.6.2. Grafting

A more robust method of anchoring materials in the pores of host membranes is the covalent attachment of the materials to the membrane. The creation of a covalent bond between the pore-filling material and the host substrate permanently "locks" the material in the membrane pores, such materials are said to be "grafted" onto the substrate. Technologies for modification of polymers using methods such as grafting have been of prime importance in polymer applications and have been reviewed in numerous articles and books over the past few years [45-49]. Two basic approaches are used to graft materials into membranes, attachment of preformed polymers and graft polymerization of monomers within the membrane.

1.2.6.2.1. Attachment of Preformed Polymers

The method of coupling preformed polymers to a membrane illustrates the advantage of being able to control the characteristics of the grafted polymer, such as molecular weight and polydispersity, prior to attachment to the membrane. Mir and coworkers end-grafted poly(styrene) chains onto silicon and then sulfonated the aromatic rings to produce a negatively charged, grafted electrolyte [50]. Poly(ethyleneglycol) chains have been grafted onto functionalized poly(styrene) latex particles [51] and poly(sulfone) surfaces [52]. Other reports of grafting preformed polymers to surfaces are abundant [53-56]. One major disadvantage of the technique of grafting of preformed polymers is the lack of control over the density of the grafting.

1.2.6.2.2. Graft Polymerization

Examples of graft polymerization of monomers within membranes are abundant [21,31,57]. Casolaro and coworkers grafted polymerized acrylic acid onto cellulose membranes using free-radical mechanisms initiated by Ce(IV) salts or oxygen plasma [58]. Imaizumi and coworkers photografted acrylic acid onto poly(ethylene) films using benzophenone as a radical initiator [59].

Membranes containing poly(vinylpyridine) moieties have been prepared by grafting techniques [37,59-67]. Childs and coworkers have reported the preparation of poly(4-vinylpyridine) grafted membranes [68-70]. These membranes were prepared by absorbing 4-vinylpyridine and a photoinitiator, benzoin ethyl ether, into the pores of a

poly(propylene) or poly(ethylene) membrane followed by UV-initiated polymerization, Scheme 1.2.

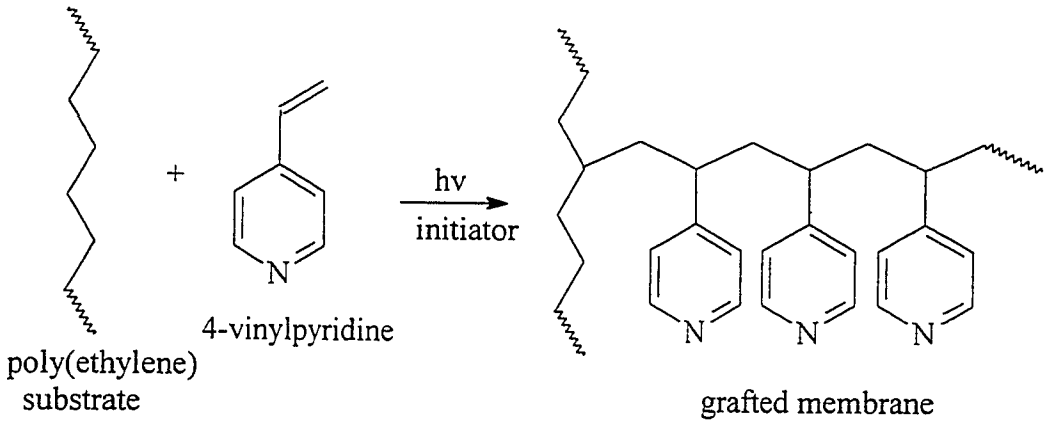

Scheme 1.2. Photografting of 4-vinylpyridine onto a poly(ethylene) membrane.

Alkylation or protonation of the membranes in Scheme 1.2 produces positively charged anion exchange membranes.

1.2.6.3. Crosslinking of the Pore-Filling Polymer

In cases where there is concern about the presence of grafting (actual formation of a covalent bond between the substrate membrane and the incorporated material), and the potential loss of the incorporated polymer, the addition of a crosslinking agent to the polymerization helps to improve the stability of the pore-filled membranes.

Childs and coworkers have prepared poly(4-vinylpyridine)-filled membranes using divinylbenzene as a crosslinker for the *in-situ* polymerization. These membranes have shown promise in the areas of acid recovery by diffusion dialysis [15] and ultra-low

pressure water softening [71]. Scheme 1.3. shows the formation of crosslinked poly(4-vinylpyridine) resulting in a three dimensional polymer gel.

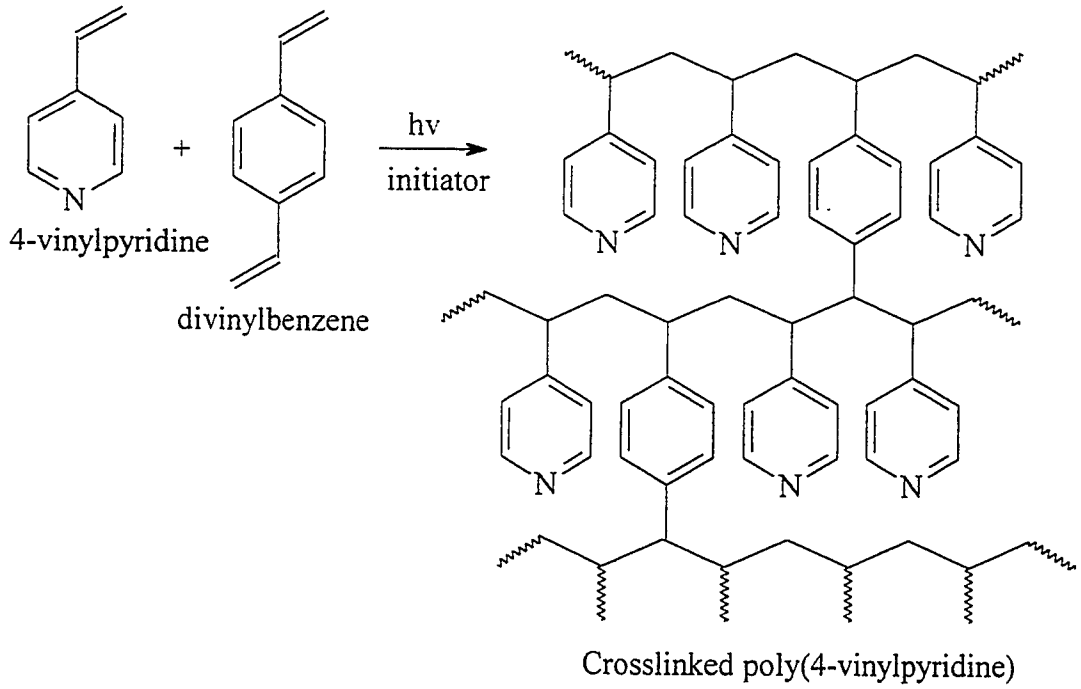

Scheme 1.3. Formation of Crosslinked Poly(4-vinylpyridine)

When a crosslinking agent is used in the polymerization within a membrane, it is no longer necessary to rely on the formation of covalent bonds between the incorporated polymer and the porous substrate to anchor the gel within the membrane. Although grafting may still be occurring, the physical entanglement of the three dimensional, crosslinked polymer gel within the pores of the host substrate will assist in locking the pore-filling material in the membrane.

1.2.6.4. Crosslinking of Preformed Polymer

The necessity of grafting a polymer onto the host membrane in order to anchor the incorporated material can be completely avoided by crosslinking a preformed polymer within the pores of the substrate. A solution of preformed polymer and a crosslinking agent is absorbed into the membrane pores and the reaction of the crosslinker with the preformed polymer entangles and locks the polymer within the substrate. This technique has been used by Iijima and coworkers to incorporate poly(4-vinylpyridine) into poly(ethyleneterephthalate) films [72,73].

This procedure has been used by Childs and coworkers to incorporate poly(4-vinylpyridine) into poly(ethylene) microporous membranes using dibromoalkanes as crosslinkers, Scheme 1.4.

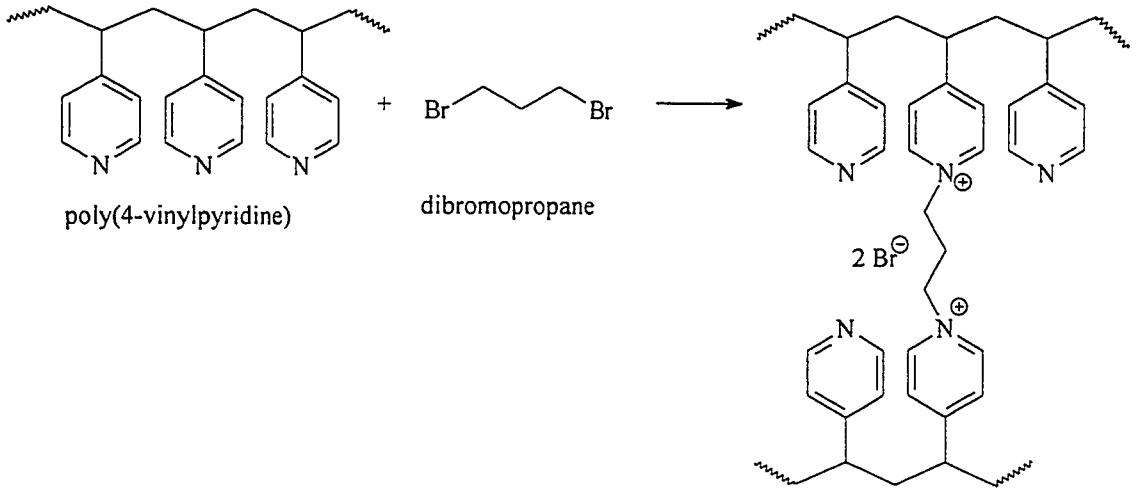

Scheme 1.4. Crosslinking of Poly(4-vinylpyridine) Using Dibromopropane

Membranes produced by this technique yield stable anion exchange membranes upon alkylation of the pyridine sites without the need for covalent bonds (grafting) between the polyelectrolyte and the host membrane.

Another route to anion exchange membranes used by Childs and coworkers is shown in Scheme 1.5, the reaction of poly(vinylbenzyl chloride) with a crosslinker such as 1,4-diazabicyclo[2,2,2]octane (DABCO) within the pores of a poly(propylene) substrate [74].

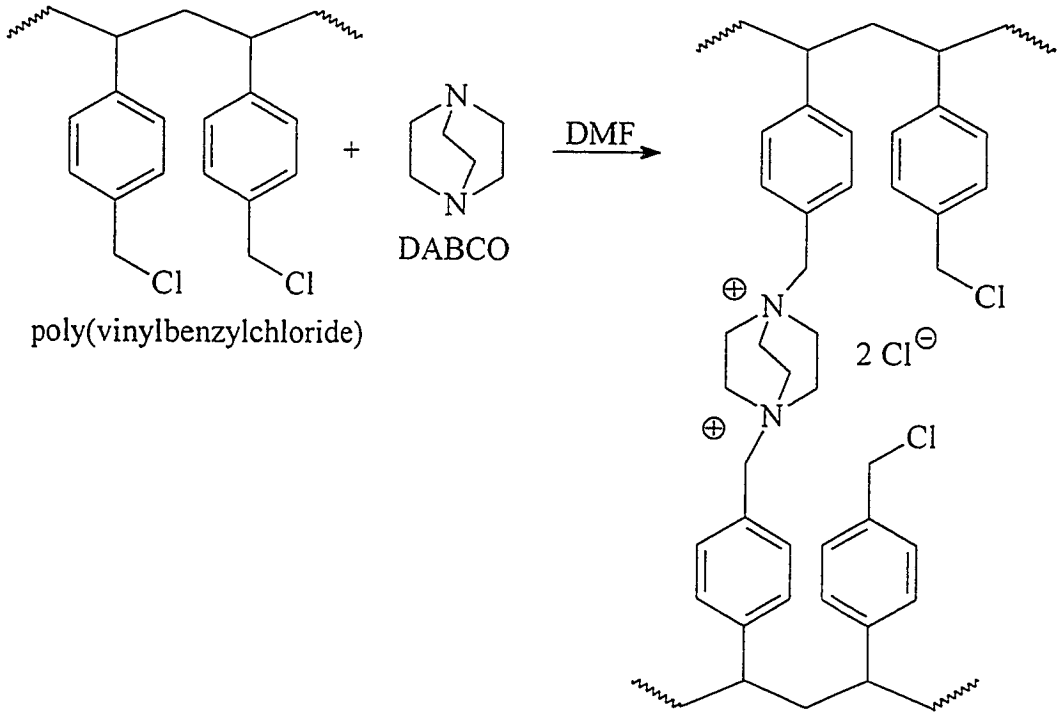

Scheme 1.5. Crosslinking of poly(vinylbenzylchloride) Using DABCO

Amination of the remaining benzylchloride groups yields a stable anion exchange membrane. One of the limitations of this technique is the limit to the amount of pore loading that can be achieved. A solvent must be used to insert the preformed polymer and

crosslinker into the porous host, thus, the amount of material that can be introduced into the substrate is limited by the amount of polymer that can be dissolved in a given amount of solvent. By comparison, the *in situ* polymerization of monomers within the pores of the host (sections 1.2.6.2. and 1.2.6.3.) does not require a solvent, hence a higher loading is possible.

1.2.7. Properties of Pore-Filled Ion Exchange Membranes

1.2.7.1. The Host Substrate

As has been mentioned, the host membrane provides the majority of the mechanical strength of the final membrane. Thus, the host plays a role in determining the properties of the pore-filled membrane. If swelling of the membrane occurs, the water content will increase and this will affect the electrical resistance, permeability and selectivity of the membrane. This requires using a host that has good tensile strength.

One of the critical factors regarding membrane use is the lifetime of the membrane under operating conditions. This calls into play the chemical and thermal stability of the host substrate. Having an incorporated polyelectrolyte with good stability is of no use if the support material is not stable.

1.2.7.2. Role of the Incorporated Polyelectrolyte

The choice of polyelectrolyte depends on the desired separation characteristics. For example, in acid recovery applications an anion exchange membrane is used since cations other than protons will be rejected. In this case a positively charged polyelectrolyte that is stable to an acidic environment is required. Conversely, for caustic recovery, a negatively charged polyelectrolyte that is stable to basic solutions is required. Water purification processes can use either anion or cation exchange membranes, the choice of which is determined based on the composition of the feed stream.

Polyelectrolytes are generally water soluble polymers. The use of crosslinking, in addition to locking the polyelectrolyte in the membrane, decreases the water solubility of the polyelectrolyte. Thus, a crosslinked polyelectrolyte will swell in water but will not dissolve and the degree of swelling depends inversely on the degree of crosslinking. Another way to decrease its water solubility is to increase the hydrophobicity of the polyelectrolyte by introduction of hydrophobic groups.

1.2.7.3. Water in Pore-Filled Ion Exchange Membranes

The water component of ion exchange membranes plays an important role in determining membrane properties since transport across the membrane occurs through the aqueous regions. The amount of water contained within the membrane is controlled by a number of factors: structure of the incorporated polymer, quantity of fixed charge sites,

degree of crosslinking and the compositions of the solutions in contact with the membrane.

A polyelectrolyte bearing more hydrophobic groups will have a lower water content than a more hydrophilic polyelectrolyte. For example, quaternization of poly(4-vinylpyridine) with long chain alkyl bromides decreases the water content of membranes containing this particular polyelectrolyte [37]. Increasing the number of fixed charge sites will increase the amount of water in a membrane because each ion exchange site and its counter ion will have water of hydration associated with it [2]. A membrane with a lower degree of crosslinking will swell with water to a greater extent than a membrane with increased crosslinking [15]. If, on first contact of a membrane with a solution of an electrolyte, the chemical potentials of the water in the two phases are not equal, an osmotic pressure difference will exist and this will cause water to be transported until the chemical potentials are equal. A membrane in contact with concentrated electrolyte solutions will experience a decrease in water content as there is a competition between the membrane and the solution for the available water [2].

It is generally accepted that water in membranes may be present in two states; namely "bound" and "free" water [75-78]. Bound water is also referred to as nonfreezable water, since it cannot be detected by differential scanning calorimetry, and is associated with the fixed charge sites and counter ions in the form of hydration shells. Free water is also referred to as freezable water and behaves more like bulk water, freezing as the sample is cooled and the heat released is detectable by differential scanning calorimetry.

It has been estimated that each ion exchange site and its counter ion have hydration shells containing approximately eight water molecules [2,15,79], therefore comprising the bound, or nonfreezable, water in the membrane.

1.2.7.4. Ion Exchange Capacity and Fixed Charge Concentration

The ion exchange capacity is usually defined as the number of milliequivalents of ion exchange sites per gram of dry membrane. While ion exchange capacity provides an indication of the amount of fixed charge sites per unit mass of membrane, it does not give a realistic picture of the membrane under operating conditions. When the membrane is hydrated and in contact with the solutions that will be used in the separation, a more useful parameter is the fixed charge concentration which can be quoted as moles of fixed charge sites per kilogram of water in the membrane.

Water content is linked to fixed charge concentration by an inverse relationship. A higher water content leads to a lower fixed charge concentration, thus, factors that affect water content have an inverse effect on fixed charge concentration. Polyelectrolytes bearing hydrophobic groups will increase the membrane fixed charge concentration, as will increasing the crosslinking of the polyelectrolyte.

The method of membrane fabrication is also important. As mentioned in section 1.2.6.4., the extent of pore loading using preformed polymers is limited by the fact that a solvent must be used to introduce the preformed polymers into the host substrate. As a result, the quantity of polyelectrolyte incorporated into the membrane and the resulting

fixed charge concentration will be lower than that obtained by using an *in-situ* polymerization technique which requires no solvent.

It is the fixed charge concentration which, in part, determines the permeability and selectivity of an ion exchange membrane according to Donnan exclusion and the Donnan potential. A monomer with a lower molecular weight will allow for a higher fixed charge concentration, provided sufficient crosslinking is used to limit membrane swelling.

1.2.8. Diffusion Dialysis for Acid Recovery Using Anion Exchange Membranes

The use of diffusion dialysis for the recovery of acid from spent solutions was first introduced in the late 1950s [24-26]. The early 1960s saw the development of anion exchange membranes for use in this area by Tokuyama Soda and Asahi Glass of Japan [32]. A typical dialysis cell is composed essentially of a sandwich of membranes with the solutions flowing between the membranes. The solutions on either side of the membranes alternate between the acid/salt feed liquor and the recovered acid solution, shown in Fig. 1.8.

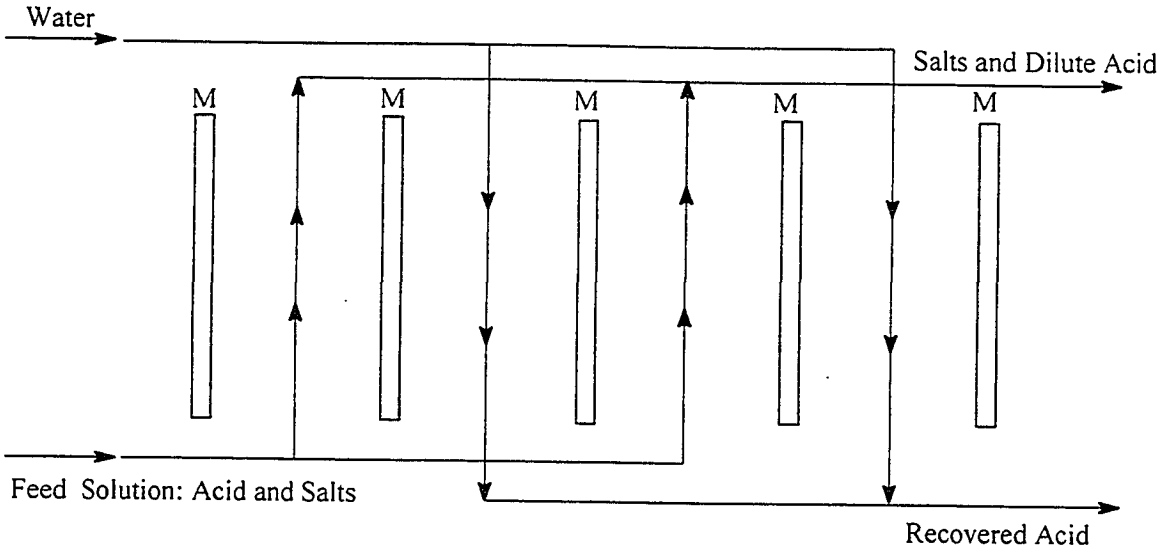

Fig 1.8. Diffusion Dialysis Flow System. M = membrane.

The feed solution is usually fed into the bottom of the dialysis unit and the water into the top. This system provides counter current flow which maintains the maximum concentration difference between the feed and permeate solutions at any given location along the membrane surface, thus giving the maximum rate of acid recovery.

Having the feed solution enter the unit at the bottom also makes use of the changing solution density as a flow promoter. As the feed solution becomes depleted of acid its density decreases, this causes a convective flow of the solution in an upwards direction, coupling with the flow that is already being pumped upwards. Likewise, the water is being pumped down the dialysis unit and, as acid is recovered, the density of the permeate solution increases. The resulting convective flow is in the same direction as the pumped flow.

The diffusion of a particular ionic species across a membrane is not an independent phenomenon [33]. The transport of any anion across a membrane must be accompanied by an equivalent transport of cations, a result of the electroneutrality requirement. For acid recovery, the facile transport of anions across an anion exchange membrane, coupled with the ability of protons to leak across an anion exchange membrane, allows for separation of acid from a mixed salt solution.

From a practical viewpoint, there are two important factors involved in the dialysis process, one of which is the rate of transport through the membrane and the other the degree of separation. These two factors are generally in conflict with one another, an increase in the rate of transport usually results in a decrease in separation, or selectivity, of the membrane.

The rate of transport of a particular species across a membrane is inversely proportional to the membrane thickness. With this in mind, it is desirable to make the membrane as thin as possible to maximize the flux of the desired species, in this case the acid. A decrease in thickness, however, results in a decrease in mechanical strength, which limits the minimum thickness of membranes.

To achieve high selectivity of acid over salts, a high fixed charge concentration is required, which leads to a decrease in transport across the membrane of all species. Therefore, the desired rate of acid recovery must be balanced by the minimum membrane thickness that is required and an acceptable selectivity of acid over salts.

Prosep Technologies of Pickering Ontario are the developers and manufacturers of a process which uses resin sorption for acid recovery. In this process the spent acid solution is passed through a resin bed which selectively absorbs the acid from the liquor. The purified acid is then desorbed from the resin with water. This process has been studied by Prosep on an economic basis and Table 1.3 gives a comparison of the cost of purification of a representative sulfuric acid bath using the resin bed technology of Prosep to that using a membrane based diffusion dialysis system [80].

Table 1.3. Summary of Annual Operating Costs for Diffusion Dialysis and Prosep Purification of H_2SO_4 Pickling Applications

Item	Diffusion Dialysis Costs ($US/yr)	Prosep Technology Costs ($US/yr)
H_2SO_4 Losses	33,570	18,720
Neutralizing Lime	15,510	8,800
Sludge Disposal	94,875	53,075
Membrane/Resin Replacement	50,000	10,000
Deionized Water Consumption	23,310	—
Process Water Consumption	—	7,435
Water Preheating and Filtration	17,760	770
Maintenance/Operating Costs	26,250	13,125
Total Annual Costs	261,275	111,925

By looking at Table 1.3, the comparison shows an annual saving of $149,350 using the resin bed process compared to a diffusion dialysis acid recovery system. It should be noted that the data were obtained from a biased source. The greater acid losses with the diffusion dialysis system result in increased disposal costs, leading to the increased costs with diffusion dialysis seen in the first three rows of the table. Row four shows the replacement cost of membranes compared to the resin bed, membranes being five times the cost of the resin bed. Water treatment and maintenance costs are also higher for the diffusion dialysis process.

It becomes clear with regard to the comparison made in Table 1.3 that if diffusion dialysis is to be a viable alternative to the resin bed technology, improvements must be made in membrane performance. Improved acid transport will help reduce the costs associated with acid losses and disposal costs. Extending the life of the membranes as well as producing less expensive membranes will reduce replacement costs. What is needed is a cheaper membrane which shows improved acid recovery performance.

With the development of the pore-filled membrane process at McMaster University, anion exchange membranes based on poly(4-vinylpyridinium) salts were investigated with respect to their ability to separate acid from mixed salt solution. Early studies indicated that the membranes exhibited high permeability towards protons relative to a commercially available diffusion dialysis membrane (Selemion DSV, Asahi Glass, Japan) and were somewhat permselective with respect to protons over sodium and magnesium ions [81]. These results indicated that perhaps McMaster membranes could

be optimized to improve their diffusion dialysis performance to exceed that of the commercial membrane.

One key feature of McMaster membranes is their potential for low cost production by using an inexpensive poly(propylene) or poly(ethylene) support. The pore-filling techniques developed at McMaster are simple and scaling up to an industrial process may be possible. This makes these membranes attractive from an economic standpoint since membrane costs form a large part of the investment in membrane systems.

1.3. Research Outline

1.3.1. Statement of Problem

At the outset of this work McMaster membranes have shown promise in the areas of water purification and, with more specific relevance to this thesis, acid recovery by diffusion dialysis. The fabrication methods used allow for the tuning of membrane properties in a well controlled and well defined manner. The pore-filled membranes produce at McMaster thus far, however, have not been optimized for acid recovery in any way and an investigation into understanding how the membranes function has not been undertaken.

Much work has been done at McMaster with respect to pressure driven water softening applications which utilize membranes with lower pore loadings than dialysis membranes. As well as differences in the composition of membranes used for water

softening, the driving force for the separation is pressure whereas acid recovery uses a concentration difference as a driving force. Thus the transport through dialysis membranes deals with different parameters than those in pressure driven applications. An understanding of the principles involved in the diffusion of ions through McMaster membranes is required.

It was thus proposed to continue the work in the direction of acid recovery applications by fabricating membranes with various pore loadings, crosslinking and nitrogen atom quaternizing groups and then to study their performance in the diffusion dialysis recovery of acid from acid/salt solutions.

The spent acid bath was simulated using a solution of hydrochloric acid, sodium chloride and magnesium chloride. Sodium and magnesium chlorides were used as representative metal ions because of the ease of quantification using the ion chromatography instrument in the laboratory.

1.3.2. Objectives

There are two general goals of this work. The first is to optimize the crosslinked poly(4-vinylpyridine)-filled microporous membranes for performance in acid recovery applications. In order to do this, the second goal is to understand the fundamental principles of ion transport through the membranes.

Poly(4-vinylpyridinium) was chosen as the pore-filling polyelectrolyte because it is easily polymerizable, simple to introduce into the nascent membrane as it is a hydrophobic liquid monomer and it is easily converted to its cationic form by

quaternization of the pyridine nitrogen atom. It was also logical to continue working with a monomer that had been shown to produce membranes effectively and exhibit promise in acid recovery applications.

To address the general goals put forth, the detailed objectives are:

1. To examine the effects of mass loading and degree of crosslinking of poly(4-vinylpyridine)-filled membranes crosslinked with divinylbenzene on membrane properties and acid recovery performance (Chapter 2);
2. To examine the effects of pyridine nitrogen atom quaternization with alkyl groups of varying chain length on membrane properties, such as water content, bound and free water contents, and acid recovery performance, and compare them with protonated membranes (Chapter 3);
3. Perform an in depth study of the mechanism of acid transport through the protonated and alkylated membranes by determining activation enthalpies and entropies of diffusion of acid through the membranes and how these parameters relate to the structure of the water contained in the membranes as well as water mobility (Chapter 4).

CHAPTER TWO

PREPARATION, CHARACTERIZATION AND DIFFUSION DIALYSIS TESTING OF POLY(4-VINYLPYRIDINE)-FILLED MEMBRANES

This chapter is based on a paper that has been published in the Journal of Membrane Science [15]. The chapter integrates the contents of the published paper with some additional data and information.

The first step in this research was the fabrication and evaluation of a well defined set of poly(4-vinylpyridine) (PVP)-filled membranes. Some preliminary work had been done in the group of Dr. Childs on PVP membranes by Mike Kovacs and their diffusion dialysis performance was examined. However, very few membranes were studied and the individual effects of mass gain and degree of crosslinking on membrane properties and performance were not thoroughly investigated.

The chemistry of the copolymerization, introduction of charged sites, materials and apparatus used, membrane characterization and diffusion dialysis performance in acid recovery are discussed in this chapter.

2.1. Introduction

The anion exchange membranes discussed in this chapter were produced using a technique whereby the pores of a polypropylene microfiltration membrane were filled with a polyelectrolyte by UV-induced polymerization of 4-vinylpyridine (4VP) containing varying amounts of divinylbenzene (DVB) [68,82]. While the actual manner in which the polymer is bound to the polypropylene support has not been determined, it is firmly anchored in the pores of the support and cannot be removed by solvent extraction or acid/base conditioning.

Ionization of the incorporated poly(4-vinylpyridine) by protonation of the nitrogen atoms produces anion exchange membranes with high ion exchange capacities which have been shown to be particularly effective in low pressure water softening [83].

The goal of the work described in this chapter was to prepare pore-filled membranes using poly(4-vinylpyridine) crosslinked with divinylbenzene in order to examine the effects of mass loading and degree of cross linking of the pore filling polymer on the properties of the membranes, such as dimensional stability, water content, and ion exchange capacity and to examine the effectiveness of the membranes in the diffusion dialysis recovery of acid.

2.2. Chemistry of the Copolymerization of 4-Vinylpyridine and Divinylbenzene

A photochemically initiated free radical polymerization was used for the copolymerization of 4-vinylpyridine and divinylbenzene (DVB) [84,85]. The

photoinitiator used was 2,2-dimethoxy-2-phenylacetophenone (DMPA). The reaction is shown in Scheme 2.1. The initiator, DMPA, decomposes upon UV irradiation at 350 nm to form free radicals (In•) capable of initiating a polymerization reaction. 4-Vinylpyridine and DVB are subsequently copolymerized within the pores of a polypropylene microporous membrane, forming a crosslinked, three dimensional polymer network that is entangled within the microporous host membrane.

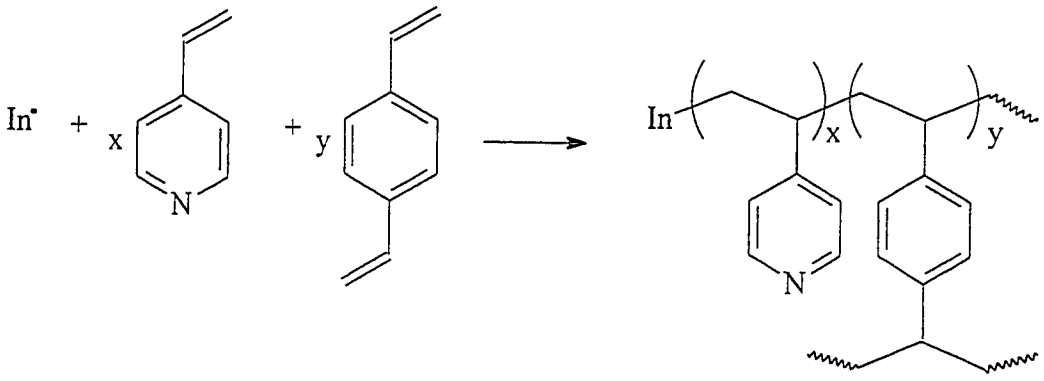

Scheme 2.1. Copolymerization of 4-Vinylpyridine and DVB

DMPA is a light sensitive compound that absorbs light in the ultraviolet range and undergoes fragmentation leading to the formation of radicals (In• in Scheme 2.1.) which subsequently initiate the copolymerization. DMPA undergoes α-cleavage to form a benzoyl and a benzoyl ketal radical which fragments further to form methylbenzoate and a methyl radical, Scheme 2.2. [86].

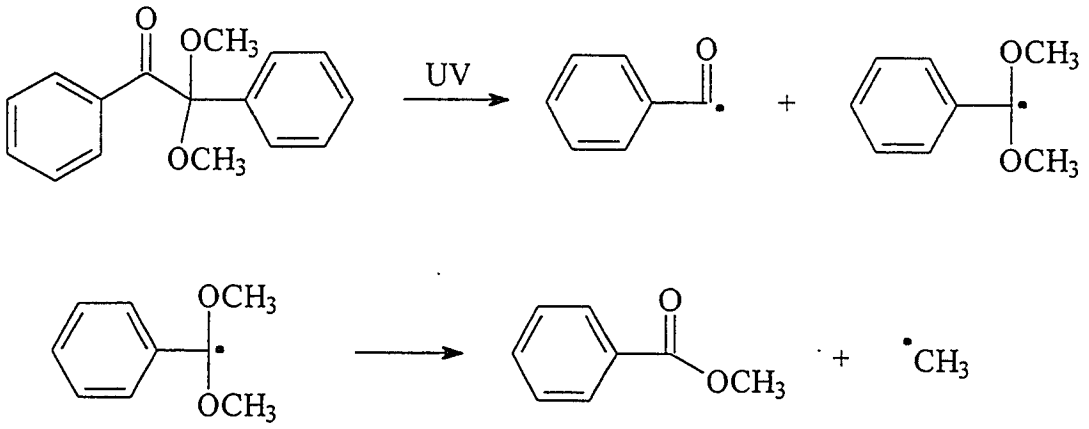

Scheme 2.2. UV Initiated Fragmentation of DMPA, Formation of Radicals

Usually only the benzoyl and methyl radicals shown in Scheme 2.2. are effective in initiating the polymerization reaction [86].

2.3. Introduction of Charged Sites on Poly(4-vinylpyridine) Chains

Poly(4-vinylpyridine) is a weak polybase and in basic solution the pyridine nitrogen atoms of the polymer are in free base form [68,70]. At lower pH values the pyridine nitrogen atoms are protonated to form the positively charged pyridinium form, Fig. 2.1.

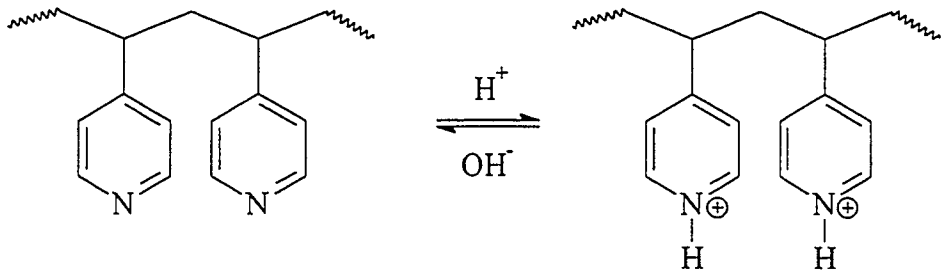

Fig. 2.1. Reversible Protonation of Poly(4-vinylpyridine)

The pK_a of poly(4-vinylpyridinium salt) in aqueous solution is a function of the degree of protonation and is reported to be in the range from 5.0, when the polymer is fully deprotonated, to approximately 3.7, when fully protonated [68]. The pK_a of poly(4-vinylpyridinium salt) anchored in a porous membrane with 50% of the pyridine groups in protonated form is reported to be 2.57 with HCl and 3.47 with H_2SO_4 [70].

Poly(4-vinylpyridine) in its free base form is fairly hydrophobic and not water soluble. Table 2.1. lists some solvents and nonsolvents for poly(4-vinylpyridine) [87].

Table 2.1. Solvents and Nonsolvents for Poly(4-vinylpyridine)

Soluble in:	Insoluble in:
Methanol	Petroleum Ether
Ethanol	Ether
2-Propanol	Butanone
tert-Butanol	Water
Chloroform	Benzene (swells PVP)
Pyridine	Toluene (swells PVP)

Poly(4-vinylpyridine) becomes water soluble in acidic solution when approximately 35% of the pyridine nitrogen atoms are protonated at pH 4.6 [70]. Copolymerization of poly(4-vinylpyridine) with a crosslinker, such as DVB which was used in this thesis, renders the polymer product insoluble in all solvents due to the formation of a macromolecular, three dimensionally crosslinked polymer. The product

can, however, be swollen by such solvents as those which solubilize non-crosslinked poly(4-vinylpyridine). Similarly, a crosslinked poly(4-vinylpyridine) polymer is swollen when contacted with an aqueous acid solution as the pyridine nitrogen atoms become protonated and water penetrates the now hydrophilic polymer. The swollen polymer can be referred to as a polymer gel.

2.4. Experimental

2.4.1. Materials

The substrate used in this study was a polypropylene (PP) microfiltration membrane with an average pore diameter of 0.26 μm, average thickness of 53 μm and porosity of approximately 60 vol% (data provided by the 3M Canada Company).

4-Vinylpyridine and divinylbenzene (approximately 55% meta and para isomers, 45% ethylvinylbenzene) (Aldrich) were purified by vacuum distillation to remove stabilizers prior to the copolymerization. 2,2-Dimethoxy-2-phenylacetophenone (Aldrich) was used as received as a photoinitiator. Methanol, hydrochloric acid, sodium chloride and magnesium chloride were reagent grade and used without further purification. Water used was carbon filtered and deionized using a Barnstead/Thermolyne system (organic removal cartridge D 8904 and deionization cartridge D 8901).

2.4.2. Experimental Procedure

The membranes were prepared by photoinitiated polymerization of 4-vinylpyridine with varying amounts of DVB in the pores of the PP substrate as described previously [68]. The nominal percent DVB content of the pore-filling electrolyte was taken as the weight ratio of DVB isomers to 4-vinylpyridine in the monomer mixture, therefore when preparing the mixture of poly(4-vinylpyridine) and DVB, the weight of the ethylvinylbenzene present in the DVB was accounted for by multiplying the required mass of DVB by 1.818 and then using that mass of DVB mixture in the copolymerization.

2.4.2.1. Pore-Filling Copolymerization of Poly(4-vinylpyridine) and Divinylbenzene

The *in-situ* polymerization of poly(4-vinylpyridine) and DVB was carried out using a procedure described previously [68] in a reaction vessel shown in Fig. 2.2. The polypropylene substrate was cut into rectangular pieces, 11.0 cm × 15.0 cm, soaked in acetone for approximately 18 h, air dried and weighed. The membrane was then placed on the inner wall of the reaction vessel (Fig. 2.2.).

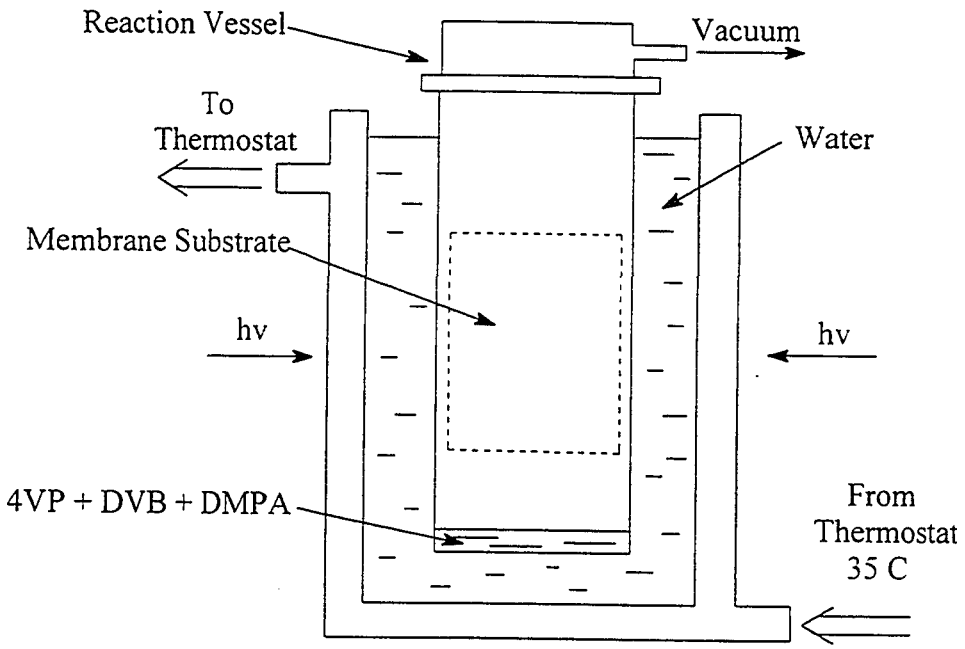

Fig. 2.2. Water Jacketed Cylindrical Photoreactor with Temperature Control, Vacuum and Uniform Light Exposure.

Approximately 2 g of a reaction mixture containing poly(4-vinylpyridine), DVB and DMPA was poured into the bottom of the reaction vessel. The vessel was capped and, together with its contents, was frozen in a dry ice-acetone bath. The vessel and its frozen contents was placed under vacuum for 0.5 h and then removed from vacuum and allowed to warm to room temperature. The reaction vessel was filled with nitrogen and the membrane was wetted evenly with the reaction mixture by rotating the vessel in a horizontal position.

The wetted membrane in the reaction vessel was then placed in the temperature controlled bath and irradiated in a Rayonet-type photoreactor equipped with 10 UV lamps at 350 nm for a given time (0.5 - 1.0 h).

2.4.2.2. Membrane Extraction and Mass Gain Determination

After polymerization, the reaction vessel was opened and filled with methanol to swell the pore-filled membrane and detach it from the wall of the vessel. The membrane was extracted with methanol (Soxhlet) to remove non-anchored polymers. The extraction was carried out until no change in mass of the dried membrane (dried in vacuum at room temperature for 1 - 2 h) was detected (usually 24 - 48 h).

The mass gain of the membrane was taken as the percent mass increase of the substrate, Eq. 2.1.:

$$\text{Mass gain} = \frac{m_d - m_o}{m_o} \times 100\ \% \qquad (2.1.)$$

where m_d was the mass of the pore-filled, extracted and dried membrane and m_o the mass of the nascent substrate prior to pore-filling. Reproducibility was within 2%.

2.4.2.3 ESEM Examination of Pore-Filled Membranes

The membrane samples were viewed in an ElectroScan model 2020 Environmental Scanning Electron Microscope (ESEM) (ElectroScan Corporation, Wilmington, MA). Membrane samples for ESEM examination were in their dry, free base form. Pieces of the membrane were cut and glued to an aluminum stub using an epoxy adhesive. Cross sections were obtained by gluing the sample on its edge and, after the glue had hardened, slicing with a razor to give a fairly clean cross section. Images were

obtained at pressures of 2.9 Torr to 3.6 Torr in an atmosphere of 99% water vapour at 20 kV. Magnifications were in the range of 950× to 1050×.

2.4.2.4. Ion Exchange Capacity (IEC)

The method for determining IEC has been described by Mika and coworkers [68]. The membrane was conditioned by alternating treatments with 1 M HCl and 1 M NaOH, and washed in between with water. This process was repeated three times. After the membrane was converted into its free base form by the final treatment with NaOH, the membrane was washed with water and placed in a dilute (~ 0.2 M) HCl solution of known volume and concentration for 24 h. The quantity of HCl solution used was so adjusted to contain approximately 50% more HCl than required for the theoretical IEC calculated from the sample mass gain.

The sample was removed from the solution and held above it while the membrane surface was rinsed with water. The residual solution was titrated with standard NaOH and the IEC was calculated from equation 2.2.:

$$\text{IEC (meq/g)} = \frac{V_{HCl}N_{HCl} - V_{NaOH}N_{NaOH}}{m_d} \times 1000 \qquad (2.2)$$

where V_{HCl} and V_{NaOH} were the volumes of the HCl and NaOH solutions and N_{HCl} and N_{NaOH} were the normalities of the HCl and NaOH solutions, respectively, and m_d was the mass of the pore-filled, extracted and dried membrane in its free base form. The IEC is thus expressed in units of milliequivalents of protonated nitrogen atoms per gram of dry,

free base membrane. This procedure was repeated twice for each membrane and the reproducibility was within 3%.

2.4.2.5. Water Content (Free Base and Protonated)

After the membrane was conditioned by alternating treatments with 1 M HCl and 1 M NaOH, the membrane was placed in its free base form by treatment with 1 M NaOH for 24 h. After rinsing with water, the membrane was placed between two sheets of damp filter paper, gently pressed to remove surface water and weighed. Water content in free base form (WC_f) was calculated by equation 2.3.:

$$WC_f(\%) = \frac{m_{wf} - m_d}{m_{wf}} \times 100\% \qquad (2.3.)$$

where m_{wf} was the mass of the water-swollen membrane in free base form and m_d was the mass of the dry membrane in free base form.

The water content in protonated form (WC_p) was calculated from equation 2.4. in a similar manner. The membrane was place in its protonated form by treatment with 1M HCl for 24 h, rinsed water, placed between two sheets of damp filter paper, gently pressed to remove surface water and weighed.

$$WC_p(\%) = \frac{m_{wp} - m_d - m_{HCl}}{m_{wp}} \times 100\% \qquad (2.4.)$$

where m_{wp} was the mass of the water-swollen membrane in protonated form, m_d was the mass of the dry membrane in free base form and m_{HCl} was the mass of HCl associated with the ion exchange sites, as determined from the IEC measurement.

2.4.2.6. Fixed Charge Concentration

The fixed charge concentration is the concentration of fixed charge sites (ion exchange sites) in the water contained in the membrane. It is expressed as equivalents of fixed charge sites per kilogram of water in the membrane and is calculated from equation 2.5. The fixed charge concentration is a function of both the IEC of the membrane and the membrane water content in protonated form.

$$\text{Fixed Charge Concentration (eq/kg)} = (\text{IEC} \times m_d)/(m_{wp} - m_d - m_{HCl}) \qquad (2.5.)$$

where IEC is the ion exchange capacity of the membrane and m_d is the mass of the dry free base membrane, therefore the numerator of equation 2.5. gives the total number of milliequivalents of fixed charge sites in the membrane. The total mass of water in the protonated membrane in grams is given by the denominator of equation 2.5. where m_{wp} was the mass of the water-swollen membrane in protonated form, m_d was the mass of the dry membrane in free base form and m_{HCl} was the mass of HCl associated with the ion exchange sites. The final units on the right hand side of equation 2.5. are milliequivalents per gram, which are equivalent to equivalents per kilogram.

2.4.2.7. Membrane Thickness (Free Base and Protonated)

The thickness of the membranes was measured using a calibrated pycnometer according to the following procedure. The sample of membrane to be measured was cut into a piece approximately 5 cm × 6 cm and equilibrated in the specific solution (1M NaOH for membranes in free base form and 1 M HCl for membranes in protonated form)

for 24 h. The pycnometer of known mass and volume was filled with the equilibrating solution and weighed. The membrane sample was then placed in the pycnometer filled with the equilibrating solution and weighed and then the membrane sample was placed between two pieces of damp filter paper, gently pressed to remove surface water and weighed. Finally, the length and width of the water swollen membrane sample was measured using a ruler with an accuracy of 0.5 mm. The thickness of the membrane in μm was calculated from equation 2.6.:

$$\text{Membrane Thickness } (\mu\text{m}) = \frac{(mass_{pyc} - mass_{tot} + mass_{mem})Vol_{pyc}}{(mass_{tot} - mass_{drypyc}) \times l \times w} \times 10{,}000 \qquad (2.6.)$$

where $mass_{pyc}$ is the mass of the pycnometer filled with the equilibrating solution in grams, $mass_{tot}$ is the mass of the pycnometer filled with the equilibrating solution and the membrane sample in grams, $mass_{mem}$ is the mass of the water swollen membrane in grams, Vol_{pyc} is the volume of the pycnometer in cm^3, $mass_{drypyc}$ is the mass of the empty, dry pycnometer in grams and l and w are the length and width of the membrane sample, respectively, in cm. The measurement was repeated twice for each membrane and the reproducibility was within 3%.

2.4.2.8. Elemental Analysis

The amounts of carbon, hydrogen and nitrogen in the pore-filled membranes were determined using a combustion method by QTI Laboratories (New Jersey, US). Membrane samples were converted to free base form by treatment with 1 M NaOH for 24

h, followed by thorough rinsing in water and a water soak for 24 h. The samples were then placed in methanol for 1 h to replace the water in the membrane and pumped dry under vacuum for 1 h. The samples were weighed, placed in plastic bottles and sent to QTI for C/H/N analysis.

2.4.2.9. Diffusion Dialysis Testing

Diffusion dialysis experiments were carried out using a cell, Fig.2.3., constructed from Lucite that consisted of two chambers of equal volume separated by the membrane with an active area of 3.14 cm^2.

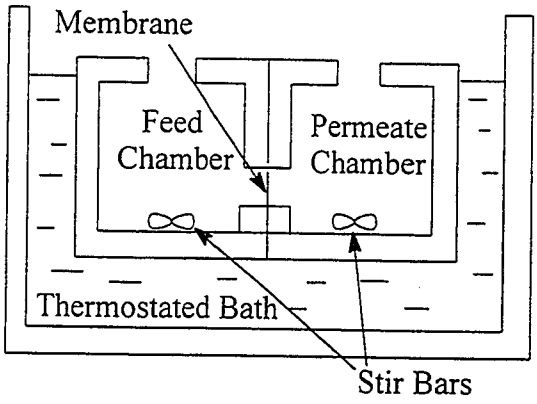

Fig. 2.3. Diffusion Dialysis Cell in Thermostat Bath

Simultaneously, the feed chamber was filled with 25 mL of a solution of 1.0 M HCl, 0.5 M NaCl and 0.5 M $MgCl_2$ and the permeate chamber with 25 mL of deionized water. The thermostated bath was maintained at 25°C. Both chambers were stirred at identical rates of 25 revolutions per second in order to minimize concentration polarization effects. (The minimization of concentration polarization was confirmed by

performing a series of acid diffusion dialysis experiments with increasing stirring speeds and determining the speed at which the dialysis coefficient reached a maximum.) Diffusion was allowed to occur for a measured time and then the solutions were removed from each side of the cell and analyzed for acid and salt composition. Acid concentration was determined by titration with standard NaOH. The Na^+ and Mg^{2+} concentrations were measured by ion exchange chromatography (Dionex, DX 100). Water transport that occurred by osmosis from the permeate side to the feed side during the experiment was calculated from the mass balance of the acid using equation 2.7.:

$$V_{H2O} = (C_{f0}V_{f0} - C_{pt}V_{p0} - C_{ft}V_{f0})/(C_{ft} - C_{pt}) \qquad (2.7.)$$

where V_{H2O} is the volume in mL of water transported from the permeate side to the feed side during the experiment, C_{f0} is the concentration of acid in the feed solution at time zero, V_{f0} is the volume in mL of the feed solution at time zero, C_{pt} is the concentration of acid in the permeate solution at time t, V_{p0} is the volume in mL of the permeate solution at time zero and C_{ft} is the concentration of acid in the feed solution at time t.

The dialysis coefficient, U (Equation 2.8.), of the membrane for each component was given by the amount of the component that was transported per unit active membrane area, per unit time and per unit concentration difference of the component:

$$\text{Dialysis Coefficient (U)} = W/A \bullet t \bullet \Delta C \qquad (2.8.)$$

where W was the amount of the component transported in moles, A was the active membrane area in square metres, t = was the time in hours and ΔC was the mean logarithm concentration difference of the component in mol/l, given by Equation 2.9.

$$\Delta C = (C_{f0} - C_{ft} + C_{pt})/\ln[C_{f0}/(C_{ft} - C_{pt})] \quad (2.9.)$$

where C_{f0} was the concentration of the feed solution at time zero, C_{pt} was the concentration of the permeate solution at time t and C_{ft} was the concentration of the feed solution at time t [88]. The reproducibility for the permeability measurement was less than ±4% for repeated measurements with a single sample of membrane and less than ±10% for different sections of the same membrane. The selectivity of the membrane with respect to one species over another is given as the ratio of the permeabilities of the two species.

2.5. Results and Discussion

Two series of membranes were prepared by absorbing a mixture of 4-vinylpyridine and DVB into the pores of a polypropylene microporous substrate and initiating polymerization by irradiation at 350 nm. The first series was comprised of membranes in which the mass loading was varied while the crosslinking was held constant. The membranes of the second series had similar mass loadings and the crosslinking was varied. The membranes had mass increases ranging from 47% to 210% and DVB contents ranging from 0.54% to 44.1%. The membranes with low mass gains were white in colour, similar to the nascent membrane, while the higher mass gain membranes were translucent with a slight yellowish colour and became brittle when dry. The high mass gain, high DVB content membranes are also somewhat brittle, even when swollen with water.

2.5.1. Characterisation of Membranes

2.5.1.1. Series One: Varying Mass Gain, Constant DVB Content

The first series of membranes was prepared to examine the effects of mass loading on membrane properties while holding the degree of crosslinking constant. The series of membranes was produced using a mixture of 4-vinylpyridine containing 4% by weight DVB. The resulting membranes had mass increases varying from 47% to 210%. Characteristics of these membranes are presented in Table 2.2. and discussed below.

Table 2.2. Series One: Properties of Membranes

Membrane	Mass Gain (%)	DVB (%)	Thickness Free Base (μm)	Thickness Protonated (μm)	IEC (meq/g)	Water Uptake (Free Base) (%)	Water Uptake (Protonated)[1] (%)	Waters per[2] ion exchange site	Fixed Charge Conc. (eq/kg)[3]
407	47	4.1	60	68	2.2	52	61	43	1.3
408	52	4.1	56	71	2.4	52	64	45	1.3
412	172	4.1	65	96	4.8	31	56	17	3.3
426	191	4.1	63	99	4.4	33	54	17	3.2
420	203	4.0	68	101	4.8	27	59	19	2.9
421	210	4.1	68	106	4.4	27	54	18	3.2

[1] Corrected for mass of HCl
[2] Calculated on the basis of total water content of the membranes in protonated form.
[3] Fixed Charge Concentration as equivalents of determined nitrogen per kg of water in the membrane in protonated form.

2.5.1.1.1. Mass Increase

The maximum mass gain was calculated for the substrate used based upon its porosity of approximately 60 %. Complete filling of the pores of the substrate with the 4-vinylpyridine/DVB copolymer would result in a maximum calculated mass gain of approximately 200%, assuming no significant change occurred in the structure of the polypropylene substrate during the polymerization. The observed mass gains range up to 210%, in close agreement to the calculated maximum mass gain.

There was some difficulty varying the mass gains using the photoinitiated procedure. Mass gains were either quite low (less than 50%) when short irradiation times were used, or near the maximum value of 200% when longer irradiation times were used. The lower mass gain membranes were produced using irradiation times of 0.5 h and the higher mass gain membranes using times of 1 h, hence there was a rough correlation between mass gain and irradiation time. Attempts to produce a membrane with a mass gain of ~100% were unsuccessful.

2.5.1.1.2. Membrane Thickness

The thicknesses of the membranes were measured in both protonated and free base forms. The results are shown in Table 2.2. As can be seen, the thicknesses of the membranes increased with increasing mass gain in both the free base and the protonated forms. At the highest mass gain, the increase in thickness in the free base form is 21% above the thickness of the nascent membrane. Such a thickness increase has previously

been shown to be caused by stretching of the porous substrate induced by swelling of the poly(4-vinylpyridine) with methanol during the extraction step involved in the preparation of the membranes [69]. Some interpenetration of the incorporated polymer into the base substrate is thought to occur, leading to swelling of the membranes after the polymerization.

Small changes were observed in the length and width of the membranes compared to the initial dimensions. For example, the membranes width increased by approximately 3% and the membranes length increased by approximately 2% after pore filling in free base form.

Protonation of the membranes with 1.0 M HCl further increases the thicknesses of the membranes relative to the free base form with a maximum thickness increase of 89% for the membrane with the highest mass gain. As reported in earlier papers in this series, the thickness change from the free base to the protonated form is fully reversible [68,69]. The lengths and widths of the membranes both increased by approximately 5% in protonated form. While the crosslinking provided by the DVB will restrict conformational changes in the pore-filling polymer, hydration of the protonated polymer will occur, resulting in additional swelling due to the osmotic pressure in the membrane.

2.5.1.1.3. Water Uptake (Free Base and Protonated Forms)

The membranes in free base form exhibit only a moderate thickness increase with increasing mass gain. As a result there is a steady decrease in the percent water uptake of

the membranes from 52% to 27%, Table 2.2, with increasing incorporation of poly(4-vinylpyridine) into the pores. In the protonated forms of the membranes, there is a substantial increase in thickness that occurs as a function of mass gain. It is interesting that the total percent water content of the membranes remains fairly constant, in the range of 54% to 64%, regardless of mass loading when the membranes are in their protonated form.

2.5.1.1.4. Fixed Charge Concentration

The concentration of fixed charge sites with the various graft yields is shown in Table 2.2. The fixed charge concentration is given in equivalents of nitrogen per kilogram of water in the protonated membrane rather than total membrane volume since the ions travel only through the aqueous phase and not the base substrate. Thus, while the weight percent water uptake of the series of membranes in their protonated form is fairly constant, it can be seen from Table 2.2 that the effective fixed charge concentration increases as the mass gain increases from 52% to 172%. The percent water uptake is a ratio of the mass of water in the membrane to the total mass of the membrane and as the fraction of poly(4-vinylpyridine) in the membrane increases with mass gains from 52% to 172% the result is an increased concentration of the ion exchange sites in the membrane water. At high mass gains the fixed charge concentration reaches a limiting value as the membrane thickness increases with mass gain and water content remains constant.

The number of waters per ion exchange site shown in Table 2.2 refers to the number of water molecules per fixed charge site in the membrane. This number is derived by simply dividing the molality of pure water by the fixed charge concentration, giving a ratio of water molecules to ion exchange site. The significance of this parameter becomes apparent in the discussion of the diffusion dialysis results, later in this chapter.

2.5.1.1.5. Ion Exchange Capacity (IEC)

The IECs of the membranes is also given in Table 2.2. Although the IEC gives an indication of the number of ion exchange groups per gram of membrane, it is with reference to the membrane in its dried state. This parameter is not very useful, however, for predicting membrane behaviour or for comparison between different membranes because the dried state is not the state in which membranes function. Membranes work and perform separations when water swollen, therefore it is more useful to characterize membranes in the state that they are found when functioning.

A membrane with a relatively high IEC may absorb a large amount of water when brought into contact with the working solution, resulting in a fairly low fixed charge concentration. Another membrane with a lower IEC but also a lower water uptake may have a higher fixed charge concentration under operating conditions. Therefore, considering only the IECs of the two membranes might result in the incorrect prediction of performance or the erroneous analysis of results if the two membranes are compared to one another.

For these reasons most of the interpretation of the data in this thesis is done in terms of fixed charge concentration and not IEC. The parameter of IEC is still used in the literature, however, so these values are given in Table 2.2 in keeping with tradition. As can be seen in Table 2.2, the IECs do correlate with fixed charge concentration. This is due to the membranes having similar chemical composition, therefore one might expect that an increase in mass gain would result in an increase in IEC.

The IECs listed in Table 2.2 are the experimental values determined by titration as described in the experimental section. In all cases, the experimental IEC was approximately 80% of the theoretical IEC calculated based on the measured mass gain. This is a common effect found with polyelectrolytes and thus is one manifestation of the polyelectrolyte effect [89]. As the polymer chain becomes protonated and acquires a positive charge it becomes more difficult to introduce more positive charges close to one another along the polyelectrolyte due to electrostatic repulsion, resulting in a limit to the degree of protonation of less than 100%. This effect has been observed by Mika and coworkers [68,70] with pore-filled membranes and is further enhanced by the confinement of the polyelectrolyte within the membrane pores.

2.5.1.2. Series Two: Similar Mass Gain, Varying DVB Content

A second series of membranes were prepared in which the mass gain was held approximately constant but the amount of DVB was varied from 0.5% to 44%. The characteristics of the membranes studied are listed in Table 2.3. All membranes were

irradiated for 1h to achieve the maximum mass gain. At the end of the polymerization the residual monomer solution in the reaction vessel was polymerized into a solid, indicating that the polymerization had gone to completion. It was assumed that all of the DVB incorporated into the pore-filling polymer was in the form of crosslinks.

The mass gain of the membranes was found to be somewhat dependent on DVB content. As can be seen in Table 2.3, the mass gain increased from 147% to 201% as the DVB content increased from 0.54 % to 15.4%. Above 15.4% DVB content the mass gain leveled off at approximately 200%. Mika and coworkers found that mass gains increased substantially with increased crosslinking for poly(4-vinylpyridine)-filled membranes crosslinked with DVB, ranging from 125% at 0.3% DVB to 210% at 3% DVB [82]. Jiang found a strong dependence of mass gain on degree of crosslinking when producing pore-filled membranes using styrene crosslinked with DVB [90]. The effect was much more pronounced with mass gains increasing from 150% to 600% as the DVB content increased from 1.0% to 4.0%. Such increases in mass gain are typically found with the introduction of crosslinkers [91].

2.5.1.2.1. Membrane Thickness

The membrane thickness was determined as a function of the concentration of DVB used in the polymerization. As can be seen from the data in Figure 2.4, the membrane thicknesses decreased with increasing DVB content for both the free base and

Table 2.3. Series Two: Properties of Membranes

Membrane	Mass Gain (%)	DVB (%)	Thickness Free Base (μm)	Thickness Protonated (μm)	IEC (meq/g)	Water Uptake (Free Base) (%)	Water Uptake (Protonated)[1] (%)	Waters per[2] ion exchange site	Fixed Charge Conc. (eq/kg)[3]
422	147	0.54	79	131	4.5	45	64	26	2.2
406	157	1.3	67	107	4.4	48	60	22	2.5
415	173	2.5	78	120	4.7	39	59	20	2.8
412	172	4.1	65	96	4.8	31	56	17	3.3
417	182	6.1	67	94	4.3	27	51	16	3.6
428	181	8.3	69	96	4.0	23	50	16	3.5
431	201	15.4	69	88	3.8	18	42	12	4.5
432	208	24.8	56	71	3.5	15	37	10	5.3
PV19	193	44.1	58	67	3.0	18	30	9	6.4

[1] Corrected for mass of HCl
[2] Calculated on the basis of total water content of the membranes in protonated form.
[3] Fixed Charge Concentration as equivalents of determined nitrogen per kg of water in the membrane in protonated form.

the protonated forms. The scatter at lower DVB content is most likely caused by the variation in graft yields in this region of the membrane series. The increase in crosslinking will restrict the swellability of the polyelectrolyte resulting in a reduction in membrane thickness. In fact, the membranes having 25 and 40% DVB had free base thicknesses of 56 and 58 μm, identical, within error, to the nascent membrane thickness, indicating that no membrane swelling occurred during the steps involved in introducing the crosslinked poly(4-vinylpyridine).

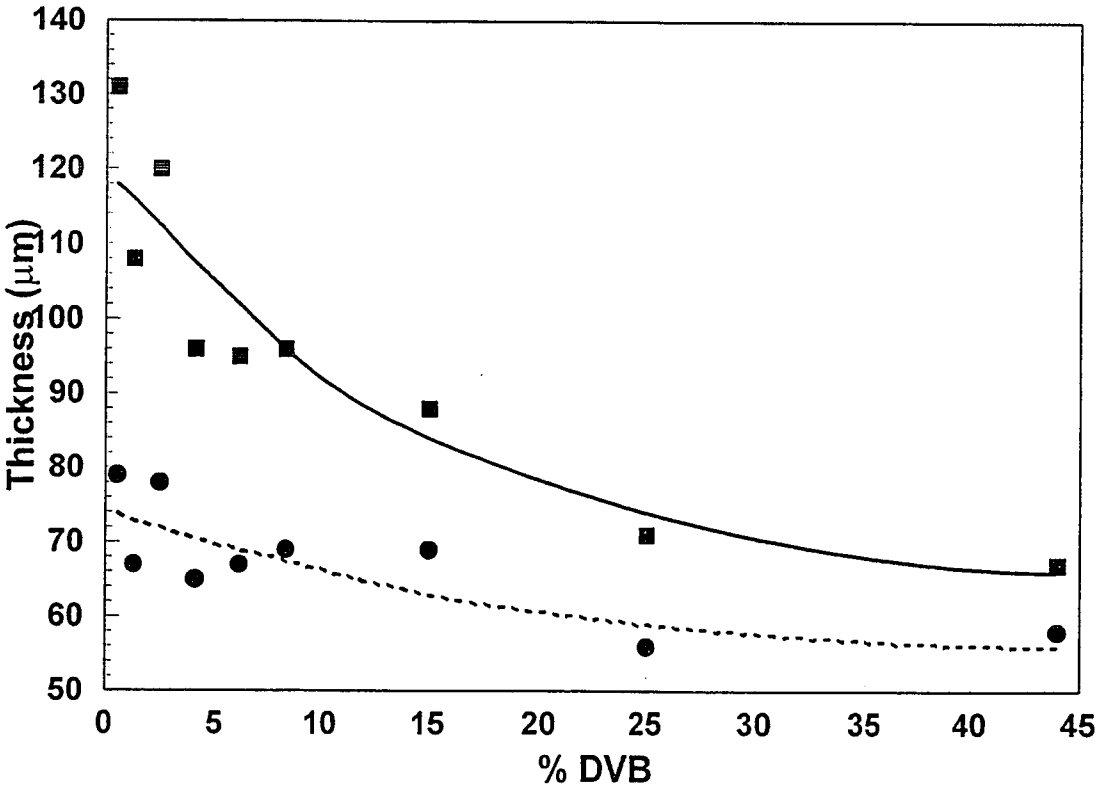

Fig. 2.4. Membrane Thickness versus Percent DVB Crosslinker - Protonated Form: Solid Line, Free Base Form: Broken Line

2.5.1.2.2. Water Uptake (Free Base and Protonated Forms)

A pronounced decrease in water uptake by the membranes in free base form was observed with increasing DVB content, Table 2.3. Unlike series one, however, there was also a dramatic decrease in water uptake by the membranes in protonated form. Water uptake dropped from 64% to 30% over the series of membranes in their protonated form. A decrease in membrane water uptake with increasing crosslinking is entirely expected and numerous examples exist in the literature [2,85].

For series one there was an increase in membrane thickness with mass loading, leading to a fairly constant water uptake for the membranes in protonated form but for series two the membrane thickness decreased while mass loading was held constant due to the increased crosslinking. This led to a decrease in membrane volume with no change in mass loading thus decreasing the membrane water content.

2.5.1.2.3. Fixed Charge Concentration

The result of the decreasing water content with increasing DVB content at constant mass loading is an increase in fixed charge concentration. As can be seen from the data summarized in Table 2.3 and shown in Fig. 2.5, the fixed charge concentration increased from 2.2 eq/kg at one half percent DVB content to 6.4 eq/kg at 44 percent DVB content.

2.5.1.2.4. Ion Exchange Capacity

The IECs of the membranes in series two showed an overall decrease with increasing DVB content, Table 2.3. This decrease is caused by a reduction in the relative amount of 4-vinylpyridine incorporated into the membranes compared to DVB. At constant mass loading, the increase in DVB content leads to a comparable decrease in 4-vinylpyridine content, thus sacrificing ion exchange groups. The small increase in IEC seen over the first four membranes in series two is caused by a small increase in mass gain over these four membranes. Following this small rise in IEC, the IECs fall over the rest of the series as the mass gain is more constant. Again, the measured IECs were approximately 80% of the total theoretical IECs, based on mass gain.

This is an example how misleading IECs can be in terms of predicting membrane fixed charge concentration and performance, as was mentioned in section 2.5.1.1.5. Even though there was a significant drop in membrane IECs with increasing DVB content, there was a dramatic increase in fixed charge concentration as a result of the markedly lower water content.

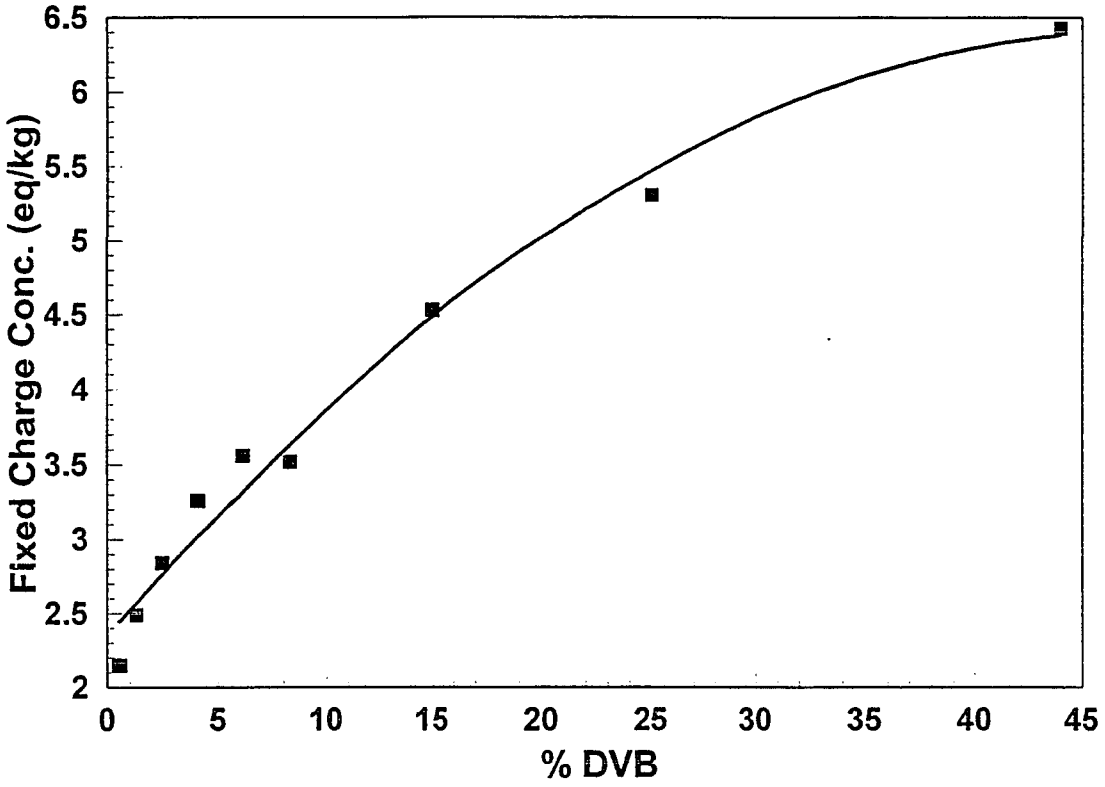

Fig. 2.5. Fixed Charge Concentration versus Percent DVB Crosslinker

2.5.1.2.5. ESEM Analysis

ESEM was used to help determine the structure of the pore-filled membranes and the location of the pore-filling polymer. ESEM pictures of the cross sections and surfaces of the nascent polypropylene membrane, membrane 422 in dry, free base form (147% mass gain, 0.54% DVB) and membrane PV19 in dry, free base form (193% mass gain, 44.1% DVB) are shown in Figs. 2.6, 2.7 and 2.8 respectively.

As can be seen by comparison of Fig. 2.6, the nascent membrane, with Figs. 2.7 and 2.8, the pore-filled membranes, both the surface and the cross section of the

membrane is altered by the pore-filling. The pore-filled membranes are no longer visibly porous. The pores on the surfaces of the membranes have been filled by the incorporated polymer and the fibrils visible in the cross section of the nascent membrane are no longer visible in the ESEM pictures of the cross sections of the pore-filled membranes. The composition of the pore-filled membranes appears uniform throughout the whole thickness of the membrane and there is no apparent surface layer. These observations are consistent with those of Mika and coworkers [68] who observed the SEM images of poly(4-vinylpyridine)-filled membranes.

(A)

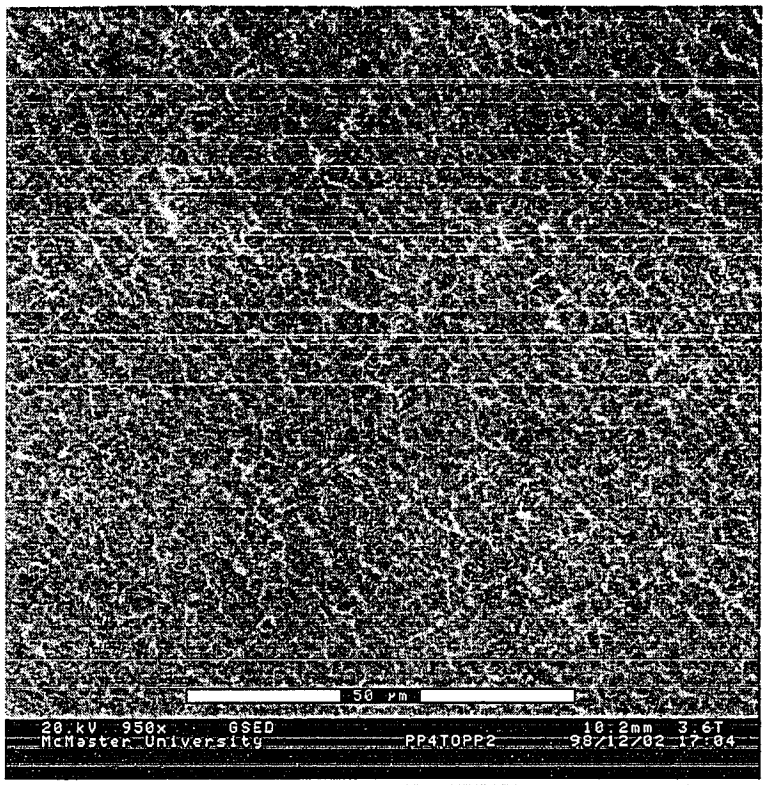

(B)

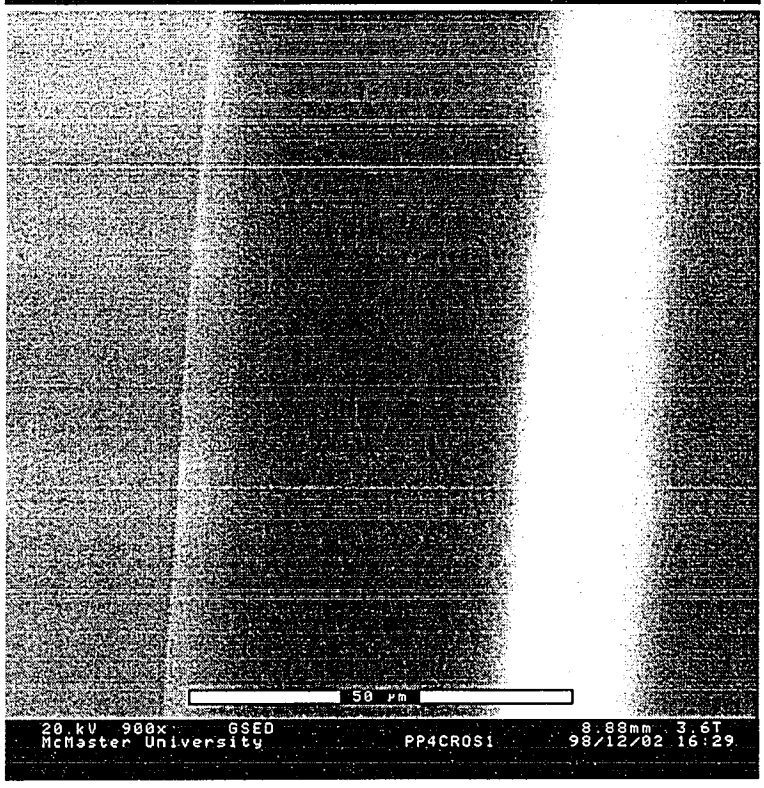

Fig. 2.6. ESEM Images of the Nascent Polypropylene Membrane
(A) Surface and (B) Cross Section

(A)

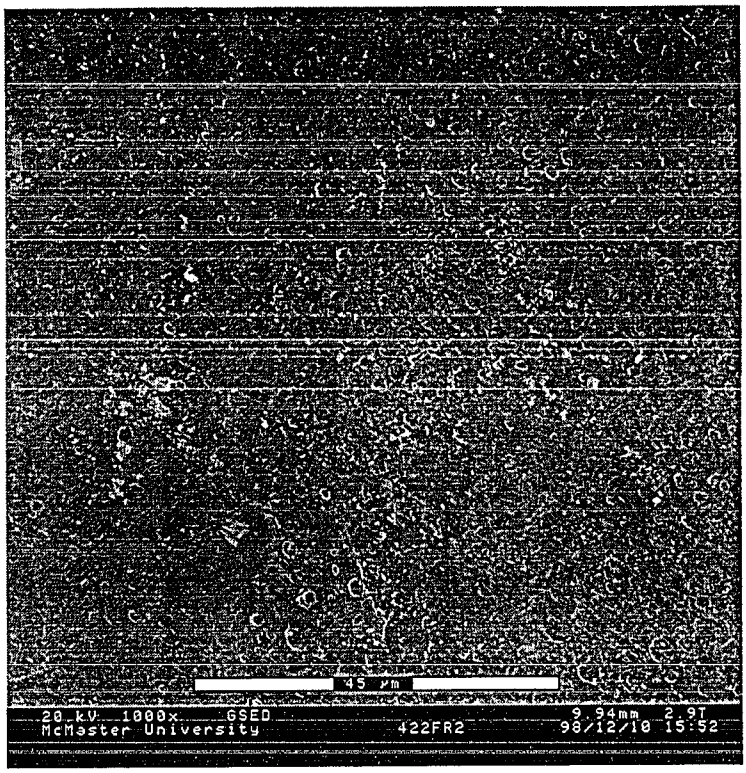

(B)

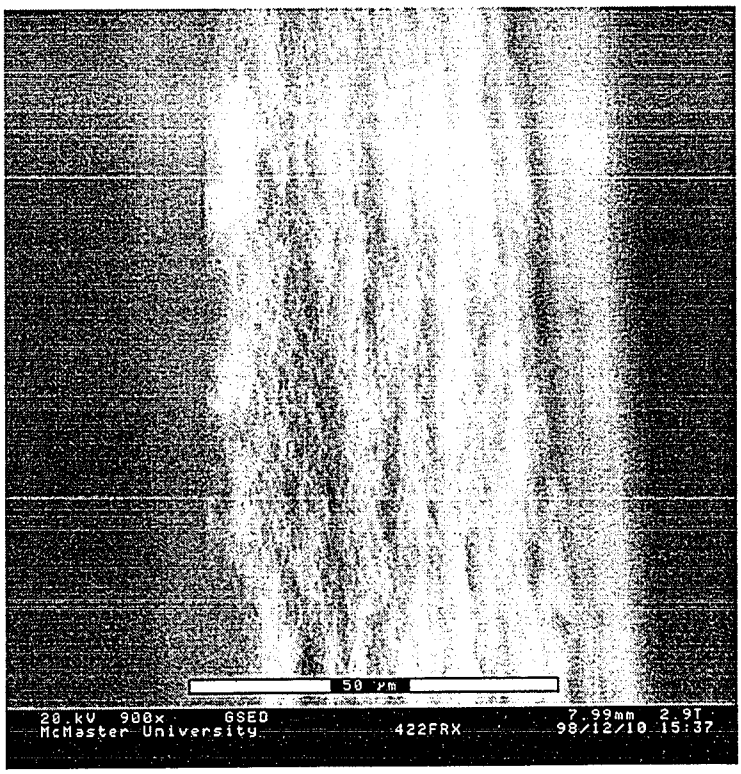

Fig. 2.7. ESEM Images of Membrane 422:
(A) Surface and (B) Cross Section

(A)

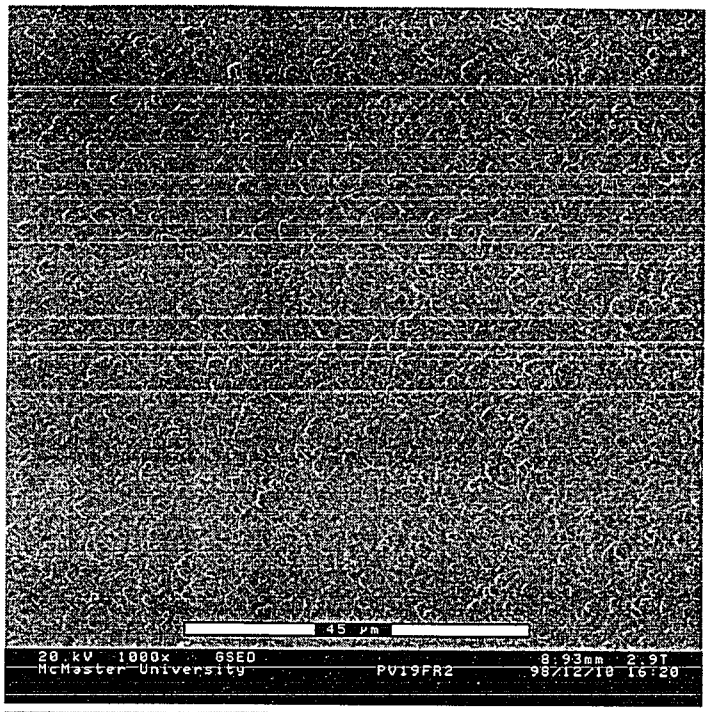

(B)

Fig. 2.8. ESEM Images of Membrane PV19:
(A) Surface and (B) Cross Section

2.5.1.2.6. Elemental Analysis

The percent DVB content assigned to the membranes studied in this thesis was assumed to be the same as the percent DVB that was present in the initial monomer mixture used for the fabrication of each membrane. Although this was considered to be a reasonable assumption, and is supported by the literature [2], confirmation of the assumption was undertaken by performing elemental analysis on a selected number of poly(4-vinylpyridine)-filled membranes.

Three samples of membranes with higher degrees of crosslinking were chosen from series two and analyzed for carbon, hydrogen and nitrogen. It was necessary to use membranes with high DVB content because the error involved in elemental analysis (~3%) needed to be significantly less than the percent DVB content. With knowledge of the mass gain of the membranes it was possible to calculate the theoretical amount of nitrogen that should be present in the membrane samples if the incorporated polymer had the same composition as the monomer feed mixture.

Membranes 431, 432 and PV19, with percent DVB contents of 15.4, 24.8 and 44.1, respectively, were put in their free base form, dried and submitted for elemental analysis. The results are shown in Table 2.4. As is shown in the last column of Table 2.4, the total percent composition based on carbon, hydrogen and nitrogen falls approximately 5% short of the expected 100%. Since the only components of the pore-filled membrane in free base form are these three elements, the missing 5% needed to be accounted for.

Table 2.4. Elemental Analysis Results

Membrane	% Carbon	% Hydrogen	% Nitrogen	Total %
431	79.3	9.2	6.1	94.6
432	81.4	9.5	5.4	96.3
PV19	81.7	9.3	4.6	95.6

Poly(4-vinylpyridine) is a rather hydrophobic polymer in free base form. It does, however, have a significant, though small, water solubility. Since the membrane samples submitted for elemental analysis were stored under ambient conditions, they may have absorbed a small amount of moisture from the room air. No drying instructions were given to the company performing the elemental analysis so one may assume that any water absorbed by the samples was still present prior to the analysis. As a result, the 5% missing from the total mass could have been accounted for as oxygen present as water.

With the assumption that some water was present in the samples during analysis, the results were recalculated to remove the water component. As well as removing the oxygen present as water, an appropriate amount of hydrogen was removed with the oxygen in a 2:1 molar ratio. The recalculated elemental analysis results are shown in Table 2.5, corrected for water content.

Table 2.5. Elemental Analysis Results: Corrected for Water Content

Membrane	Carbon (%)	Hydrogen (%)	Nitrogen (%)	Total (%)	Calculated Nitrogen (%)	Expt'l N / Calculated N
431	84.4	9.1	6.5	100	6.9	0.94
432	84.9	9.5	5.6	100	6.2	0.90
PV19	85.9	9.2	4.9	100	4.8	1.02

After removing the water from the elemental analysis results, the final column of Table 2.5 shows the ratio of the experimentally determined nitrogen content to the calculated nitrogen content based upon the mass gain of the membrane. The differences between the calculated and experimentally determined nitrogen contents range from +2% to -10%. This indicates that assuming that the incorporated polymer is of the same composition as the initial monomer feed is fairly good.

2.5.2. Diffusion Dialysis Testing

Diffusion dialysis testing of the membranes was carried out using solutions of HCl containing sodium and magnesium chlorides. Dialysis coefficients of the acid and each salt were calculated based on changes in concentration in both compartments of a dialysis cell. Since the nascent membrane is hydrophobic, it was pre-wetted with methanol and then solvent exchanged with the diffusion dialysis test solution before testing.

It must be noted at this point that the dialysis coefficients obtained from these diffusion dialysis experiments are, strictly speaking, apparent dialysis coefficients. This is because the feed solution used was a mixture of an acid and two salts. The presence of the acid influences the salt dialysis coefficients and vice versa, therefore the dialysis coefficients are only true with respect to this particular feed solution composition.

Confirmation that the effects of concentration polarization due to inadequate stirring were minimized was obtained by performing a series of diffusion dialysis experiments at various stirrer speeds. The results were obtained by measuring the acid dialysis coefficient of a representative membrane as a function of stirrer speed, the results are shown in Fig. 2.9.

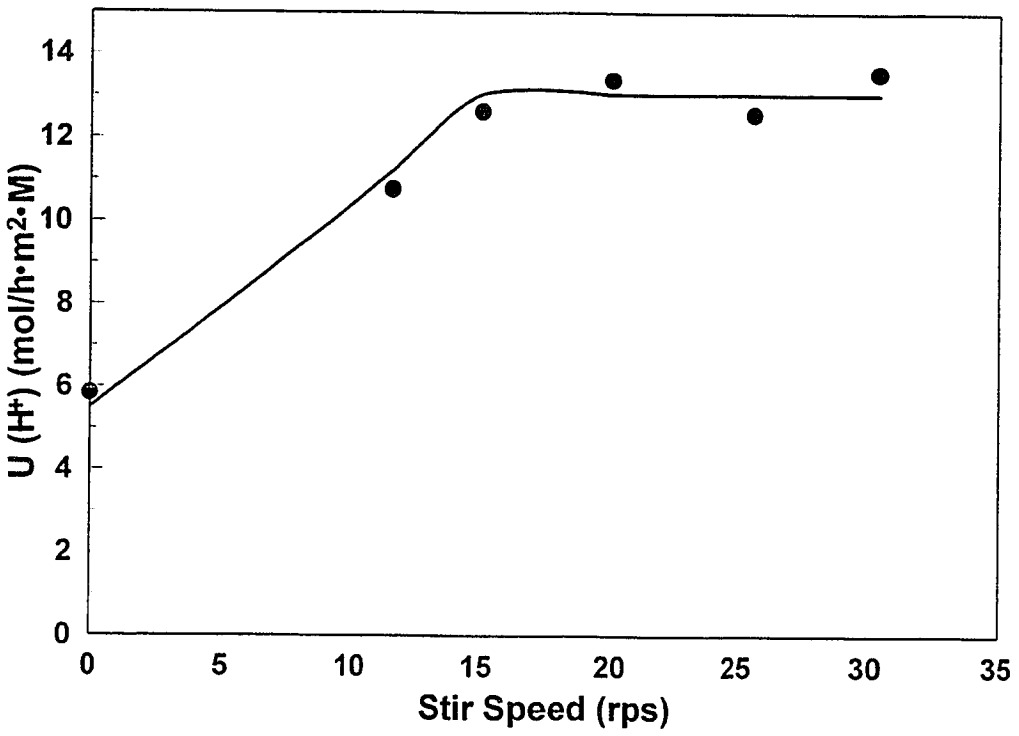

Fig. 2.9. Acid Dialysis Coefficient vs Stir Speed

As can be seen in Fig. 2.9, an increase in stirring speed from zero revolutions per second (rps) to 15 rps resulted in an increase in acid dialysis coefficient from 5.8 mol/h•m^2•M to 12.6 mol/h•m^2•M. Increasing the stir speed above 15 rps resulted in a fairly constant acid dialysis coefficient of approximately 13 mol/h•m^2•M, indicating that the stirring efficiency was at a maximum. Based on the results shown in Fig. 2.9, a stirring speed of 25 rps was chosen for all diffusion dialysis experiments to ensure optimum mixing of the solutions.

2.5.2.1. Effect of Mass Gain on Dialysis Coefficient and Selectivity, Series One

The results of testing of the first membrane series are shown in Table 2.6, an investigation into the effects of varying mass gain with constant DVB content on diffusion dialysis performance. The nascent, ungrafted polypropylene substrate when tested in the diffusion dialysis cell, had selectivities of 5.3 and 9.8 for the permeability of HCl over NaCl and $MgCl_2$, respectively. These selectivities arise from the different diffusion coefficients of proton, sodium ion and magnesium ion. The diffusion coefficients of these ions in water at 25°C at infinite dilution are [35]: $D_{H+} = 9.31 \times 10^{-9}$ $m^2\ s^{-1}$, $D_{Na+} = 1.33 \times 10^{-9}\ m^2\ s^{-1}$ and $D_{Mg2+} = 0.71 \times 10^{-9}\ m^2\ s^{-1}$ giving ratios of diffusion coefficients of: $D_{H+}/D_{Na+} = 7.0$ and $D_{H+}/ D_{Mg2+} = 13.1$. As would be expected, the estimated ratios are in good agreement with the values observed here with the nascent polypropylene membrane.

Table 2.6. Dialysis Coefficients and Selectivities With Varying Mass Gain

Membrane	Mass Gain (%)	Acid Dialysis Coefficient (U)[1]	NaCl Dialysis Coefficient (U)	$MgCl_2$ Dialysis Coefficient (U)	Selectivity (U HCl) / (U NaCl)	Selectivity (U HCl) / (U $MgCl_2$)
nascent	0	39 ± 3	7.4 ± 0.2	4.0 ± 0.1	5.3 ± 0.2	9.8 ± 0.2
407	47	46 ± 1	7.4 ± 0.2	3.8 ± 0.1	6.2 ± 0.4	12.1 ± 0.7
408	52	46 ± 2	7.1 ± 0.2	3.8 ± 0.1	6.5 ± 0.2	12.1 ± 0.4
412	172	34 ± 2	2.7 ± 0.1	0.65 ± 0.05	12.6 ± 0.5	52 ± 3
426	191	37 ± 1	2.7 ± 0.1	0.82 ± 0.05	13.7 ± 0.2	45 ± 1
420	203	37 ± 1	2.9 ± 0.1	0.89 ± 0.05	12.8 ± 0.4	42 ± 1
421	210	37 ± 1	2.9 ± 0.1	0.91 ± 0.05	12.8 ± 0.2	41 ± 1

[1] $U = mol/hr \cdot m^2 \cdot \Delta C$

The acid dialysis coefficients of the membranes in Series 1, Table 2.6, with the lower mass gains are larger than for the nascent membrane. The dialysis coefficients of sodium and magnesium chlorides remain fairly constant in the low mass gain membranes and similar to those found with the nascent membrane. Membranes with mass gains in the range of 170% to 200% have similar acid dialysis coefficients to that of the nascent membrane while the dialysis coefficients of sodium and magnesium chlorides decrease.

The increase in the acid dialysis coefficient at low mass gain, as compared to that of the nascent membrane, could possibly be a result of facilitated transport of protons by the nitrogen atoms of the pyridine rings. This results in an increase in selectivity of acid over sodium and magnesium chlorides for the low mass gain membranes even though the dialysis coefficients of the metal chlorides remain similar to those found for the nascent membrane. It should be noted that the dialysis coefficients have not been corrected for the increase in thickness that occurs with the pore-filled membranes. This correction would have the effect of further increasing the dialysis coefficients of all species through the thicker pore-filled membranes, therefore the lower mass gain membranes would show an even greater increase in the acid dialysis coefficient compared to the nascent membrane. The selectivity of acid over salts, however, would not change with a correction for membrane thickness because the dialysis coefficients of all species change proportionately.

As the mass gain associated with incorporated poly(4-vinylpyridine) increased to about 170%, the HCl dialysis coefficient decreases and levels off to a similar value as that

of the nascent membrane. However, a correction for the increase in membrane thickness with increasing mass gain would result in similar acid dialysis coefficients for all of the six membranes in this series. It should be noted that the water uptake of the pore-filled membranes in protonated form is relatively constant for this series of membranes, Table 2.2. The result that the membranes have similar water contents and similar acid dialysis coefficients, when corrected for membrane thickness, indicates the possibility that membrane water content may be a controlling factor in determining acid permeability. The results discussed in the following chapters continue the investigation into this relationship.

The fixed charge concentration increases with mass gain leading to more efficient Donnan exclusion of co-ions. This is evident in the decrease of the dialysis coefficients of NaCl and $MgCl_2$ compared to that of HCl. The net result is that the selectivity of HCl over sodium and magnesium chlorides increases with increasing fixed charge concentration as the permeability of the two metal ions is markedly reduced as the fixed charge concentration is increased. Divalent magnesium cations are expected to be excluded from the membrane more efficiently than monovalent cations due to Coulombic repulsion with the membrane fixed positive charges.

The fixed charge concentration reaches a maximum of 3.3 eq/kg at a mass gain of 172% and then plateaus. The acid dialysis coefficient decreased somewhat with increasing mass gain, however the selectivities of acid over sodium and magnesium chlorides were much greater for the high mass gain membranes as the fixed charge

concentration within the membranes reduced the permeability of sodium and magnesium ions relative to protons.

By comparing the data in Tables 2.2 and 2.6, it is apparent with the solutions used in these tests that fixed charge concentrations within the membrane must approach approximately 3 eq/kg to achieve any significant selectivity in terms of HCl dialysis coefficient relative to NaCl and $MgCl_2$ dialysis coefficients. This is not surprising if one looks at the fixed charge concentration relative to the ionic concentration of the diffusing solution. The cation concentration in the feed solution, being the sum of proton, sodium and magnesium ion concentrations, was approximately 2.5 M. The Donnan potential of the membrane, which acts to exclude co-ions from the membrane, is greater with dilute than with concentrated solutions [33,88]. If the concentration in the external solution is higher than the membrane fixed ion concentration, the membrane acts as if it were neutral and no Donnan exclusion of co-ions takes place.

2.5.2.2. Effect of Crosslinking on Dialysis Coefficient and Selectivity: Series Two

Diffusion dialysis test results of the second membrane series are shown Table 2.7. The effect of DVB content on the acid dialysis coefficient and selectivity of acid over sodium and magnesium chlorides is shown in Figs. 2.10 and 2.11 respectively. As can be seen from Fig. 2.10, the acid dialysis coefficient decreased from 49 mol/h•m^2•ΔC at 0.54% DVB content to 5.7 mol/h•m^2•ΔC at 44.1% DVB content. The selectivity of acid over sodium and magnesium chloride diffusion increased markedly with increasing DVB

content, Fig. 2.11. The dialysis coefficients of NaCl and $MgCl_2$ showed a dramatic decrease resulting in a net eight-fold increase in selectivity of acid over NaCl and a sixty-fold increase in selectivity of acid over $MgCl_2$ as the DVB content increased.

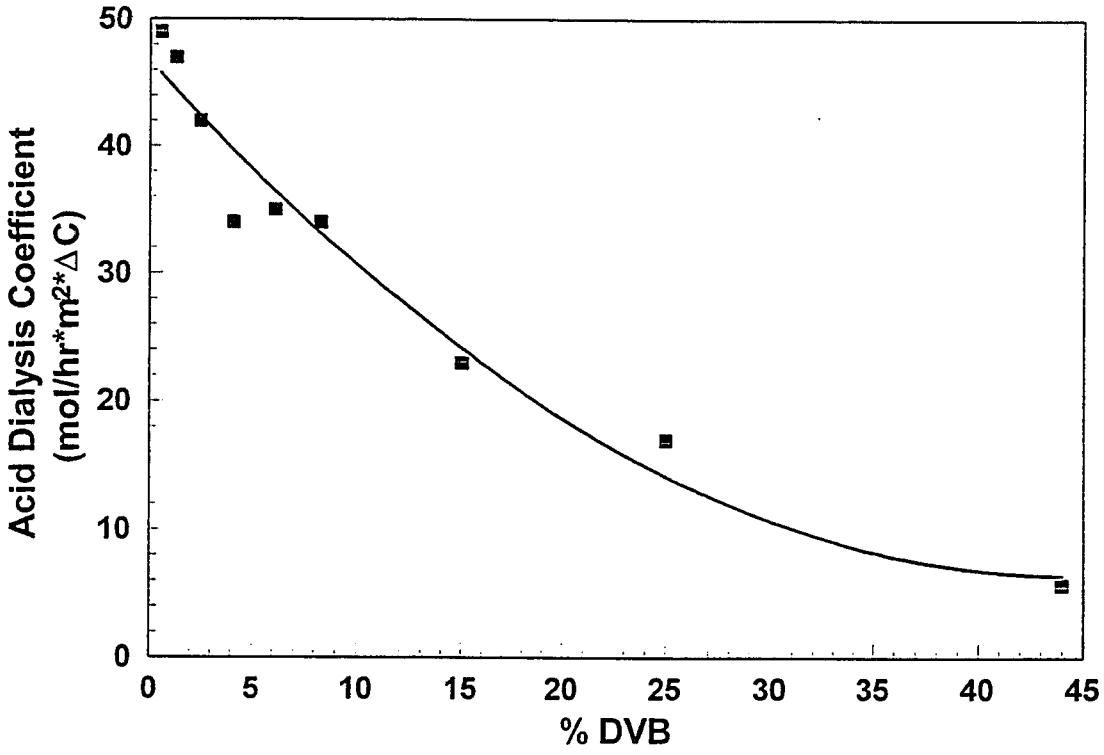

Fig 2.10. Acid Dialysis Coefficient versus Percent DVB Crosslinker

Table 2.7. Dialysis Coefficients and Selectivities With Varying DVB Content

Membrane	% DVB	Acid Dialysis Coefficient (U)[1]	NaCl Dialysis Coefficient (U)	$MgCl_2$ Dialysis Coefficient (U)	Selectivity (U HCl) / (U NaCl)	Selectivity (U HCl) / (U $MgCl_2$)
422	0.54	49 ± 2	5.2 ± 0.2	2.25 ± 0.16	9.4 ± 0.5	22 ± 1
406	1.3	47 ± 2	4.8 ± 0.1	1.79 ± 0.11	9.8 ± 0.5	26 ± 1
415	2.5	42 ± 2	3.7 ± 0.1	1.3 ± 0.1	11.3 ± 0.5	32 ± 2
412	4.1	34 ± 2	2.7 ± 0.1	0.65 ± 0.05	12.6 ± 0.5	52 ± 3
417	6.1	35 ± 2	2.5 ± 0.1	0.72 ± 0.05	14 ± 0.6	49 ± 2
428	8.3	34 ± 2	2.1 ± 0.06	0.51 ± 0.04	16 ± 0.8	67 ± 3
431	15.4	23 ± 1	0.89 ± 0.04	0.15 ± 0.01	26 ± 1	150 ± 8
432	24.8	17 ± 0.8	0.47 ± 0.02	0.043 ± 0.003	36 ± 2	390 ± 20
PV19	44.1	5.7 ± 0.3	0.073 ± 0.004	0.0044 ± 0.0003	78 ± 4	1300 ± 60

[1] $U = mol/hr \cdot m^2 \cdot \Delta C$

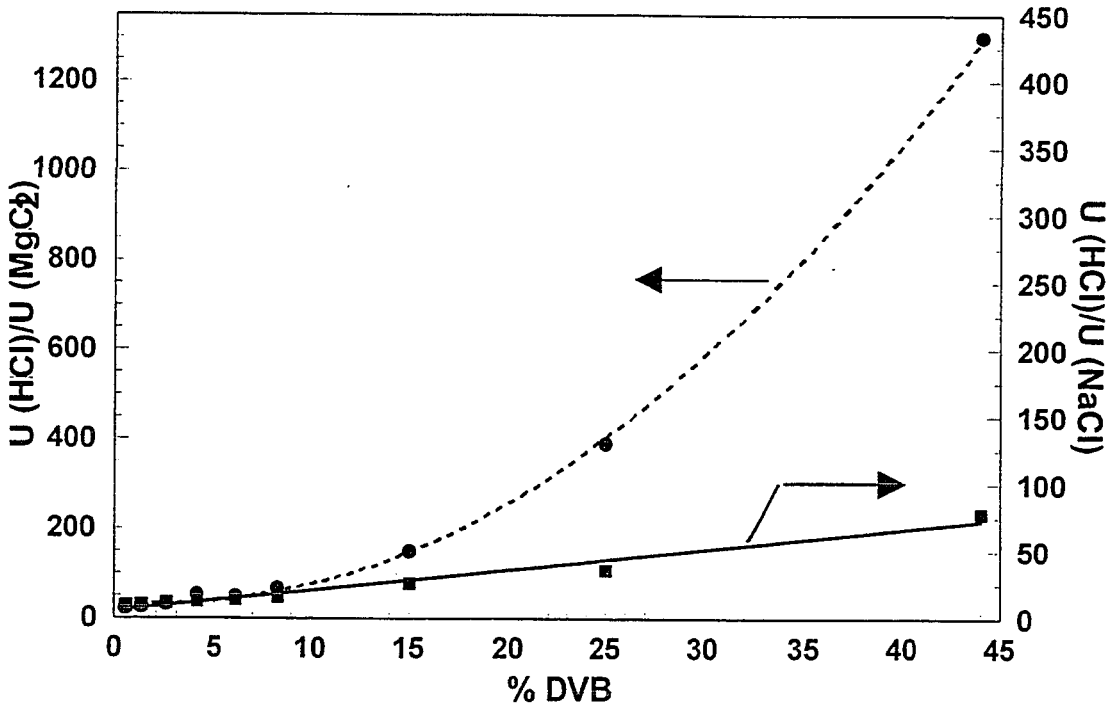

Fig. 2.11. Selectivity versus Percent DVB Crosslinker:
Solid Line; HCl/NaCl, Broken Line; $HCl/MgCl_2$

These results can be understood in terms of the varying water content of these membranes. The proton leakage through anion exchange membranes has been considered from the view point of a three-phase membrane model where the membrane consists of hydrophobic polymer, an active ion exchange zone and an interstitial zone comprised of water not taken up in the hydration shells of the ions in the membrane [11,12]. The water that is sorbed into the membrane is divided between the active and interstitial zones. Tugas and coworkers have found that the mobility of anions in the active zone to be much greater than the mobility of anions in the interstitial zone [12]. This was interpreted as the result of different conduction mechanisms in the two regions. The anions are thought to

move by a hopping mechanism in the active zone, transferring from one exchange site to another, while in the interstitial region a "dragging" mechanism (restricted diffusion) occurs whereby hydrated ions experience friction as they move through the membrane [12]. The portion of water in the membrane that is found in the solvation shells of the fixed ions and their counter ions is not free to move within the membrane and will exert drag on ions moving through the membrane. Hydrated ions will require a certain volume of water within the membrane to permit migration through the membrane.

Cation transport occurs mainly through the interstitial zone where the repulsive force caused by the ion exchange sites is minimal [11]. Therefore, the quantity of water in the interstitial zone (the free water) relative to the quantity of bound water associated with the ion exchange sites should affect cation permeability. This effect is clearly seen in the results described here. As the total water content of the membranes decreases, a decrease in cation permeability is observed.

The number of molecules of water per ion exchange site can be used to give some insight into the amount of free water within the membrane. These numbers have been calculated for the series of membranes described here, the results are presented in Table 2.3. Water contents have been reported for commercial ion exchange membranes as between 11 and 14 molecules of water per ion exchange site [12].

In membranes described here, each ion exchange site consists of a pyridinium and chloride ion, each of which must possess a hydration shell. It has been estimated that the average number of H_2O molecules in the combined hydration shells of these two ions is

between 4 and 8 [79]. Using the total water contents given in Table 2.3, and after estimating the number of water molecules in the hydration shells of the fixed ions and the counter ions at six, the number of free water molecules dropped from approximately 20 to 3 per ion exchange site as the DVB content increased from 0.54 to 44%.

This drop in water content greatly affects the mobility of sodium and magnesium ions in the membrane since these ions must migrate as hydrated species. Estimates put the hydration number of the sodium ion at approximately 4 and the magnesium ion at approximately 8 [79]. Proton migration can occur by hopping from one water molecule to another, including water found in the hydration shells of the ions as well as free water. It is unlikely that transport of protons is accompanied by the transport of water, since proton hopping is the cause of their extraordinary mobility [11]. It has also been shown by Gavach and coworkers that the ratio of the ionic mobilities of H^+ and Cl^- in the membrane phase of three commercial anion exchange membranes does not differ widely from that in water [12]. This indicates that the mechanism of proton transport through the membranes is the same as that in water and involves proton hopping rather than simple diffusion. Gavach has, however, reported significant acid sorption into the anion exchange membranes studied [12,13,17,22] and determined that there are two factors forming the basis of the greater permeability for acid than salts, the first being the higher mobility of protons with respect to other cations and the second being the higher degree of sorption of the acid in the membrane [17]. No measurements of acid sorption were made for the

pore-filled membranes discussed in this thesis so the relationship between acid sorption and acid permeability was not determined.

The increase in fixed charge concentration that was observed with increasing DVB content, Fig. 2.5, resulted in increased Donnan exclusion of cations (co-ions) from the membranes. With respect to the difference in selectivity of acid over sodium chloride compared to acid over magnesium chloride, the bivalent co-ion Mg^{2+} is more effectively excluded from the membranes than the monovalent Na^{+} co-ion due to the Donnan effect. The electrostatic repulsion between the fixed positive charges and a bivalent co-ion are greater than that for a monovalent co-ion, increasing the separation of bivalent co-ions.

Anderson and coworkers have studied the effects of polymer chains fixed to stationary surfaces on the diffusion of molecules and found a dependence on the molecule's size [44]. It was found that as the size of the diffusing molecule increased, the permeability of the molecule decreased. This is in agreement with the results found in this work with the permeabilities of sodium and magnesium. The magnesium ion, having a hydrated radius of 4.3 Å, consistently showed a lower permeability than the sodium ion, which has a hydrated radius of 3.6 Å [79].

Comparison was made with a commercial diffusion dialysis membrane, Selemion DSV, manufactured by Asahi Glass. When tested under the same conditions as the membranes presented in this work, the DSV membrane showed an acid dialysis coefficient of 5.6 mol/h•m^2•ΔC and selectivities of HCl over NaCl and $MgCl_2$ of 100 and 2500 respectively while the membrane prepared with 44% DVB content, PV19, showed

an acid dialysis coefficient of 5.7 mol/h•m^2•ΔC and selectivities of HCl over NaCl and $MgCl_2$ of 78 and 1300 respectively.

Through high pore loadings and high crosslinking, the pore-filled membranes studied in this chapter achieved good selectivity but in order to achieve the selectivities of the DSV through continued increases in the DVB content, an extremely high amount of crosslinking would be required. Based on the results of this chapter, a further increase in the DVB content would decrease the acid dialysis coefficient to a very low value, much lower than that for the DSV. This indicates that the DSV membrane is achieving its superior performance as a result of some membrane property that is different from the pore-filled membranes studied in this chapter.

2.6. Conclusions

This chapter has shown that poly(4-vinylpyridine) filled microporous membranes can be modified by inclusion of DVB as a cross-linker to yield anion exchange membranes that perform efficiently in the diffusion dialysis recovery of acid from acid/salt mixtures. The increase in mass gain combined with increasing amounts of DVB, up to 44% by weight, produces membranes with low water content and low cation dialysis coefficients that show high selectivities towards HCl relative to NaCl and $MgCl_2$.

Membrane thickness was found to increase with increasing mass gain at constant DVB content leading to a fairly constant percent water uptake while membrane thickness decreased with increasing DVB content at constant mass gain resulting in a decrease in

percent water uptake and a dramatic improvement in the selectivity of the membranes for diffusion dialysis.

Comparison with a commercial diffusion dialysis membrane, Selemion DSV, indicates that the membranes presented in this work perform well for acid recovery by diffusion dialysis but differ in some fundamental property from the DSV which limits their selectivity. The selectivities of the membranes approach those found with the DSV, and membrane optimization could likely result in performance that matches or exceeds that of the Selemion DSV.

As yet, the relative amounts of free and bound water in the pore-filled membranes have not been determined. An investigation into the structure of the membrane water is undertaken in Chapter 3 which will answer this question. As well, in Chapter 3, the effects of quaternization of the pore-filled membranes using various alkyl groups on membrane performance is probed which addresses the question of why the Selemion DSV shows superior acid recovery performance.

CHAPTER THREE

TUNING THE ACID RECOVERY PERFORMANCE OF POLY(4-VINYLPYRIDINE)-FILLED MEMBRANES FOR ACID RECOVERY

This chapter is based on a paper that has been prepared for publication in the Journal of Membrane Science.

Analysis of the results of diffusion dialysis testing of the membranes described in Chapter Two resulted in the conclusion that the pore-filled membranes produced at McMaster University showed potential for use in acid recovery. It was concluded that a high pore loading and a significant degree of crosslinking were necessary to produce membranes suitable for acid recovery. However, the membranes were still not able to achieve the selectivities displayed by the commercial membrane, the Selemion DSV.

In this chapter the effect of quaternization of the nitrogen atom of poly(4-vinylpyridine) with alkyl groups of various lengths is examined with the interest of further improving the properties of the pore-filled membranes.

3.1. Introduction

Ideally, anion-exchange membranes are impermeable to cations. While in practice no membrane is ideal and some leakage of cations will occur through an anion-exchange membrane, proton mobility through the membranes is abnormally high. Proton migration can occur by two mechanisms: diffusion, similar to other ions, or the Grotthus mechanism in which protons transfer from one water molecule to another [13]. This high proton mobility as compared to metal ions permits the recovery of acid from solutions containing other cationic species [16-19,22].

We have recently described a new approach to constructing anion-exchange membranes in which the pores of a host microfiltration membrane are filled with a suitable polyelectrolyte [68,71]. The polyelectrolyte gel is anchored in and constrained by the pores of the microporous support. The properties of the membranes can be tuned for a variety of applications, including ultra-low pressure water softening [83], by variation of the gel polymer concentration (volume fraction).

Membranes of this pore-filling construct, made by the uv-induced copolymerization of 4-vinylpyridine and divinylbenzene, show considerable promise for use in diffusion dialysis [15]. These anion exchange membranes, in which the positive charge results from protonation of the pyridinium nitrogen atoms, exhibit high acid dialysis coefficients. However, their selectivity in terms of discriminating between acid (proton) and metal ion salts was less than desirable. The purpose of this work is to see if the transport properties and, particularly, proton/metal cation selectivity of the

incorporated poly(4-vinylpyridine) gels could be enhanced by alkylation rather than protonation of the pyridine nitrogens.

Sata and Yamamoto have previously reported that the water content and proton mobility of poly(4-vinylpyridine) based membranes can be modified by variation in the alkyl substituents placed on the pyridine nitrogen atoms [37]. It is clear from this work that proton mobility is related to the water content of the membranes, however no work has been reported on the effect of such changes on metal cation mobility [37,92]. It has also been reported that the rate of acid permeation through Neosepta anion exchange membranes, manufactured by Tokuyama Soda Co. Ltd. Japan, can be decreased by the formation of poly(pyrrole) in the membrane matrix [93,94]. The permselectivity of anions through poly(vinylbenzyl ammonium salt)-based membranes has been shown to depend on the nature of the N-alkyl groups on the ammonium sites with higher selectivities being found with more hydrophobic, lower water content membranes [38,95-99]. As such it might be expected that metal ion permeability could be affected by the water content in anion exchange membranes. Indeed, our previous work with protonated poly(4-vinylpyridine)-based membranes showed that increasing the degree of cross-linking with divinylbenzene led to a reduction in water content and an increase in fixed charge concentration. These changes were accompanied by an increase in selectivity of the membranes in terms of acid and metal salt diffusion.

In addition to the effect of water content on membrane properties, knowledge of the nature of the water in the membrane is also important. There has been much debate

over the structure of water in polymer systems [77]. Views range from describing the water as being present in as many as three states; bound water, interfacial water and free water, to more or less a broad continuum of varying water states that are not distinctly separate. In general, it is accepted that water contained in ion exchange membranes, resins and hydrogels is present in two states [75-78], the first state being a quantity of water bound to the ion exchange sites in the form of hydration shells and the second state being free water which has properties similar to those of bulk water. Differential scanning calorimetry (DSC) is a thermal analysis technique that can be used to quantify the amount free water present in materials by determining the amount of energy required to freeze the water or melt the ice contained in the material. This technique is used in this chapter to probe the nature of the water contained in the membranes in terms of "free" and "bound" water as a result of alkylation of the pyridine nitrogen atoms.

In this work we systematically explore the effects of changing the pyridine-N-alkyl groups in poly(4-vinylpyridine) pore-filled membranes on the content and nature of the incorporated water, the nominal charge densities of the resulting membranes, and the permeabilities of both acid (HCl) and simple metal salts. It is shown that decreasing the water content of the membranes by making the pyridine N-alkyl group larger, markedly reduces salt diffusivity. The diffusion of acid is affected to a much smaller degree and, as a result, the selectivity of the membranes in acid recovery is greatly enhanced.

3.2. Experimental

3.2.1. Materials

The porous substrate used in this study was a polypropylene microfiltration membrane with an average pore diameter of 0.26 μm, an average thickness of 53 μm and a porosity of approximately 60 vol% (3M Company). 4-Vinylpyridine and divinylbenzene (55% meta and para isomers, 45% ethylvinylbenzene) (Aldrich) were purified by vacuum distillation. 2,2-Dimethoxy-2-phenylacetophenone (DMPA) (Aldrich) was used as a photoinitiator. *N,N*-Dimethylformamide (DMF), dimethylsulfate, bromoethane, 1-bromopropane, 1-bromobutane, 1-bromopentane, 1-bromohexane and benzylbromide (Aldrich) were used as received. Methanol, hydrochloric acid, sodium chloride, magnesium chloride, lithium chloride, potassium chloride and sodium sulfate were reagent grade and used without further purification. The water used was carbon filtered and deionized.

3.2.2. Preparation of the Membranes

The membranes were prepared by a photo-initiated radical copolymerization of 4-vinylpyridine and DVB in the pores of the polypropylene substrate as described previously in section 2.5.2. The nominal percent DVB content of the pore of the pore-filling polymer was taken as the weight ratio of DVB isomers to 4-vinylpyridine in the monomer mixture. The membranes were extracted with hot methanol (Soxhlet) and

equilibrated in a three-fold cycle involving 1M HCl, a water rinse, followed by 1M NaOH. The equilibration time in each solution was 12 h. After the last base cycle the membranes were soaked in deionized water followed by methanol and then dried under vacuum prior to quaternization.

The membranes were characterised by mass gain, thickness, ion exchange capacity and water content as described in Chapter 2. Differential scanning calorimetry was used to examine the membrane water and then the membranes were tested by diffusion dialysis with a solution composed of hydrochloric acid, sodium chloride and magnesium chloride, as described in Chapter 2.

3.2.2.1. Alkylation of the Pyridine Nitrogen Atoms

All quaternization reactions were conducted in DMF solutions at room temperature. N-methylation was achieved using a 10% (v/v) solution of dimethylsulfate for 3 days. N-ethylation and N-propanation were achieved using 50% (v/v) solutions of bromoethane or 1-bromopropane, respectively, for 10 days. The N-butyl and N-pentyl derivatives were prepared by treatment of the membrane with 50% (v/v) solutions of 1-bromobutane or 1-bromopentane, respectively for 15 days. Reaction with 50% (v/v) solution of 1-bromohexane for 9 days gave the N-hexyl derivative. N-benzylation was achieved with a 5% (w/w) solution of benzyl bromide for 3 days. After the quaternization reactions were complete, the membranes were soaked in methanol for 0.5 h, deionized

water for 2 h, and 1M NaCl for approximately 18 h to convert the membranes into their chloride forms.

3.2.2.2. Degree of Quaternization and Water Content

A membrane, approximately 6 cm × 6 cm, in its chloride form was soaked in deionized water to remove excess NaCl present. This treatment was repeated three times. The membrane was then placed in 100 mL of 740 ppm aqueous Na_2SO_4 solution overnight to displace the chloride ions and convert the membrane to its sulfate form. The solution was retained while the membrane was treated with a second 100 mL of the Na_2SO_4 solution and allowed to soak overnight. The solutions were combined, diluted to 500 mL, and the chloride concentration was determined by ion exchange chromatography (Dionex, DX 100). The degree of quaternization that was achieved for each membrane was calculated based on the theoretical maximum that could be expected if 100% of the pyridine groups present in the membrane were reacted. The experiment was repeated twice. The reproducibility for the measured percent quaternization was ±3%, based on two observations.

The total water content of the quaternized membranes was determined as in Chapter 2 using the following equation:

$$\text{mass of } H_2O = m_{w,q} - m_{d,u} - m_{q,c}$$

Where $m_{w,q}$ is the mass of the wet, quaternized membranes, $m_{d,u}$ is the mass of the dry membranes prior to quaternization and $m_{q,c}$ is the mass of the quaternizing groups and

associated counterions, quantities which were determined by ion exchange chromatography.

3.2.3. Diffusion Dialysis Testing

Diffusion dialysis experiments were carried out using a cell constructed from Lucite that consisted of two chambers of equal volume separated by the membrane with an active area of 3.14 cm^2 as described in section 2.5.2.9. Initially, one chamber contained a solution of 1.0 M HCl, 0.5 M NaCl and 0.5 M $MgCl_2$ (or in some instances a solution of 1.0 M HCl, 0.5 M LiCl, 0.5 M NaCl and 0.5 M KCl) and the other deionized water. The cell temperature was maintained at 25°C. Both chambers were stirred at identical rates of 25 revolutions per second in order to minimize concentration polarization effects. Diffusion was allowed to occur for a measured time and then the solutions were removed from each side of the cell and analyzed for acid and salt composition. Acid was determined by titration with NaOH. The metal ion concentrations were measured by ion exchange chromatography (Dionex, DX 100).

The apparent dialysis coefficient, U, of the membrane for each component was determined using equations 2.8 and 2.9 from section 2.5.2.9. The experiment was repeated three times for each membrane. The reproducibility for the measured dialysis coefficients was ±5%, based on three observations. The results were compared with those of the second series of membranes tested in Chapter 2.

3.2.4. Differential Scanning Calorimetry (DSC)

DSC analysis was performed with a TA Instruments DSC 2910 calorimeter using a standard DSC cell interfaced to a thermal analysis data system and cooled with liquid nitrogen. The membrane samples were equilibrated in 0.1 M HCl, the surfaces patted dry and weighed pieces were placed in aluminum pans with lids crimped on. The samples were equilibrated at 20°C and cooled at 5°C/min to -60°C. The exothermic peak in the DSC thermogram was integrated to obtain the enthalpy of freezing of water in the membrane given in Joules per gram of sample. The amount of freezable water was then calculated using the enthalpy of fusion of water as 333 J/g. The experiment was repeated twice for some of the membrane samples. The reproducibility for the DSC measurement was within ± 10%. The amount of non-freezable or bound water was calculated by subtracting the amount of freezable water from the total amount of water in the membrane. The second series of membranes from Chapter 2 were also subjected to the DSC experiments.

3.3. Results

The pore-filled membranes studied in this work were prepared by photoinitiated copolymerization of 4-vinylpyridine and divinylbenzene (DVB) within the pores of a polypropylene microporous substrate. The host membrane selected had a pore size of 0.2 μm and porosity of 60%. This host membrane possesses sufficient mechanical strength to limit the swelling of the incorporated polyelectrolyte. From the previous work it was

found to be important to largely fill the pores of the host membrane [15]. Thus the polymerizations were continued until the membranes had mass gains associated with the incorporated poly(4-vinylpyridine) copolymer in the range of 150% to 208%. The positive charge was introduced into the membranes by one of two routes, protonation of the nitrogen atoms of the pyridine rings by HCl or N-alkylation.

There is general agreement that the quaternization reaction involving the pyridine nitrogen atom occurs by an S_N2 mechanism, that is a bimolecular reaction [100]. The mechanism of a generic alkylation of the pyridine nitrogen atom by an alkyl bromide is given in Scheme 3.1. This type of S_N2 reaction is known to proceed well in polar aprotic solvents such as *N*,*N*-dimethylformamide (DMF).

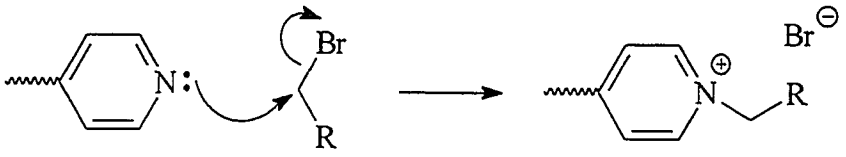

Scheme 3.1. Alkylation of Pyridine Nitrogen Atom

Many studies have been carried out involving the quaternization of poly(4-vinylpyridine) [100-104]. It has been found that there was a departure from the overall second order kinetics that were observed for alkylation of the monomeric species. This is evident in an enhanced retardation of the alkylation reaction with poly(4-vinylpyridine), which was initially attributed to charge build up during the reaction [100].

For example, Boucher and coworkers studied the quaternization of poly(4-vinylpyridine) extensively [100-102]. In their early studies, using solutions of 1-bromopropane in sulfolane, the retardation effect was analyzed according to a neighbouring group model with rate constants k_0, k_1 and k_2 used for the reaction of pyridyl groups with zero, one and two already reacted neighbours. Allowing for a limiting reaction of approximately 95%, the ratios of rate constants were: $k_1/ k_0 = 0.80$ and $k_2/ k_0 = 0.37$. Although these results substantiated the neighbouring group model used, it was not clear whether steric or electrostatic factors were responsible for the rate constant ratios less than one [100].

Later work by Boucher using n-alkyl bromides of different chain lengths (C_2, C_3, C_4 and C_6) as quaternizing agents for poly(4-vinylpyridine) yielded rate constant ratios k_1/ k_0 and k_2/ k_0 which decreased with increasing chain length of the n-alkyl bromide [101]. These results indicated that the retardation as the reaction proceeded was due predominantly to steric, rather than electrostatic effects. This conclusion has been confirmed by a number of similar subsequent studies [102-104].

In this work, N-alkylation of the anchored poly(4-vinylpyridine) was carried out by treatment with a series of alkyl bromides in DMF. The N-alkyl groups incorporated ranged from methyl to *n*-hexyl and benzyl, scheme 3.2, in order to vary the degree of hydrophobicity of the membranes. The degree of N-alkylation, or quaternization, achieved for all membranes was between 75% to 80% of the calculated maximum based on the total pyridine groups available.

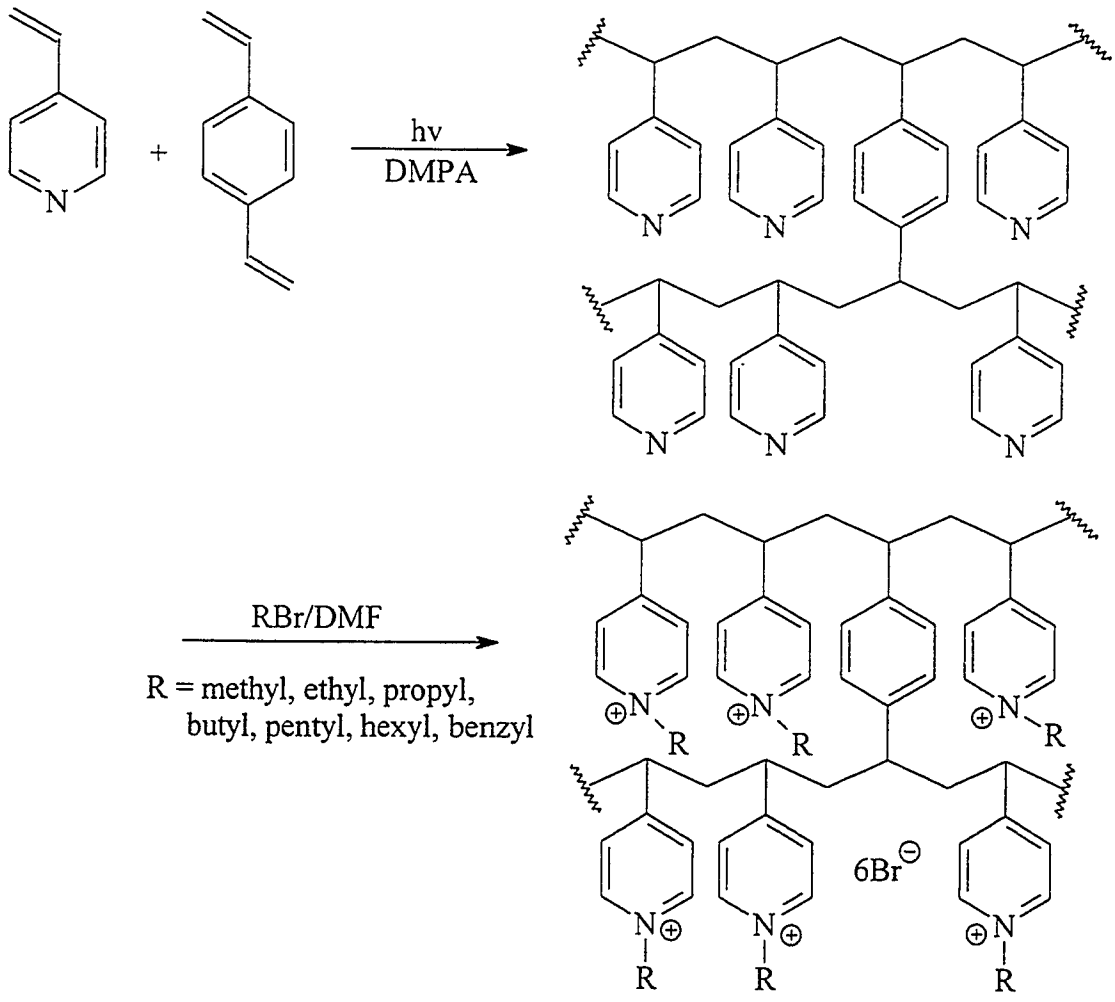

Scheme 3.2. Formation and Alkylation of Membranes: 422 through PV19, R = hydrogen; 406me, 426me, 431me and 432me, R = methyl; 432et, R = ethyl; 432pr, R = n-propyl; 432bu, R = n-butyl; 432pe, R = n-pentyl; 432he, R = n-hexyl; 432bz, R = benzyl.

3.3.1. Properties of Membranes

The membranes were characterized in terms of their physical dimensions, particularly thickness, mass-loading, and ion-exchange capacity. The data for the membranes studied in this work are summarized in Table 3.1. The first nine membranes in Table 3.1 were taken from the second series of membranes in Chapter 2, except for

membrane 426, and have DVB contents ranging from 0.54% to 44.1%, mass loadings in the range of 147% to 208%, thicknesses from 131μm to 67μm. These membranes were all tested in protonated form. Membranes 406me, 426me, 431me and 432me were produced by methylation of pieces of membranes 406, 426, 431 and 432 respectively, producing a series of four membranes with similar mass loadings but varying DVB contents. This series allows for the examination of the effects of methylation on the membrane properties and performance in diffusion dialysis in comparison to the membranes in protonated form. Membranes 432et, 432pr, 432bu, 432pe, 432he and 432bz were produced by N-alkylation of pieces of the single membrane 432 with the appropriate alkyl bromide. Including membrane 432me, this gave a series of seven membranes with identical initial mass loadings and DVB contents with which to study the effects of changing the hydrophobicity of the membranes.

Table 3.1. Properties of Membranes

Membrane	Group on Nitrogen	DVB (%)	Mass Gain[1]	Thickness[2] (μm)	Ion Exchange Capacity (meq/g)[3]
422	hydrogen	0.54	147	131	4.5
406	hydrogen	1.3	157	107	4.4
415	hydrogen	2.5	173	120	4.7
426	hydrogen	4.1	191	104	4.4
417	hydrogen	6.1	182	94	4.3
428	hydrogen	8.3	181	96	4.0
431	hydrogen	15.4	201	88	3.8
432	hydrogen	24.8	208	71	3.5
PV19	hydrogen	44.1	193	67	3.0
406me	methyl	1.3	157	119	4.1
426me	methyl	4.1	191	109	4.1
431me	methyl	15.4	201	86	3.6
432me	methyl	24.8	208	85	3.3
432et	ethyl	24.8	208	73	3.2
432pr	n-propyl	24.8	208	73	3.0
432bu	n-butyl	24.8	208	73	2.9
432pe	n-pentyl	24.8	208	73	2.8
432he	n-hexyl	24.8	208	76	2.7
432bz	benzyl	24.8	208	78	2.6

[1] Mass loading of membrane by percent weight before quaternization, ±3%.
[2] Thickness of membrane in 1 M HCl solution after quaternization, ±3%.
[3] Ion exchange capacity in milliequivalents per gram of dry membrane, ±5%.

3.3.2. Membrane Water Contents and DSC Results

The total water contents of the membranes were determined gravimetrically. The water contents, taken in conjunction with the ion exchange capacities, Table 3.1, allow calculation of the fixed charge concentrations (equivalents of ion exchange sites per kg of water in the membrane), Table 3.2. As a probe of the nature of the water present in the membranes they were studied using differential scanning calorimetry (DSC) in order to determine their "freezable" water content. In each case the membrane sample was cooled from room temperature down to -60°C producing thermograms with exothermic peaks in the range of -15°C to -20°C. The freezable water content of the membranes was calculated from the measured enthalpy values assuming that the enthalpy of fusion of water (333 J/g) is not affected by its incorporation into the membrane. The difference between the total water contents of the membranes, determined gravimetrically, and the freezable water contents, determined by DSC, gave the amount of nonfreezable or bound water in the membranes. The total water, freezable water and bound water contents (expressed as the number of water molecules per ion exchange site) are given in Table 3.2.

Table 3.2. Membrane Water Contents and DSC Results

Membrane	Total H_2O per Fixed Charge[1]	Free H_2O per Fixed Charge[2]	Bound H_2O per Fixed Charge	Fixed Charge Conc. (eq/kg)[3]
422	25.8	18	7.8	2.2
406	22.3	16.3	6.0	2.5
415	19.5	13.6	5.9	2.9
426	17.4	12	5.4	3.2
417	15.6	10.3	5.3	3.6
428	15.7	8.3	7.4	3.5
431	12.1	4.6	7.5	4.6
432	10.4	3.6	6.8	5.3
PV19	8.7	0.17	8.5	6.4
406me	27.5	14.5	13	2.0
426me	19.5	9.5	10	2.9
431me	14.7	4.9	9.8	3.8
432me	13.5	3.7	9.8	4.1
432et	12.1	2.5	9.6	4.6
432pr	11.3	2.3	9.0	4.9
432bu	10.7	1.2	9.5	5.2
432pe	10.5	1.1	9.4	5.3
432he	8.3	0.96	7.3	6.7
432bz	7.7	0.35	7.3	7.3

[1] Total number of water molecules per ion exchange site determined gravimetrically, ±5%.
[2] Molecules of free water per ion exchange site as determined by DSC, ±1 water molecule.
[3] Fixed charge concentration as equivalents of ion exchange sites per kg of water in the membrane, ±5%.

3.3.3. Diffusion Dialysis Testing

All membranes were subjected to diffusion dialysis testing using a stirred cell as described in section 2.5.2.9 with a feed solution composed of 1 M HCl, 0.5 M NaCl and 0.5 M $MgCl_2$ separated by the membrane from a permeate solution initially containing deionized water. The results are shown in Table 3.3 with the apparent dialysis coefficients of the acid and salts listed, as well as the selectivities of acid over salts.

Table 3.3. Diffusion Dialysis Results for HCl/NaCl/$MgCl_2$ Test Solution

Membrane	U (HCl)[1]	U (NaCl)	U ($MgCl_2$)	$\frac{U(HCl)^2}{U(NaCl)}$	$\frac{U(HCl)}{U(MgCl_2)}$
422	49	5.2	2.25	9.4	22
406	47	4.8	1.79	9.8	26
415	42	3.7	1.3	11.3	32
426	41	3.2	0.89	13	46
417	35	2.5	0.72	14	49
428	34	2.1	0.51	16	67
431	23	0.89	0.15	26	150
432	17	0.47	0.043	36	390
PV19	5.7	0.073	0.0044	78	1300
406me	67	6.1	2.8	11	24
426me	55	3.4	1.5	16	37
431me	47	1.3	0.38	37	120
432me	34	0.67	0.15	51	230
432et	31	0.40	0.72	78	430
432pr	20	0.18	0.025	110	800
432bu	15	0.088	0.01	170	1500
432pe	9.3	0.02	0.0019	460	5000
432he	6.0	0.014	0.0009	440	6660
432bz	3.6	0.007	0.0008	490	4500

[1] U = apparent dialysis coefficient in mol/h•m^2•ΔC, ±5%.
[2] Reproducibility of selectivity measurements: ±7%.

3.3.4. Diffusion Dialysis Using Monovalent Salts

In order to investigate the effects of varying ion size at constant ionic charge on diffusion dialysis performance, a selected number of membranes were tested using a feed solution of 1 M HCl and 0.5 M each of LiCl, NaCl and KCl. The apparent dialysis coefficients for the alkali metal salts are given in Table 3.4 for a nascent polypropylene membrane with no incorporated polyelectrolyte, two protonated membranes, 422 and PV19, with different DVB contents as well as two membranes quaternized with either methyl or benzyl group, 432me and 432bz, with both membranes having the same DVB content. The selectivities for KCl over NaCl and LiCl dialysis coefficients are also given in Table 3.4.

Table 3.4. Diffusion Dialysis Results for HCl/LiCl/NaCl/KCl Test Solution.

Membrane	Fixed Charge Conc. (eq/kg)	U (KCl)	U (NaCl)	U (LiCl)	U (KCl) / U (NaCl)	U (KCl) / U (LiCl)
Nascent	0	9.8	7.6	6.4	1.3	1.5
422	2.2	8.1	5.7	3.9	1.4	2.1
PV19	6.4	0.27	0.19	0.17	1.4	1.6
432me	4.1	1.0	0.85	0.98	1.2	1.0
432bz	7.3	0.0086	0.0085	0.011	1.0	0.78

3.4. Discussion

3.4.1. Effects of Methylation of Membranes

The four N-methylated membranes, 406me, 426me, 431me and 432me, have similar mass loadings but DVB contents varying from 1.3% to 24.8%. Examination of the results summarized in Table 3.1 show that the measured ion exchange capacities of the N-methylated membranes are slightly less than their protonated counterparts. The ion exchange capacity is expressed on the basis of the dry weight of the membrane and this decrease in capacity simply reflects the increased mass of the membrane resulting from N-methylation.

In general there is a small increase in thickness of the N-methylated membranes as compared to their protonated counterparts. There is no obvious pattern to the thickness changes.

As can be seen from Table 3.2, as the DVB content of the four membranes is increased, the fixed charge concentration (equivalents of ion exchange sites per kg of water in the membrane) is increased. This result parallels that observed with the corresponding N-protonated membranes, Chapter 2. There appears to be a relationship between the increase in the fixed charge concentration and the decrease in both the acid and salt dialysis coefficients as well as the increases in selectivity of acid over sodium and magnesium chlorides, Table 3.3.

The DSC results, Table 3.2, indicate that the number of water molecules that are bound to each ion exchange site remain relatively constant in the range of 6.5 ± 1 for the four membranes tested in protonated form. The number of free water molecules per ion exchange site, however, is seen to decrease from 16.3 to 3.6 with increasing fixed charge concentration. Since co-ion mobility is greater in regions of free water [11,12,33], the decrease in dialysis coefficients of all species would seem to be a result of the decrease in free water. The increase in selectivity of acid over salts results from sodium and magnesium chloride diffusion decreasing more rapidly than acid diffusion as the free water content of the membranes decreased.

The data for membranes 406me, 426me, 431me and 432me yield interesting results when compared to their protonated counterparts, as shown in Tables 3.1, 3.2 and 3.3. Before discussing the trends in the data it is important to stress that the degrees of protonation and alkylation of all the membranes tested are very similar (approximately 80%). Thus, in comparing the data, the number of charged sites in a protonated or alkylated membrane with the same initial mass loading are very similar. Therefore, variations in fixed charge concentrations will largely be due to differences in the amount of water present in the membranes. The fixed charge concentration of each membrane decreases as a result of methylation, as the total number of water molecules per fixed charge site increases compared to their protonated form, Table 3.2. This decrease in fixed charge concentration results in an increase in the dialysis coefficients of sodium and magnesium chlorides and a large increase in acid dialysis coefficients for the methylated

membranes. Despite the increase in dialysis coefficients, there is a significant increase in selectivity of acid over NaCl observed for all four membranes upon conversion from protonated to methylated form. This result is contrary to the decrease in selectivity which accompanies a decrease in fixed charge concentration for membranes in protonated form, as was observed in Chapter 2.

These results indicate that methylated membranes do not exhibit the same properties as protonated membranes. A small decrease is seen in the selectivity of acid over $MgCl_2$ for membranes 426me, 431me and 432me compared to membranes 426, 431 and 432 while no decrease is seen for membrane 406me compared to membrane 406 even though the fixed charge concentration of membrane 406me is less than that of membrane 406. Again, this observation is contrary to what would be expected if the fixed charge concentration decreased and the membranes were in protonated form.

These apparently anomalous results can be explained by referring to Table 3.2. It can be seen that the decrease in fixed charge concentration resulted from an increase in water content of the membranes after methylation compared to the protonated form. The increased number of water molecules per ion exchange site, however, did not result in an increase in the membrane free water content, rather an increase in the membrane bound water. In fact, membranes 406 and 426 showed decreases in the number of free waters per ion exchange site from 16.3 to 14.5 and 12 to 9.5 respectively upon conversion from protonated to methylated form. Membranes 431 and 432 remained practically unchanged in free water content upon conversion from protonated to methylated form. Membranes

406me and 426me doubled their numbers of bound waters per ion exchange site compared to membranes 406 and 426 while membranes 431me and 432me showed an in increase in bound water per ion exchange site of 1.3 times and 1.4 times those of membranes 431 and 432 respectively. This increase in bound water does contribute to ion migration, as is seen in the results of Table 3.3, but the contribution to the acid dialysis coefficient is much greater than the contribution to the dialysis coefficients of the salts.

The results obtained from the methylated series discussed above indicates that alkylation improves acid recovery performance of the membranes compared to quaternization by protons. It would seem that the structure of the membrane water in terms of "bound" and "free" water is affected by the presence of an alkyl group at the ion exchange site. This prompted an investigation of the effects of various alkyl groups as quaternizing agents on membrane water structure and acid recovery performance.

3.4.2. Effects of Different Alkyl Groups

A second series of seven membranes was prepared in which the mass loading was held constant at 208% and the DVB content was held constant at 24.8%. These membranes were subsequently quaternized with groups containing one to seven carbon atoms, namely; methyl, ethyl, n-propyl, n-butyl, n-pentyl, n-hexyl and benzyl groups, designated as membranes 432me, 432et, 432pr, 432bu, 432pe, 432he and 432bz respectively. Properties of these membranes are given in Tables 3.1, 3.2 and 3.3. As can be seem from Table 3.2, there is a marked increase in fixed charge concentration with

increasing carbon number, values rising from 4.1 eq/kg with methyl to 7.3 eq/kg with benzyl, as a result of the lowered water content.

A decrease in acid dialysis coefficient from 34 mol/h•m^2•ΔC with methyl to 3.6 mol/h•m^2•ΔC with benzyl was found, Table 3.3. Sata and coworkers used long chain alkyl bromides to modify the properties of anion exchange membranes and observed an increase in fixed charge concentration from 6 eq/kg to 12 eq/kg as a result of lowered water content from 45% to 20% [37]. A decrease in the apparent diffusion coefficient of HCl through the membranes upon incorporation of the hydrophobic groups was also observed [37,92], with which this work is in agreement.

Diffusion dialysis testing of the seven alkylated membranes gave the ratios of the dialysis coefficients of acid over NaCl and $MgCl_2$ shown in columns five and six of Table 3.3, respectively. Selectivity of acid over NaCl rose from 51 to 490 as the quaternizing group was varied from methyl to benzyl. Selectivity of acid over $MgCl_2$ increased dramatically from 230 to 6660 as the quaternizing group was varied from methyl to hexyl and dropped to 4500 with the benzyl group. The rise in selectivity with increased fixed charge concentration results from the fact that the mobility of cations such as sodium and magnesium is much more affected by a decrease in membrane water content than the mobility of protons.

Although these trends are in agreement with the work of the previous chapter on protonated membranes, the extent to which the selectivity of acid over sodium and magnesium chlorides increased with fixed charge concentration is far greater than that

obtained with protonated membranes. For example, comparing a protonated membrane to a membrane quaternized with the hexyl group having similar mass increases, fixed charge concentrations and acid dialysis coefficients, the following results are obtained. The protonated membrane, PV19, had a fixed charge concentration of 6.4 eq/kg, an acid dialysis coefficient of 5.7 mol/h•m^2• ΔC and selectivities of acid over NaCl and $MgCl_2$ of 78 and 1300 respectively. The membrane quaternized with the hexyl group, 432he, had a fixed charge concentration of 6.7 eq/kg, an acid dialysis coefficient of 6.0 mol/h•m^2• ΔC but achieved selectivities of acid over NaCl and $MgCl_2$ of 440 and 6660! Although the two membranes had very similar fixed charge concentrations and acid dialysis coefficients, the hexyl quaternized membrane had a selectivity of acid over NaCl that was 5.6 times greater than that with the protonated membrane and a selectivity of acid over $MgCl_2$ that was 5.1 times greater. This again indicates that alkylated membranes have different properties than protonated membranes.

A comparison was made with a commercially available diffusion dialysis membrane manufactured for use in acid recovery by Asahi Glass, the Selemion DSV. The DSV membrane showed an acid dialysis coefficient of 6.1 mol/h•m^2•ΔC with selectivities of HCl over NaCl and $MgCl_2$ of 100 and 2600 respectively. As is seen in Table 3.3, the membranes quaternized with pentyl and hexyl groups have similar or higher acid dialysis coefficients and much higher selectivities than the DSV. The membrane quaternized with the benzyl group has a somewhat lower acid dialysis coefficient but much higher selectivities than the DSV.

3.4.3. Comparison of Alkylated to Protonated Membranes in Terms of Fixed Charge Concentration

A comparison of alkylated to protonated membranes can be made based on the fixed charge concentration of the membranes, regardless of the nature of the alkylating group. The protonated membranes include membranes 422 through PV19. This comparison is shown in Figure 3.1 where the selectivity of acid over NaCl versus fixed charge concentration for both alkylated and protonated membranes is plotted.

The fixed charge concentration of the protonated membranes increases with increasing DVB content, as was described in Chapter 2, with the mass loadings of the membranes remaining relatively constant. The increase in fixed charge concentration for the alkylated membranes is a result of two separate factors. The four data points at lower fixed charge concentration for the alkylated series in Fig. 3.1 represent the methylated membranes 406me, 426me, 431me and 432me. The increase in fixed charge concentration in these four membranes is a result of increasing DVB content. The six data points at higher fixed charge concentration for the alkylated series represent membranes 432et, 432pr, 432bu, 432pe, 432he and 432bz which have identical DVB contents. The increase in fixed charge concentration for these six membranes results from the increase in the size of the alkylating group.

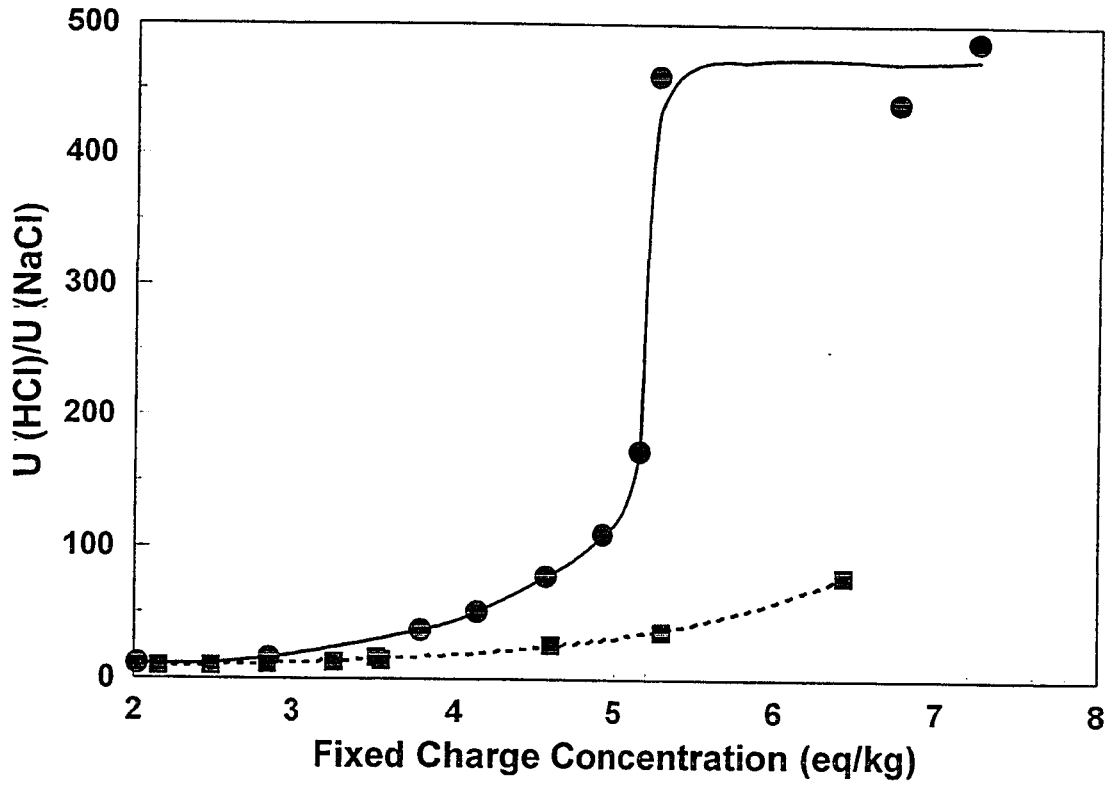

Fig 3.1. Selectivity of Acid over NaCl versus Fixed Charge Concentration: Alkylated-solid line; Protonated-broken line.

As can be seen in Figure 3.1, selectivity increases with fixed charge concentration for both alkylated and protonated membranes. The alkylated membranes are more selective for acid over NaCl than the protonated membranes given the same fixed charge concentration, with the difference becoming most pronounced at higher fixed charge concentrations. The selectivity of the alkylated membranes for acid over NaCl appears to reach a limiting value of approximately 470 at fixed charge concentrations over 5.2 eq/kg for membranes 432pe, 432he and 432bz. The selectivity of the protonated series has a maximum at 78 for membrane PV19 which has a fixed charge concentration of 6.4 eq/kg.

This difference in selectivity between the two series of membranes can be a result of either higher acid dialysis coefficients of the alkylated membranes compared to protonated membranes at a given fixed charge concentration, lower NaCl dialysis coefficients or both. Figure 3.2 is a plot of the log of the acid and NaCl dialysis coefficients of alkylated and protonated membranes versus fixed charge concentration.

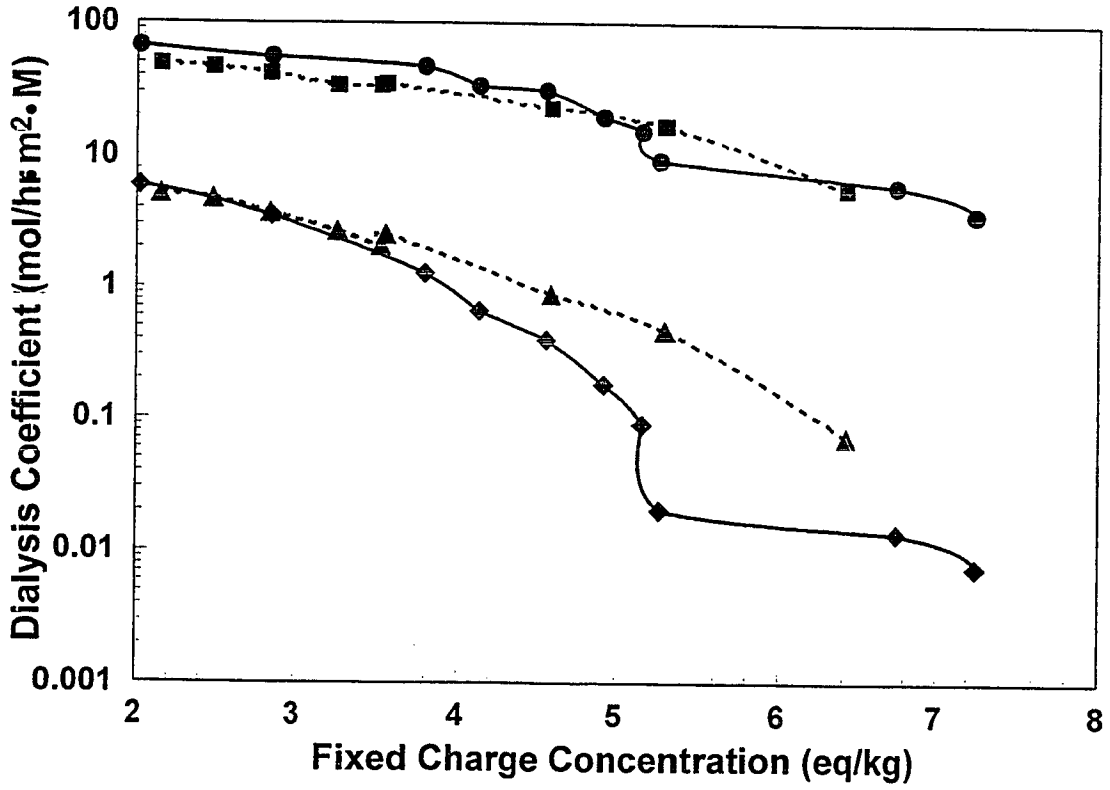

Fig 3.2. Log of the Acid and NaCl Dialysis Coefficient
versus Fixed Charge Concentration:
Alkylated-solid line; Protonated-broken line; ● and ■-HCl; ◆ and ▲-NaCl

At lower fixed charge concentrations the alkylated membranes show somewhat higher acid dialysis coefficients than the protonated membranes but at fixed charge concentrations in the range of 4 eq/kg to 7 eq/kg the acid dialysis coefficients of the two

series of membranes are similar. This means that the higher selectivity of the alkylated membranes at higher fixed charge concentrations cannot be attributed to higher acid dialysis coefficients of alkylated membranes compared to protonated membranes but to lower NaCl dialysis coefficients.

This is confirmed in Figure 3.2 where it can be seen that in the fixed charge concentration range of 4 eq/kg to 7 eq/kg the NaCl dialysis coefficients of alkylated membranes are significantly lower than those of the protonated membranes, indicating that it is the lower salt dialysis coefficients and not higher acid dialysis coefficients that result in the higher acid/salt selectivity of the alkylated membranes.

3.4.4. DSC Results and Comparison of Alkylated and Protonated Membranes

It is apparent from the results of the diffusion dialysis testing of the membranes that there is a fundamental difference in the behaviour of the alkylated membranes compared to the protonated membranes. In order to investigate the role of the membrane water in the diffusion dialysis performance of the membranes, an investigation into the nature, or the structure, of the water in the membranes was undertaken by performing DSC experiments on membrane samples.

DSC has been applied to polyelectrolyte gels [105], wet pulp and paper samples [75], poly(vinylalcohol) membranes [106] and hydrophilic hydrogels [77,107-110]. Differential thermal analysis has also been used on organic composite membranes [111]. It is important to note that it is the quantity of "free" water in the material or membrane

which is formally measured by the DSC experiment. Only by knowing the total amount of water that the membrane actually contains and then subtracting the amount of "free" water measured by DSC is the amount of "bound" water determined.

The DSC experiments yielded thermograms with exothermic peaks in the range of -15°C to -20°C which, when integrated, gave enthalpies of freezing of the free water contained in the membrane samples when cooled from +20°C to -60°C. The enthalpy values were converted to numbers of water molecules per ion exchange site and the results are shown in Table 3.2.

A comparison of the alkylated and protonated membranes can be seen in Figure 3.3, a plot of the number of free waters per ion exchange site versus fixed charge concentration. In the range of 2 eq/kg to 5.2 eq/kg, there is an average of approximately three fewer molecules of free water per ion exchange site in the alkylated membranes than in the protonated membranes at a given fixed charge concentration.

It can also be seen in Figure 3.3 that the number of free waters per ion exchange site for the alkylated series plateaus at a minimum near zero at a fixed charge concentration of 5.2 eq/kg while the protonated series reaches zero free waters per ion exchange site at a significantly higher fixed charge concentration of 6.4 eq/kg. At high fixed charge concentrations the quantity of freezable water in the membranes is small and within the errors associated with the DSC measurement and the differences between the alkylated and protonated membranes disappear.

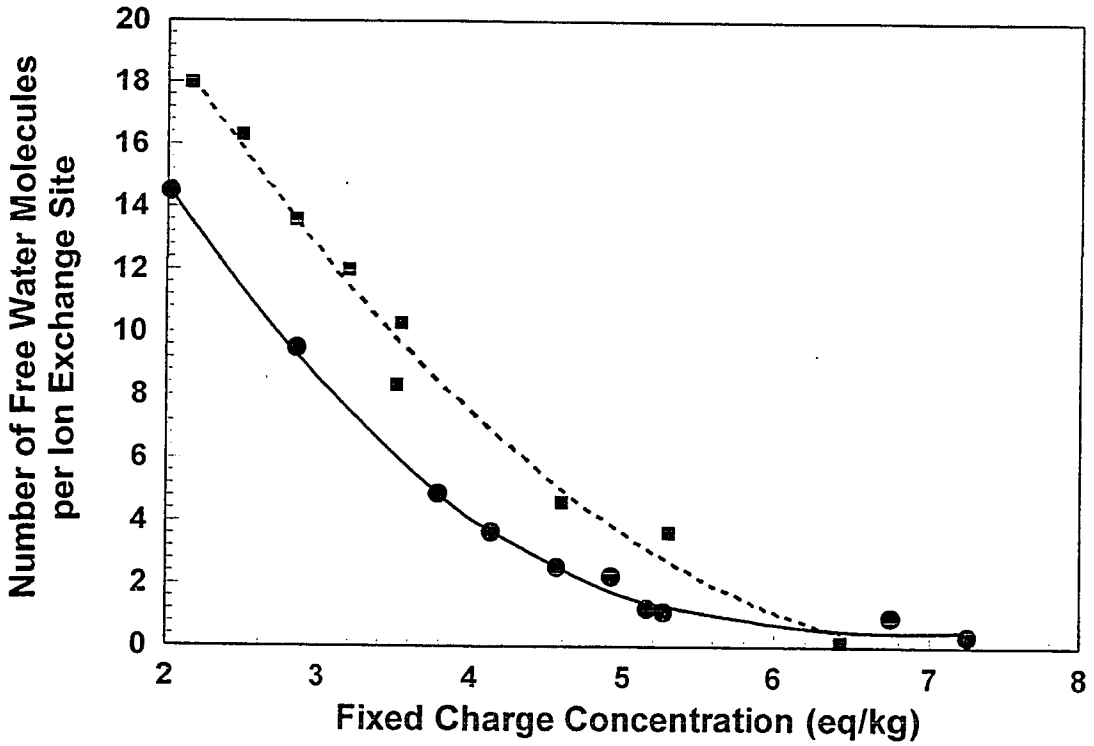

Fig 3.3. Free Water Molecules per Ion Exchange Site versus Fixed Charge Concentration: Alkylated-solid line; Protonated-broken line.

Since, at a given fixed charge concentration, the total number of water molecules per ion exchange site is the same for the both the alkylated and protonated membranes, the lower number of free water molecules per ion exchange site seen for the alkylated membranes resulted in an increase in the number of bound waters for this series.

The quantity of bound water for each membrane was calculated by subtracting the quantity of free water determined by DSC from the total water content of each membrane determined by gravimetric water uptake measurements and is given in Table 3.2. On average, the alkylated membranes have approximately three more bound water molecules per ion exchange site than the protonated membranes, which must, of course, agree with

the difference observed in free water contents from Figure 3.3. Both series of membranes maintained a fairly constant amount of bound water, the protonated membranes having, on average, 6 to 8 water molecules bound to each ion exchange site whereas the alkylated membranes have, on average, 9 to 10. The decrease in the number of bound waters per ion exchange site at fixed charge concentrations in the vicinity of 7 eq/kg for the alkylated series, Table 3.2, is caused by the overall decrease in water content of the membranes at this high fixed charge concentration, not an increase in the number of free waters per ion exchange site.

Each ion exchange site consists of both a pyridinium ion and a chloride ion and it has been estimated that the average number of water molecules in the combined hydration shells of these two ions is between 4 and 8, with the chloride ion having only one water of hydration [79]. It therefore appears that the alkylated membranes reported in this work contain slightly more bound water than would be found in simple pyridinium chloride model compounds.

In light of the DSC results, the results shown in Figures 3.2 can be explained. The relatively linear decrease in acid dialysis coefficients with increasing fixed charge concentration for both series of membranes shown in Figure 3.2 plus the similar acid dialysis coefficients of the alkylated and protonated membranes at a given fixed charge concentration suggest that the rate of acid transport through the membranes is dependent upon the total amount of water associated with each fixed charge site, that is the sum of free and bound water, independent of the quaternizing group being alkyl or proton.

The NaCl dialysis coefficient, however, does not decrease linearly with increasing fixed charge concentration for either series of membranes nor is the dialysis coefficient similar between the two series at a given fixed charge concentration, as seen in Figure 3.2. These differences in salt transport may possibly be due to the differences in free water content of the two series of membranes. Salt mobility is higher in regions containing free water as opposed to bound water [33], therefore the NaCl dialysis coefficients are higher in the protonated membranes, which contain a higher quantity of free water, and lower in the alkylated membranes, which contain less free water. The more rapid decrease in NaCl dialysis coefficients with increasing fixed charge concentration compared to the decrease in acid dialysis coefficients is caused by the fact that the free water content, which influences the salt transport, is decreasing at a faster rate than the total water content, which influences the acid transport. This results in the high selectivities observed at high fixed charge concentrations.

3.4.5. The Structure of Water

One of the pervasive themes in this thesis is the interpretation of the transport of species through the membranes in terms of the membrane water. Whether the membrane water is discussed with respect to its percent weight fraction in the membrane, or in terms of its structure, such as the degree of hydrogen bonding, or the concentration of fixed ionic groups in the membrane water, it is the water in the membrane through which the species are transported.

3.4.5.1. The Structure of Ice

Both X-ray and neutron diffraction have been used to determine the structure of ice [112]. The crystal structure adopted by ordinary ice is a tetrahedral orientation of hydrogen atoms about the oxygen atoms, based upon hydrogen bonds. Each water molecule can form four hydrogen bonds, two in which it acts as a hydrogen donor and two in which it acts as an acceptor. Neighbouring oxygen atoms are about 2.76 Å apart while the nearest nonhydrogen bonded neighbours are 4.5 Å apart, resulting in the relatively open structure and low density of ice, compared to liquid water.

3.4.5.2. The Structure of Liquid Water

The short range order in liquid water might be expected to resemble the short range order in ice since, as was indicated above, the latter is dictated by the properties of the H_2O molecule itself [112]. Indeed, X-ray diffraction studies of liquid water, which provide a radial distribution function for water molecules in a coordinate system in which the centre of one molecule is the origin, indicate that the number of nearest neighbour molecules is about 4.4, evidence that the local order about a given water molecule remains close to tetrahedral [112]. The radial distribution function also indicates that at distances of 8 Å or above the positions of water molecules are completely randomized, indicating that rapidly fluctuating structural changes are occurring.

3.4.5.3. Effects of Hydrophobic Groups on Water Structure

There is much evidence that dissolved nonpolar solutes such as hydrocarbons bring about changes in the state of water molecules, often referred to as the hydrophobic effect.

Calorimetric measurements of the transfer of hydrocarbons from organic solvents to water often yield negative enthalpy changes, indicating the formation of more hydrogen bonds or hydrogen bonds of greater strength. This is contrary to an increase in enthalpy of solution which would occur if the introduction of the hydrocarbon caused hydrogen bonds to be broken as the structure present in the water near the hydrocarbon was disrupted and the hydrocarbon itself could not form hydrogen bonds.

Transfer of hydrocarbons to water is also accompanied by a negative entropy change. The explanation for this phenomenon is that the water molecules around the nonpolar solute rearrange themselves to regenerate the broken hydrogen bonds and in doing so they create a higher degree of local order than exists in pure water, thereby producing a decrease in entropy [78,112].

In general, the hydrophobic effect, caused by introduction of hydrophobic groups into water, is the increase in the degree or strength of hydrogen bonding of the water surrounding the nonpolar solute and the resulting increase in the ordering of the water. The effect imposed on the structure of the water by hydrophobic groups can persist over several layers of molecules out from the hydrophobic groups.

Grigera and coworkers performed a molecular dynamics simulated study of a wall-water interface to probe the effects of hydrophobic surfaces on water structure [113]. A comparison was made between a hydrophilic and a hydrophobic wall, composed of water molecules and argon atoms respectively. It was concluded that the hydrophilic wall induced strong order on the water near to it, forcing the liquid into an icelike structure. The order, however, extended for only a few molecular diameters. For the hydrophobic wall, the ordering effect was milder but extended for several molecular diameters into the bulk water. These results agreed with their previous experimental data on the dielectric relaxation of water near hydrophobic compounds [114] where it was observed that the dielectric relaxation rate of water was slowed down by the dissolution of largely hydrophobic solutes, the rotational motions of water molecules in the hydration layers being two and three time slower than those of the bulk water.

Near infrared studies of the state of water in aqueous solutions of tetraalkylammonium bromides have yielded some insight into the effects of these hydrophobic cations on the structure of water. The IR bands caused by bonded and free OH species of HOD in D_2O were observed and the relative intensities of these bands were measured as a function of temperature [115]. As the temperature was increased there was a large increase in the intensity of the free OH band accompanied by a diminished intensity of the band of hydrogen bonded species. Addition of tetrabutylammonium bromide resulted in an increase in band intensity of the hydrogen bonded species and was

said to have "structure-making" character. Poly(vinylpyrrolidone) was also found to be a structure-maker [115].

Jolicoeur and coworkers have also studied the infrared spectra of aqueous solutions of tetraalkylammonium ions [116,117]. For R_4N^+ (R = Me to *n*Bu) it was found that the hydrogen bonding equilibrium was shifted in favour of hydrogen bonded species, similar to spectral changes produced by lowering the temperature of pure water.

Neutron scattering studies of the hydration structure near hydrophobic and hydrophilic amino acids has determined that the organization of the water hydrogen bonded network near the hydrophobic side chain was greater than in the case of the hydrophilic side chain [118]. Besseling has concluded, based on lattice fluid theory for water and molecular modeling, that the dissolution of small apolar molecules leads to a subtle enhancement of the pronounced structuring that is intrinsically present in water [119,120], a similar conclusion has been found by Mancera [121].

The results in this work are consistent with the conclusions found in the literature. In general, the introduction of hydrophobic molecules increase the number of hydrogen bonds present in adjacent water molecules [113]. In the membranes studied here, this corresponds to the increase in the amount of bound water that is seen upon the introduction of N-alkyl groups.

This increased ordering of the membrane water caused by the hydrophobic alkyl quaternizing groups is able to inhibit the transport of sodium and magnesium cations, as seen in the high selectivities found with the alkylated membranes in this chapter, thus the

ordered water is functioning as "bound" water. As it was discussed earlier, the relative amounts of bound and free water have little effect on proton transport, it is the total water content which determines the proton permeability.

Another possible explanation for the high selectivity of acid over metal chlorides in the alkylated membranes with a high fixed charge concentration is the formation of more discrete hydrophobic and hydrophilic regions in the membranes which would impede ionic diffusion. Eisenberg proposed the initial theory of clustering of ions in organic polymers [122]. He proposed the existence of two types of ionic aggregates: small aggregates consisting of pairs, triplets, quartets, etc. of ionic sites termed multiplets and larger aggregates, called clusters, resulting from the association of multiplets. At high fixed charge concentrations, the distance between multiplets decreases and their interaction increases to the point where clustering occurs, resulting in the formation of ionic domains separated by hydrophobic domains.

Other theories for ionic clustering have been proposed [40] and small angle X-ray scattering studies of the perfluorinated ionomer membrane Nafion have been explained on the basis of the formation of ionic clusters [41]. A model for the Nafion membrane has been proposed, consisting of approximately spherically shaped ionic clusters with a diameter of 4 nm, interconnected by short, narrow channels with a diameter of 1 nm estimated from hydraulic permeability data.

Impedance spectroscopy studies of a pH sensitive membrane containing poly(acrylamidocaproic acid) showed an increase in tortuosity of the ionic pathway with a

decrease in pH and temperature, explained on the basis of membrane water content and the formation of hydrophobic domains [123]. At high pH the hydration shells of the fixed ions were large enough to overlap, allowing ions to pass through the membrane in a unidirectional fashion. At low pH hydrophobic aggregation occurred, breaking the hydration shell links and giving a more tortuous pathway.

As the size of the quaternizing alkyl group increased in the membranes studied in this work, the water content decreased. This could allow for the formation of hydrophilic domains separated by hydrophobic domains created by the alkyl groups, thus markedly decreasing the transport of metal ions. In protonated membranes, even at high fixed charge concentrations, the formation of hydrophobic domains would not be as likely, and metal ion transport would not be reduced as effectively.

Preliminary investigations of the alkylated membranes studied in this thesis have been done to detect the presence of hydrophilic or hydrophobic domains within the membranes. Small angle x-ray scattering experiments were performed on some benzylated membrane samples, which detects domains in the size range of approximately 3 Å to 15 Å, and no clustering was found. Therefore, this effect cannot be confirmed as contributing to the increased selectivity of the alkylated membranes.

3.4.6. Effects of Ion Size on Transport Through Membranes

The higher selectivity of acid over magnesium chloride compared to acid over sodium chloride in diffusion dialysis testing of the membranes in this thesis has been

attributed to the more effective Donnan exclusion of the bivalent magnesium ion. Another possible consideration is that the larger hydrated size of the magnesium ion, compared to the sodium ion, might restrict its transport through the membranes with lower water contents and thus increase acid selectivity. In order to confirm that it is indeed the higher charge on the magnesium ion and not the larger hydrated size of the ion that results in the high selectivities found for membranes with high fixed charge concentrations, an investigation into the effect of ion size at constant ionic charge on diffusion through the membranes was performed.

The hydrated size rather than the crystallographic radius of ions determines their diffusivities in solution. Ionic diffusivities in membranes containing high percentages of water vary in the same order as in solution. For example, for the monovalent ions K^+, Na^+ and Li^+ in water the diffusion coefficients in 10^{-9} m^2/sec are: 1.96, 1.33 and 1.03 respectively [35]. The same trend in diffusivity is seen in membranes with high water contents [33]. The ionic diffusion coefficient is inversely proportional to the hydrated ion size, with size increasing in the order $K^+ < Na^+ < Li^+$. However, it has been reported that in membranes with low water contents the order of the diffusion parameters may be reversed and the crystallographic radius ($Li^+ < Na^+ < K^+$) determines the diffusion parameters [33,124].

In order to study the effects of ion size at constant charge on transport through the protonated and alkylated membranes, thereby removing any difference in selectivity based on electrostatic repulsion, a selected number of membranes were tested with a

diffusion dialysis solution containing 1.0 M HCl, 0.5 M LiCl, 0.5 M NaCl and 0.5 M KCl. The results are given in Table 3.4. The diffusivity of the cations is coupled to that of the counterion, in this case chloride, and therefore the diffusivity of a salt is a combination of the diffusivities of the two ions that move as a pair to maintain electroneutrality. The combined diffusion coefficient of two ions can be calculated from the equation 3.1:

$$D_{AB} = 2/(1/D_A + 1/D_B) \qquad (3.1)$$

where D_A and D_B are the diffusion coefficients of the cation A and the anion B. From this, the ratio of the apparent dialysis coefficients of two salts, obtained from diffusion dialysis experiments, can be compared to the ratio of the diffusion coefficients of the same two salts in bulk water. From equation 3.1 and using literature values for diffusion coefficients [35] it is found that in bulk water: $D_{KCl}/D_{NaCl} = 1.24$ and $D_{KCl}/D_{LiCl} = 1.46$.

The nascent polypropylene membrane with no pore-filling was tested by diffusion dialysis with the mixed monovalent acid/salt solution and the results were compared to those obtained from testing two protonated and two alkylated membranes, Table 3.4. As is shown in Table 3.4, the nascent membrane containing no incorporated poly(4-vinylpyridine) gave ratios of dialysis coefficients of pairs of salts that were in good agreement with the ratios estimated from the combined diffusion coefficients listed above. The protonated membranes, 422 and PV19, gave somewhat higher dialysis coefficient ratios than the nascent membrane, Table 3.4. However, the trend in diffusivity ratios remains the same as for the nascent membrane and is consistent with the diffusion

of the hydrated ions with potassium having the smallest hydrated radius and lithium the largest. The selectivity of potassium over sodium did not change as the water content of the membranes decreased from 422 to PV19. The selectivity of potassium over lithium showed a decrease with decreasing water of the membranes. This indicates that the increase in selectivity of acid over magnesium chloride compared to acid over sodium chloride that accompanies a decrease in water content for the protonated membranes is largely caused by an increase in Donnan exclusion as the fixed charge increases and not the size of the magnesium ion.

The alkylated membranes, 432me and 432bz, exhibit a reversal of the aqueous diffusivity order and appear to display a trend based on nonhydrated radius. This reversal is most evident in the case of 432bz. It is interesting to note that while membrane 432me has a much higher water content, and therefore a lower fixed charge concentration, than membrane PV19, 432me behaves as if it has a relatively low free water content that makes it difficult for hydrated cations to diffuse through the membrane. This is again an indication that there is a fundamental difference in the nature of the water in the alkylated membranes compared to the protonated membranes. If the size of the hydrated ion governed the rate of ion transport through the alkylated membranes, the selectivity of potassium chloride over lithium chloride would have increased with the benzylated membrane. Instead, the crystallographic size of the ions became a contributing factor to the membrane selectivity for ions of the same charge magnitude.

If the size of the non-hydrated ion were the only parameter controlling diffusion of cations through these membranes, the selectivity of acid over magnesium chloride compared to acid over sodium chloride would decrease with decreasing membrane water content since the crystallographic size of the magnesium ion is less than that of sodium. However, there is a dramatic increase in selectivity of acid over magnesium chloride compared to acid over sodium chloride, as seen earlier in this chapter, confirming that it is indeed the increase in Donnan exclusion with decreasing water content and increasing fixed charge concentration that is the cause of the high selectivity.

3.5. Conclusions

It has been shown in this chapter that poly(4-vinylpyridine)-filled microporous membranes quaternized with alkyl bromides produced anion exchange membranes that outperform a commercial membrane, Selemion DSV, in acid recovery by diffusion dialysis. Comparisons with membranes which were quaternized by protons, taken from Chapter 2, has shown that quaternization with alkyl groups produces membranes that show superior performance. This difference in behaviour is related to the amount and nature of the water contained in the membrane. The results have been interpreted in terms of the commonly used model of water being either "free" or "bound". While other models for the nature of the water in the membranes could be used, the important feature of these results is that the nature of the water is different in the alkylated membranes compared to the protonated membranes.

As the number of carbon atoms in the alkylating group increased, the membrane fixed charge concentration increased, the dialysis coefficients decreased and the selectivity of acid over sodium and magnesium chlorides increased dramatically. The acid dialysis coefficients of both the alkylated and protonated membranes were found to be dependent on the total membrane water content, that is the sum of bound and free water, while the salt dialysis coefficients were found to be more dependent on the free water content and the Donnan exclusion mechanism.

CHAPTER FOUR

ACID TRANSPORT MECHANISM AND WATER MOBILITY WITHIN POLY(4-VINYLPYRIDINE)-FILLED MEMBRANES

The transport of water soluble species through the membranes discussed in this thesis occurs within the aqueous domains of the membranes. It has been shown in Chapter three that the incorporation of hydrophobic groups into the membranes in the form of N-alkyl groups caused changes to occur in the degree of structure of the water in the membranes. This resulted in a dramatic increase in selectivity of acid transport over salt transport for the alkylated membranes compared to the protonated membranes.

The water within ion-exchange membranes is frequently thought of as being of two types, namely "free" and "bound" water. Differential scanning calorimetry was used to measure the relative amounts of free and bound water within the membranes. The alkylated membranes were found to have a higher amount of bound water than the protonated membranes, which led to a decrease in salt transport but little change in acid transport. These results were taken to suggest that acid transport occurring through both bound water and free water domains while salt transport was restricted to free water domains.

Two major questions arise from the work described in Chapter 3. The first concerns the mechanism of acid transport through the membranes and what, if any, are the differences in the transport mechanism between the protonated and alkylated membranes? The second concerns the mobility of the water in the membranes and, if there are any differences in membrane water mobility between the protonated and alkylated membranes, how do these differences relate to the transport of acid through the membranes?

This chapter reports an investigation into the mechanism of acid transport through the membranes as a function of the nature of the water in the membranes. The membranes are analyzed with respect to their total water content since Chapter 3 concluded that acid transport occurs through all of the membrane water, both bound and free. The fixed charge concentration is assumed not to play a significant role in determining the acid transport since protons are able to migrate through the membrane by the Grotthus mechanism, unaffected by Donnan exclusion, as described in section 1.2.3. Analyzing the behaviour of the membranes as a function of membrane water content allows for a fundamental comparison of protonated membranes to alkylated membranes. In this manner, questions regarding the differences in the mechanism of acid transport between the protonated and alkylated membranes can be answered. The activation energies of acid diffusion as well as the entropy terms associated with the acid diffusion process have been measured. These parameters are used to help describe the mechanism of acid

transport and understand the differences in behaviour of the protonated and alkylated membranes.

The results of the DSC experiments described in Chapter 3 were analyzed in terms of the relative amounts of free and bound water in the protonated and alkylated membranes. An examination of the mobility of the water in the membranes will allow for a more thorough interpretation of the DSC results and assist in the interpretation of the mechanism of acid transport through the membranes. Pulsed Field Gradient NMR has become an increasingly popular technique for examining the mobility of molecules in heterogeneous systems such as water in membranes. This technique is used here to determine the self diffusion coefficients of water in the protonated and alkylated membranes.

The determination of electrical properties of the membranes, such as membrane resistance, provides information about the transport of ions through the membranes. The membrane electrical resistance can be related to the results obtained from the diffusion studies thus providing further information about ion mobility within the membranes. Impedance spectroscopy (IS) is a technique that can be used to determine the electrical resistance of materials, as well as other electrical properties, and is used here to determine the resistances of the protonated and alkylated membranes.

The combined results of this chapter produce a consistent picture which explains both the mechanism of acid transport through the membranes and the observed differences between the alkylated and protonated membranes.

4.1. Acid Diffusion Through Membranes

In section 1.2.3 the transport of protons through membranes was described as occurring by a combination of simple diffusion and the Grotthus mechanism, in order to account for the anomalously high diffusion coefficient of the proton. In order to study the mechanism of acid transport through the membranes discussed in this thesis, it was necessary to perform diffusion dialysis experiments using acid alone, without the presence of any other salt.

The introduction of salt into the acid feed solution results in the determination of an apparent dialysis coefficient for acid rather than a true dialysis coefficient. The transport of protons, or any other cation, across the membrane from the feed solution to the permeate solution is always accompanied by the transport of an equivalent amount of a counterion. Thus, the driving force for diffusion has two components, the difference in chemical potential of the cation between feed and permeate solutions and the difference in chemical potential of the anion between feed and permeate solutions. If the feed solution is composed of only an acid solution, such as hydrochloric acid, then the differences in chemical potentials, and therefore driving forces, of the cation and anion are equal and the dialysis coefficient found for the acid will be a true dialysis coefficient. If, however, the feed solution contains an additional salt, sodium chloride for example, the difference in chemical potential of the chloride ion will be greater than that of the protons. This results in an increase in the apparent dialysis coefficient of the acid in the presence of added salt because the driving force, ΔC, used in the equation to calculate the

apparent dialysis coefficient, is the acid concentration difference which is smaller than the chloride concentration difference. As the selectivity of the membranes towards acid over salt increases, this effect further increases the apparent dialysis coefficient of acid since little salt transport is occurring and chloride transport is largely accompanied by proton transport.

4.2. Pulsed-Gradient Spin-Echo NMR

There has been an increase in the use of magnetic field gradients in NMR over the last decade [125]. An example of one such application is the use of pulsed-gradient spin-echo (PGSE) NMR for measuring the self diffusion coefficients in multicomponent systems [126].

Any echo sequence is susceptible to the effects of diffusion. Diffusion measurements are generally performed with some variation of the Hahn spin echo or stimulated echo pulse sequences incorporating field gradient pulses [125]. Fig 4.1 shows the Stejskal and Tanner pulsed field gradient (PFG) sequence, the simplest sequence and the one that was used to perform the experiments in this chapter [127]. It is a Hahn spin echo pulse sequence with a gradient pulse inserted into each τ period. The second half of the echo is used as the free induction decay (FID).

The main magnetic field is in the z direction, and the gradient pulses are also applied along the z direction. The application of the $\pi/2$ pulse rotates the magnetization of

the spins from the z axis into the x-y plane. The spins then dephase during the first τ period. At a time, τ, a π pulse is applied which reverses the dephasing process so that an echo is formed at time 2τ. The first applied magnetic field gradient pulse spatially "labels" the spins (molecules) with respect to their position along the z axis. The spins then continue to diffuse during the time Δ, at which point they are subject to a second gradient pulse of equal but negative magnitude. If the spins have not moved with respect

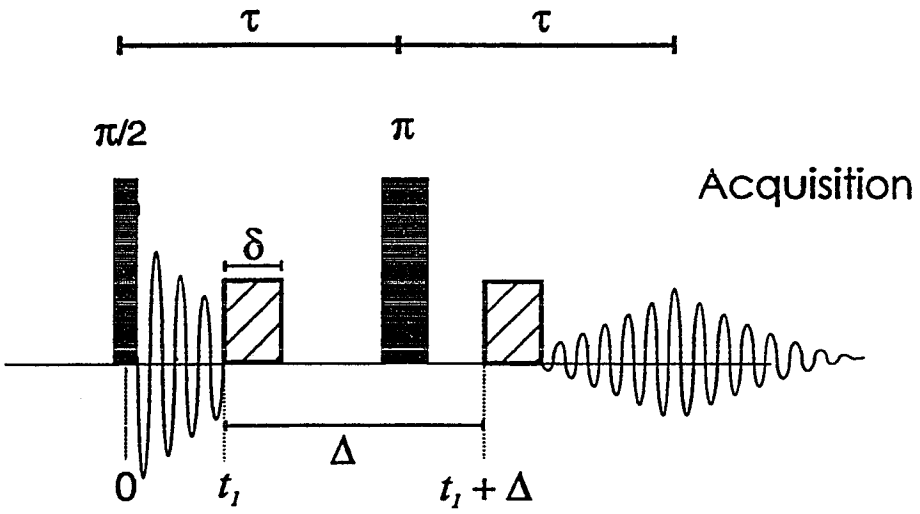

Fig. 4.1. The Stejskal and Tanner PFG sequence. A Hahn spin echo pulse sequence with a gradient pulse of duration δ and a magnitude G inserted into each τ period. The separation between the leading edges of the gradient pulses is denoted by Δ.

to the z axis the effect of the two applied gradient pulses cancel, but if the spins have moved, the degree of dephasing due to the applied gradient is proportional to the displacement in the direction of the gradient. Any dephasing will result in a diminished echo signal, at time 2τ, and thus the effect of diffusion is monitored by the attenuation of the echo signal [125].

The spin echo signal is generally normalized by dividing the echo signal obtained from the pulsed field gradient experiment by the echo signal obtained in the absence of field gradients. The normalized signal intensity is related to the diffusion coefficient according to Equation 4.1:

$$I/I_0 = \exp[-(\gamma G\delta)^2(\Delta - \delta/3)D] \qquad (4.1)$$

where I is the echo amplitude of the pulsed field gradient experiment, I_0 is the initial echo amplitude in the absence of field gradients, γ is the magnetogyric ratio of the nucleus, G is the strength of the gradient pulse, δ is the gradient pulse duration, D is the self-diffusion coefficient and Δ is the interval between the two gradient pulses. The experiment is performed by varying one of the experimental variables, δ, Δ or G. In this thesis, δ is varied and the self diffusion coefficients of water in the membranes is determined by plotting the logarithm of the ratio of I/I_0 as a function of $(\gamma G\delta)^2(\Delta - \delta/3)$. The slope of the resulting straight line plot is the negative of the self diffusion coefficient of the membrane water. This information on the mobility of the membrane water lends insight into the structure of the water within the membranes and assists in understanding the differences in transport behaviour between the alkylated membranes and the protonated membranes.

4.3. Impedance Spectroscopy

Impedance spectroscopy (IS) is a powerful alternating current (AC) method of characterizing many of the electrical properties of materials. It may be used to investigate

the dynamics of bound or mobile charge in the bulk or interfacial regions of any kind of solid or liquid material: ionic, semiconducting, mixed electronic-ionic and even insulators (dielectrics) [128,129]. IS has been used for purposes ranging from conductivity measurements of solid electrolytes to the study of corrosion in metals [130]. The most common approach to the IS experiment is to measure impedance by applying a single frequency voltage to the system under study and measuring the phase shift and amplitude of the resulting current at that frequency.

Although there are direct current (DC) techniques available for electrical measurement, AC methods represent the most popular approach to determining the electrical properties of polymer electrolytes. The data from AC techniques carry information not only about the long range migration of ions but also about polarization phenomena occurring within the cell, the relaxation of trapped ions, for example [131]. The application of a DC potential also results in the accumulation of an ionic charge at one side of the sample at the sample/electrode interface to balance the accumulation or depletion of electrons at the electrode. The charge accumulation creates an interfacial potential which rises rapidly on the application of a direct current. The interfacial potential can be rendered negligible by using an alternating current.

The impedance experiment consists of applying a sinusoidal voltage to the cell (a cell is made up of the sample under study and the electrodes on either side of the sample) at a specific frequency and measuring the resulting current passing through the cell. In a DC measurement the current flowing, I, is related to the potential, V, by just one

parameter, the resistance, R, by a relationship known as Ohms law: $R = V/I$. The resistance, R, can be related to the electrical properties of the cell. In the case of an AC voltage, however, as is applied in an IS experiment, two parameters are required to relate the current to the applied potential. One represents the opposition to the flow of charge and is equal to the ratio of the voltage and current, analogous to the resistance in DC measurements [131]. The other parameter, θ, is the phase difference between the voltage and current (generally the current is not in phase with the voltage). The combination of these parameters represents the impedance, Z, of the cell.

Generally both the magnitude of the impedance $|Z| = V/I$ and its phase angle θ are functions of the applied frequency. IS involves measuring the impedance of the cell as a function of the frequency of the applied signal over a wide frequency range, typically 1 mHz to 1 MHz. The impedance of a cell is a vector quantity, possessing both magnitude and phase, and as such it may be represented as a point on a vector diagram, Fig. 4.2.

The impedance for each frequency is measured and represented by a point on the vector diagram. The distance of the point from the origin corresponds to the magnitude of the impedance and the angle formed with the x-axis corresponds to the phase difference between the voltage and current.

The impedance vector may also be represented by its x and y components, $|Z|\cos\theta$ and $|Z|\sin\theta$, or by a complex number represented by the symbol Z^* where $Z^* = Z' - jZ''$, Fig. 4.2. The use of j rather than i as the complex number operator, $\sqrt{-1}$, avoids confusion with the commonly used symbol for current.

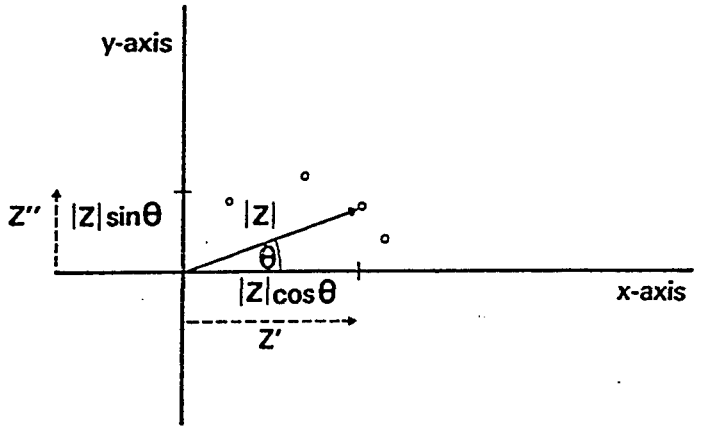

Fig. 4.2. Representation of the impedance, Z, of a cell on a vector diagram. Z' and Z'' are respectively the real and imaginary components of the complex impedance $Z^* = Z' - jZ''$.

The IS experiment typically consists of acquiring the impedance of a cell as a function of the signal frequency at a constant potential and presenting the results in the form of a complex impedance plot. The complex impedance plot is then interpreted by comparison with a model electrical circuit, generally comprised of resistors and capacitors. A sinusoidal voltage applied across a resistor is always in phase with the current passing through it, $\theta = 0$, and the magnitude of the impedance is simply given by the resistance $|Z| = R$. The impedance is independent of frequency and is represented in the complex plane by a point at a distance R along the real axis (the x axis). In the case of a capacitor, the voltage lags behind the current by 90° and the magnitude of the impedance is frequency dependent: $|Z| = 1/\omega C$, where ω is the angular frequency in radians and C represents the capacitance [131]. Therefore, large capacitances or high frequencies give rise to small impedances. The impedance of a capacitor is represented by a vertical spike coincident with the imaginary axis in the complex plane.

Two models of electrical circuits, each composed of a resistor and a capacitor, will now be examined to illustrate how these models can help in the interpretation of the complex impedance plot obtained from the IS experiment. The first model is that of a resistor and a capacitor in series. The schematic of the model and the resulting complex impedance plot is shown in Fig. 4.3(a). The impedance of the model is given by Equation 4.2. and defines a vertical spike displace a distance R along the real axis in the complex impedance plot.

$$Z^* = R - j/\omega C \tag{4.2}$$

As the frequency is increased, the impedance of the capacitor is reduced and the contribution of the imaginary component to the impedance decreases.

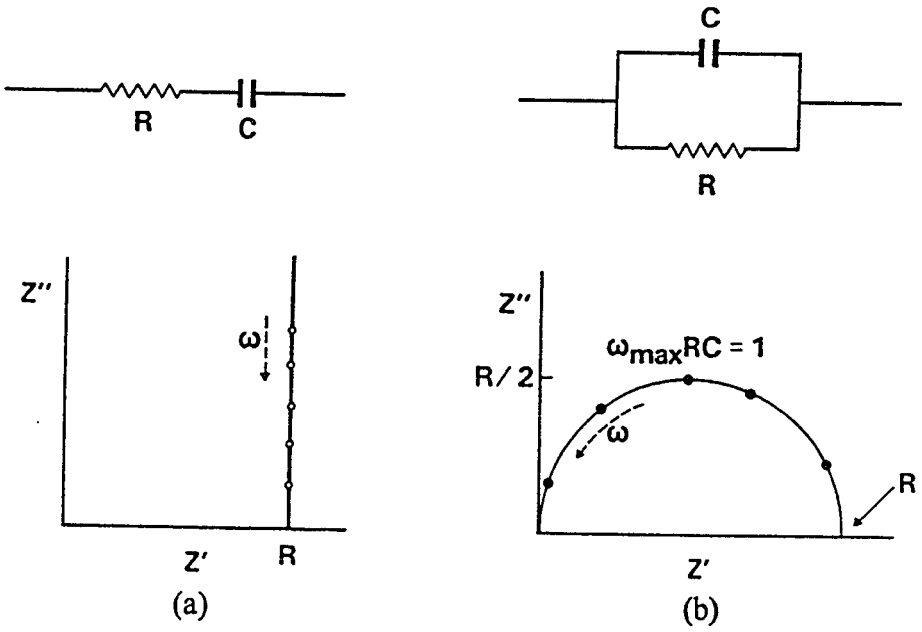

Fig. 4.3. Model circuits and complex impedance plots for a combination of a resistor, R, and a capacitor, C, (a) in series and (b) in parallel.

The second model is that of a resistor and capacitor in parallel, Fig. 4.3(b). When the two components are connected in parallel, the impedance is given by Equation 4.3.

$$Z^* = 1/(1/R + j\omega C)$$

$$= R[1/(1 + (\omega RC)^2)] - jR[\omega RC/(1 + (\omega RC)^2)] \quad (4.3)$$

Equation 4.3 defines a semicircle in the complex impedance plane with a diameter R extending along the real axis from the origin, Fig. 4.3(b).

In terms of the study of ion exchange membranes by IS, the cell can be described as being composed of a solid electrolyte sandwiched between two blocking electrodes, which means that the mobile species in the electrolyte do not participate in any electrode reactions. An AC voltage is applied to the cell and the frequency is varied. The equivalent circuit representing this cell is the same as that in Fig. 4.3(b), namely a resistor and capacitor in parallel. The electrodes become alternately positively and negatively charged and the alternating field across the ion exchange membrane causes the mobile ions to migrate back and forth in phase with the voltage. The resistance to migration of the mobile ions is represented by the resistor, R, which represents the bulk resistance of the sample. Concomitantly, the fixed charges on the polyelectrolyte become polarized in the alternating field. This dielectric polarization is represented by the capacitor, C. The bulk polarization and resistance are physically in parallel in the cell, therefore their representative components, R and C, are connected in parallel. Thus, the bulk resistance, R, of the membrane sample in the cell can be extracted from the intercept of the semicircle with the real axis in the complex impedance plot.

The pore-filled membranes studied in this work are examples of solid electrolytes and are therefore suitable for study by IS techniques. The information obtained from such experiments provides insight into the ionic mobility within the membranes in terms of the electrical impedance. IS provides another probe with which to examine the ionic transport behaviour of the membranes under electrochemical conditions which may be compared to their behaviour under diffusion dialysis conditions and assist in understanding the differences in the properties of the protonated and alkylated membranes.

4.4. Experimental

4.4.1. Materials

The substrate used in this chapter is the same as that used in the previous chapters, a polypropylene microfiltration membrane with an average pore diameter of 0.26 μm, an average starting thickness of 53 μm and a porosity of approximately 60 vol% (3M Company). 4-Vinylpyridine and divinylbenzene (55% meta and para isomers, 45% ethylvinylbenzene) (Aldrich) were purified by vacuum distillation. 2,2-Dimethoxy-2-phenylacetophenone (DMPA) was used as a photoinitiator. *N,N*-Dimethylformamide, dimethylsulfate, bromoethane, 1-bromopropane, 1-bromobutane, 1-bromopentane, 1-bromohexane and benzylbromide (Aldrich) were used as received. Mesityl oxide was distilled prior to use. Methanol, hydrochloric acid and sodium sulfate were reagent grade and used without further purification. The water used was carbon filtered and deionized.

4.4.2. Membrane Preparation

The membranes of the four hundred series (membranes with identification numbers beginning with 4) were prepared by a photo-initiated radical copolymerization of 4-vinylpyridine and DVB in the pores of the polypropylene substrate as described previously in section 2.5.2. Membranes of the five hundred series (membranes with identification numbers beginning with 5) were also prepared using the same radical copolymerization reaction but with a different apparatus.

Instead of using the photo reactor that was described in section 2.5.2.1 which did not allow for good control over the mass loadings of the membranes, the five hundred series membranes were irradiated while sandwiched between release sheets. The substrate membrane was placed on a glass plate and the monomer solution (not degassed) containing 4-vinylpyridine, DVB and initiator (DMPA) was distributed over the membrane using a Pasteur pipette. The nominal percent DVB content of the pore-filling polymer was taken as the weight ratio of DVB isomers to 4-vinylpyridine in the monomer mixture. The monomer solution was distributed evenly over the membrane by a teflon roller. The membrane, now filled with the monomer solution, was then lifted off the glass plate and placed between two overhead transparencies (release sheets) on top of another glass plate. The transparency/membrane sandwich was then pressed from the center outwards to remove excess monomer solution and air pockets from between the membrane and the release sheets. The perimeter of the sandwich was then sealed with transparent tape.

The membrane sandwich was irradiated at 350 nm for 1 h at room temperature, removed from the glass plate and the top release sheet was peeled away from the pore-filled membrane. It was then necessary to soak the membrane in methanol for a short period of time to release it from the bottom release sheet.

The membranes were extracted with hot methanol (Soxhlet) and equilibrated in a three-fold cycle involving 1M HCl, a water rinse, followed by 1M NaOH. The equilibration time in each solution was 12 h. After the last base cycle the membranes were soaked in deionized water followed by methanol and then dried under vacuum prior to quaternization.

The membranes were characterised by mass gain, thickness, ion exchange capacity and water content as described in Chapter 2. Diffusion dialysis experiments at varying temperatures were performed using a solution of hydrochloric acid, PGSE NMR experiments were done to determine the self diffusion coefficients of the membrane water, diffusion dialysis experiments using a solution of mesityl oxide in water were performed and the membranes were finally tested by impedance spectroscopy.

4.4.2.1. Alkylation of the Pyridine Nitrogen Atoms

All quaternization reactions were conducted in DMF solutions at room temperature as described in section 3.5.2.1. Membranes 406me, 426me and 431me were prepared by placing the membranes in their free base form into a 10 % (v/v) solution of dimethylsulfate for three days. Membrane 513 was used to produce the seven membranes

which comprise the series of membranes with identical DVB contents but different alkyl groups.

Membrane 513 was cut into pieces approximately 5 cm × 6 cm and the pieces in their free base form were placed in the appropriate solution of alkyl bromide. N-methylation and N-benzylation of pieces of membrane 513 (producing membranes 513me and 513bz) were achieved using 10% (v/v) solutions of dimethylsulfate and benzylbromide, respectively for 7 days. The N-ethyl, N-propyl, N-butyl, N-pentyl and N-hexyl derivatives of membrane 513 (denoted as 513et, 513pr, 513bu, 513pe and513he) were prepared by treatment of the membranes with 50% (v/v) solutions of bromoethane, 1-bromopropane, 1-bromobutane, 1-bromopentane and 1-bromohexane, respectively for 21 days. The membranes were then removed from the quaternizing solutions, soaked in methanol, 0.5 h, deionized water, 2 h, and 1M NaCl for approximately 18 h to convert the membranes into their chloride forms.

The degree of quaternization and water content were determined as described in section 3.5.2.2.

4.4.3. Diffusion Dialysis Testing With Hydrochloric Acid at Varying Temperatures

Diffusion dialysis experiments were carried out using the cell described in section 2.5.2.9 with an aqueous feed solution of 25 mL of 2 M HCl and a permeate solution initially composed of 25 mL of deionized water. Four experiments were performed with each membrane, two experiments at approximately 4°C and two experiments at

approximately 38°C. Diffusion of the acid was allowed to occur for a measured time and then the solutions were removed from each side of the cell and analyzed for acid content by titration with NaOH. The acid dialysis coefficient, U (HCl), was determined using equations 2.8 and 2.9 from section 2.5.2.9.

In order to compare the acid transport properties of different membranes, it was necessary to convert the acid dialysis coefficient to an apparent diffusion coefficient, D_{app}, normally expressed in units of m^2/s. This normalizes the data to allow for comparisons to be made between the membranes as if they were all the same thickness. The conversion of the dialysis coefficient, U, which has units of $mol/h \bullet m^2 \bullet \Delta C$ (or $L/h \bullet m^2$), to the apparent diffusion coefficient was done using Equation 4.4.:

$$D_{app} = U \bullet 2.777 \times 10^{-13} \bullet l \qquad (4.4)$$

where D_{app} is the apparent diffusion coefficient in m^2/s, U is the dialysis coefficient in $mol/h \bullet m^2 \bullet \Delta C$ and l is the membrane thickness in micrometres.

4.4.3.1. Determination of the Activation Energy of Diffusion of HCl

The activation energy of diffusion of hydrochloric acid through the membranes was determined from Equation 4.5, the Arrhenius equation, by plotting the natural logarithm of D_{app} versus 1/T in a typical Arrhenius plot for each membrane, the slope of which equals $-E_a/R$:

$$D_{app} = A \exp(-E_a/RT) \qquad (4.5)$$

where A is the preexponential factor, in m^2/s, E_a is the activation energy of diffusion, in J/mol, R is the gas constant, 8.314 J/Kmol and T is the absolute temperature in Kelvin.

4.4.3.2. Determination of the Entropy of Activation of Diffusion of HCl

The entropy of activation, $\Delta S^{\ddagger}$, for diffusion of HCl through the membranes is measured indirectly as the quantity $d(\exp(\Delta S^{\ddagger}/R)^{1/2})$, estimated from the absolute reaction rate equation for D_{app}, Equation 4.6, introduced by Eyring [132]:

$$D_{app} = (ed^2kT/h)\exp(\Delta S^{\ddagger}/R)\exp(-E_a/RT) \qquad (4.6)$$

where e is the base of natural logarithms, 2.71828, d is the distance between equilibrium positions in the process of diffusion in metres, k is Boltzmann's constant, 1.38×10^{-23} J/K, T is the absolute temperature in Kelvin, h is Planck's constant, 6.626×10^{-34} J•s, R is the gas constant and E_a is the experimentally determined activation energy of diffusion.

In the absence of information as to the correct value of d, Equation 4.6 may be applied to estimate the quantity $d(\exp(\Delta S^{\ddagger}/R)^{1/2})$. The relative value of this function may give an indication of the mechanism of diffusion. Larger values of this function may suggest that the diffusion is accompanied by the breakage of bonds or by significant structural changes [133,134], while smaller values may imply that an increase in ordering is occurring in the diffusion step.

4.4.4. Self Diffusion Coefficient of Water by Pulsed Gradient Spin Echo NMR

4.4.4.1. Sample Preparation

All membrane samples to be measured were cut to approximately 5 cm × 2 cm in size and equilibrated in 1 M HCl. They were then rolled into a tight cylindrical shape and placed in standard, 5 mm diameter NMR tubes with the 1 M HCl solution. Immediately before the NMR experiment, the HCl solution was withdrawn from the NMR tubes with a syringe and the tubes were inverted and excess solution was shaken out. The tubes were capped and placed in the NMR spectrometer.

4.4.4.2. PGSE NMR Diffusion Coefficient Measurements

The PGSE NMR measurements were made using a MRI (magnetic resonance imaging) probe with actively shielded gradient coils (Doty Scientific, Columbia, SC) installed in a Chemagnetics CMX-300 NMR spectrometer operating at 300 MHz for protons. Experiments were performed in the facilities of Dr. P. M. MacDonald at the University of Toronto, at Mississauga. A standard Stejskal-Tanner PGSE sequence was employed, [$(90°_x)$-τ-$(180°_y)$-τ-acquisition], with gradient pulses applied during τ. The PGSE experiments were performed at 25°C with a 24 μs 90° pulse length, a 100 ms delay between gradient pulses, and 8 scans. The gradient pulse was applied to the z-direction only and the duration of the gradient pulse was ramped from 1 ms to 5.75 ms by 0.25 ms

increments. The gradient strength was 56.0 G/cm and was calibrated by using the diffusion coefficient of 2 vol% H_2O in D_2O ($D_{H2O} = 1.902 \times 10^{-9}$ m^2/s [135]).

The self diffusion coefficient of the water in the membrane was determined by plotting the logarithm of the ratio of I/I_o as a function of $(\gamma G\delta)^2(\Delta - \delta/3)$ (Equation 4.1.). The slope of the resulting straight line plot is the negative of the self diffusion coefficient.

4.4.5. Diffusion Dialysis Testing With Mesityl Oxide

Diffusion dialysis experiments were carried out using the cell described in section 2.5.2.9, the same cell used for acid diffusion experiments. The feed and permeate chambers were simultaneously filled with 25 mL each of a 0.003 M solution of mesityl oxide in water and deionized water, respectively. The cell temperature was maintained at 25°C and both chambers were stirred at 25 revolutions per second. Diffusion was allowed to occur for a measured time and then the solutions were removed from each chamber. The experiment was repeated three times for each membrane tested. The permeate solution was analyzed for mesityl oxide concentration by UV absorption spectrophotometry using a CARY 50 UV/VIS Spectrophotometer (Varian). The mesityl oxide concentration in the feed solution at the end of the diffusion experiment was calculated based upon the amount of mesityl oxide transported to the permeate chamber and assuming no water transport or volume changes in the two chambers. The absorption band at 244 nm was measured. The molar absorptivity of MO of 10,770 cm^{-1} M^{-1} was

determined by calibration with a series of mesityl oxide standard solutions of concentrations ranging from 10^{-5} M to 10^{-4} M.

The time allowed for diffusion of the mesityl oxide in the diffusion dialysis experiment was adjusted so that the resulting permeate solution had a mesityl oxide concentration within the range of the standard solutions and no dilution was required prior to UV analysis.

The mesityl oxide dialysis coefficient, U (MO), was determined using equations 2.8 and 2.9 from section 2.5.2.9 and was converted to an apparent diffusion coefficient using equation 4.4.

4.4.6. Impedance Analysis of Membranes

Stainless steel circular electrodes were used in this study with a diameter of 1 cm and a thickness of 0.5 cm. The area of the electrodes was 0.785 cm^2. A stainless steel machine screw was threaded into the side of each electrode to serve as an electrical connection. The membrane samples were equilibrated in 1 M HCl and cut into disks with a 1 cm diameter punch. Immediately prior to the impedance experiment, the membrane disk was removed from the 1 M HCl solution, its thickness was measured by micrometer and sandwiched between the two electrodes without surface drying the membrane sample in order to establish a good electrical contact between the membrane and the electrode. The sandwich was held together by a spring clip to provide a reproducible pressure and a good contact between the sample and the electrode. The membrane thickness was

measured again after the impedance experiment and no significant decrease in sample thickness due to the spring clamp pressure was detected. Two sample disks cut from each membrane were tested and the impedance measurement was performed two times for each disk.

Electrical impedance measurements were taken over the frequency range of 0.5 Hz to 1 MHz at a potential of 60 mV using a Schlumberger SI1250 frequency response analyzer. The data were processed with Z-Plot software.

4.5. Results and Discussion

4.5.1. Membrane Preparation

The membranes discussed in this chapter include the four hundred series that were discussed in chapters 2 and 3 as well as a new series of membranes, denoted as the five hundred series, produced by a different method than the four hundred series.

Fig 4.4 shows how the mass gains of the five hundred series membranes vary with irradiation time with a constant DVB content and initiator concentration. An S shaped curve is obtained which is typical of polymerization reactions. An induction period of approximately 10 minutes is apparent in Fig. 4.4 where no significant mass gain occurs, followed by a steady increase in mass gain with time which levels off at approximately 200% at an irradiation time of one hour, consistent with the previously calculated

maximum mass gain, based upon the available pore volume present in the polypropylene substrate.

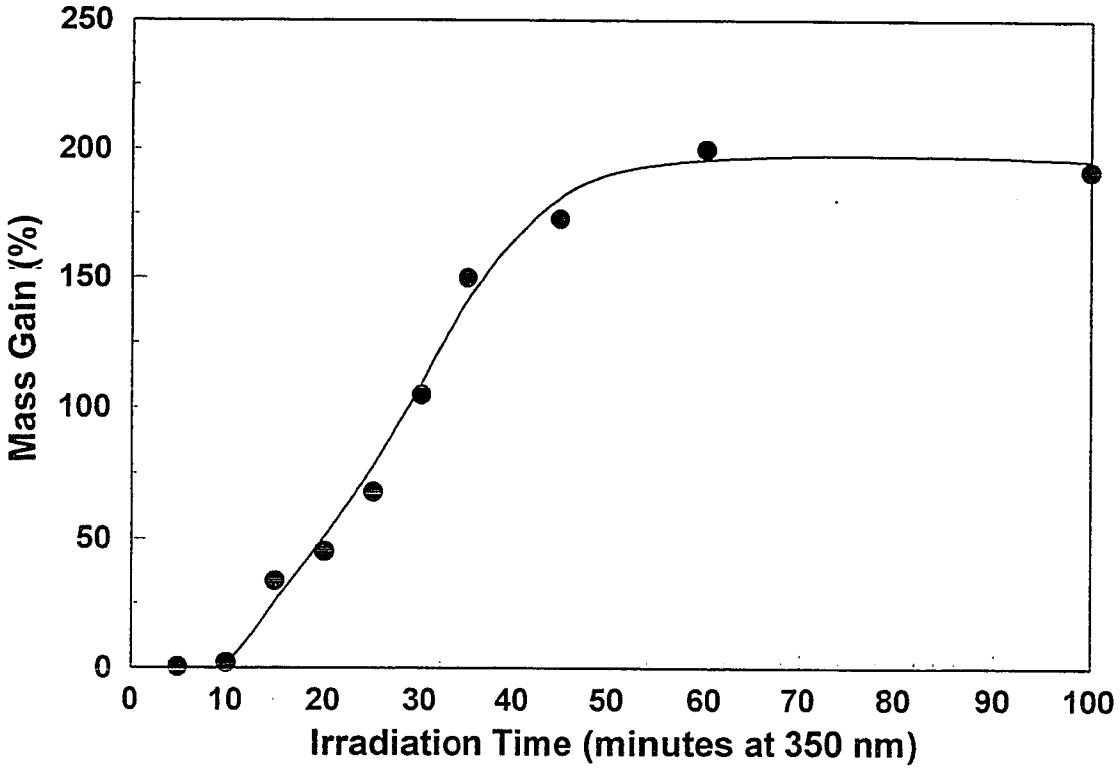

Fig. 4.4. Mass Gain versus Irradiation Time

The fabrication method used to produce the five hundred series membranes, as described in section 4.2.2, gave good control over the mass loading of the membranes, as can be seen in Fig. 4.4. This control was not possible using the photo reactor method described in section 2.5.2.1 where one side of the membrane was exposed to a nitrogen atmosphere during the irradiation and polymerization step. By sandwiching the monomer filled membrane between release sheets and then irradiating, it was found that the mass loading of the membranes could be controlled by varying the irradiation time.

Based upon the optimum irradiation time of one hour, as determined from Fig. 4.4, membrane 513 was produced by irradiation for one hour, to produce a membrane with the same mass gain and DVB content as membrane 432, which was used to form some of the alkylated membranes discussed in chapter 3. N-alkylation of pieces of membrane 513 was carried out by treatment with a series of alkyl bromides, in the same manner as discussed in section 3.6. The degree of N-alkylation that was achieved was between 75% and 80% of the calculated maximum based upon the total pyridine groups available. This degree of alkylation is comparable to the results obtained for the alkylation of the four hundred series membranes.

4.5.2. Characterization of Membranes

The membranes were characterized in terms of their thickness, mass-loading, fixed charge concentration and water content. The data for the membranes studied in this chapter are summarized in Table 4.1. The first nine membranes in Table 4.1 were taken from the second series of membranes in Chapter 2 and have DVB contents ranging from 0.54% to 44.1%, mass loadings in the range of 147% to 208%, thicknesses from 131 μm to 67 μm and were all tested in protonated form.

Membranes 406me, 426me, 431me and 513me were produced by methylation of pieces of membranes 406, 426, 431 and 513 respectively, producing a series of four membranes with similar mass loading, identical alkylating groups but DVB contents ranging from 1.3% to 25.2% and thicknesses ranging from 119 μm to 72 μm.

Table 4.1. Properties of Membranes

Membrane	Group on Nitrogen	DVB (%)	Mass Gain[1] (%)	Thickness[2] (μm)	Fixed Charge Conc. (eq/kg)[3]	% Water Content[4]
422	hydrogen	0.54	147	131	2.2	67
406	hydrogen	1.3	157	107	2.5	63
415	hydrogen	2.5	173	120	2.9	62
412	hydrogen	4.1	172	96	3.3	59
417	hydrogen	6.1	182	94	3.6	55
428	hydrogen	8.3	181	96	3.5	53
431	hydrogen	15.4	201	88	4.6	46
432	hydrogen	24.8	208	71	5.3	41
PV19	hydrogen	44.1	193	67	6.4	33
406me	methyl	1.3	157	119	2.0	65
426me	methyl	4.1	191	109	2.9	57
431me	methyl	15.4	201	86	3.8	46
513me	methyl	25.2	191	72	4.2	41
513et	ethyl	25.2	191	71	4.4	39
513pr	n-propyl	25.2	191	71	4.5	38
513bu	n-butyl	25.2	191	72	4.9	35
513pe	n-pentyl	25.2	191	72	5.9	30
513he	n-hexyl	25.2	191	71	6.2	29
513bz	benzyl	25.2	191	70	6.9	26

[1] Mass loading of membrane by percent weight before quaternization, ± 3%
[2] Thickness of membrane in 1 M HCl solution after quaternization, ± 5%
[3] Fixed charge concentration as equivalents of ion exchange sites per kg of water in the membrane, ± 5%
[4] Percent water content by weight, ± 5%

Membranes 513et, 513pr, 513bu, 513pe, 513he and 513bz were produced by N-alkylation of pieces of membrane 513 with the appropriate alkyl bromide. Including membrane 513me, this gave a series of seven membranes with identical mass loadings and DVB contents, but varying alkyl groups on the pyridine nitrogen atom.

4.5.2.1. Fixed Charge Concentration and Water Content

The first nine membranes in Table 4.1 have been discussed previously with respect to the increase in fixed charge concentration with increasing DVB content, section 2.6.1.2.3. The observed trend was attributed to the decrease in water content of the membranes with increasing DVB content.

A clear trend is seen with the alkylated membranes in terms of their fixed charge concentrations and water contents. A steady increase in fixed charge concentration from 2.02 eq/kg to 6.88 eq/kg is seen for membrane 406me through to membrane 513bz, Table 4.1. This is a result of a decrease in membrane water content from 65% to 26%, seen for membrane 406me through to membrane 513bz. The first four alkylated membranes, 406me, 426me, 431me and 513me, are all alkylated with the methyl group and the decrease in water content is a result of the increase in DVB content and decrease in membrane thickness over these four membranes.

The last seven alkylated membranes, 513me, 513et, 513pr, 513bu, 513pe, 513he and 513bz have identical DVB contents and mass gains, prior to alkylation, but were quaternized with alkyl groups of increasing size. The membranes in this series all have

similar thicknesses in the range of 70 μm to 72 μm. The decrease in water content over these seven membranes is caused by an increase in the size of the N-alkyl group.

4.5.3. Mechanism and Thermodynamic Parameters of Acid Diffusion Through Membranes

In order to determine the activation energy of acid diffusion and the entropy term associated with the acid diffusion process the nineteen membranes from Table 4.1 were all subjected to variable temperature diffusion dialysis experiments using a feed solution of 2 M HCl. The experiments were conducted at two temperature ranges, approximately 4°C and approximately 38°C. The apparent diffusion coefficient of acid through the membranes at 25°C was calculated by interpolation of the Arrhenius plot, $\ln(D_{app})$ versus 1/T. The results of the experiments are given in Table 4.2 where the membranes and their water contents are given along with the apparent acid diffusion coefficients, D_{app}, at 25°C, the apparent acid diffusion coefficients at the high and low temperature limits, the activation energies of diffusion, E_a, and the entropy term, $d(\exp(\Delta S^{\ddagger}/R)^{1/2})$.

It should be noted that the term D_{app} contains the partition coefficient, K, which is the ratio of the acid concentration inside the membrane to the acid concentration of the external solution, as well as the diffusion coefficient. The assumption was made that K is small and does not change over the series of membranes and, therefore, the diffusion coefficient is the dominant factor affecting the D_{app} term.

Table 4.2. Acid Diffusion Dialysis Results

Membrane	% Water[1]	D_{app} (Low)[2]	D_{app} (High)[3] (10^{-9} m^2/s)	D_{app}[4] (10^{-9} m^2/s)	E_a[5] (kJ/mol)	$d\exp(\Delta S^{\ddagger}/R)^{1/2}$ (10^{-10} m)
422	67	0.66 (6.1)	1.37 (37.7)	1.04	16.4	2.2
406	63	0.67 (5.5)	1.41 (37.3)	1.07	16.9	2.4
415	62	0.57 (5.0)	1.22 (37.7)	0.93	16.7	2.2
412	59	0.45 (4.4)	0.98 (37.9)	0.74	16.9	2.0
417	55	0.41 (4.4)	0.90 (37.6)	0.68	16.7	1.9
428	53	0.38 (4.2)	0.84 (37.8)	0.63	16.9	1.9
431	46	0.27 (4.6)	0.60 (38.4)	0.45	17.0	1.6
432	41	0.19 (4.8)	0.43 (37.8)	0.32	17.2	1.4
PV19	33	0.053 (3.5)	0.12 (39.5)	0.090	16.8	0.69
406me	65	0.68 (5.8)	1.49 (37.6)	1.11	18.0	3.0
426me	57	0.60 (6.3)	1.27 (37.5)	0.96	17.5	2.6
431me	46	0.36 (5.9)	0.78 (37.7)	0.59	17.6	2.0
513me	41	0.18 (4.7)	0.41 (38.2)	0.30	17.6	1.5
513et	39	0.15 (4.8)	0.36 (38.6)	0.26	18.3	1.6
513pr	38	0.12 (3.3)	0.32 (37.6)	0.23	19.6	1.9
513bu	35	0.088 (3.0)	0.22 (37.5)	0.16	19.1	1.5
513pe	30	0.061 (3.2)	0.15 (38.6)	0.11	18.3	1.0
513he	29	0.038 (3.5)	0.10 (39.1)	0.070	19.6	1.1
513bz	26	0.020 (3.2)	0.057 (39.0)	0.040	20.1	0.99

[1] Percent water content by weight, ± 5%
[2] Apparent diffusion coefficient at low temperature (temperature indicated in parentheses) ± 5%
[3] Apparent diffusion coefficient at high temperature (temperature indicated in parentheses) ± 5%
[4] Apparent diffusion coefficient at 25°C, ±5%
[5] Activation energy and entropy terms determined from Arrhenius plot, ±5%

4.5.3.1. Apparent Acid Diffusion Coefficients

The apparent diffusion coefficients at 25°C, D_{app}, for hydrochloric acid range from 1.04×10^{-9} m^2/s to 0.09×10^{-9} m^2/s for the protonated membrane series and 1.11×10^{-9} m^2/s to 0.04×10^{-9} m^2/s for the alkylated membrane series, Table 4.2. D_{app} was found to increase with increasing membrane water content for each membrane series.

Sata and coworkers studied the acid transport properties of membranes containing poly(4-vinylpyridine) crosslinked with divinylbenzene formed by the paste method. The pyridine groups were N-alkylated using octyl bromide, dodecyl bromide and hexadecyl bromide [37]. Diffusion dialysis experiments were performed using a 3 M HCl feed solution. D_{app} for the acid was found to increase with increasing membrane water content, increasing from 0.08×10^{-9} m^2/s for membranes with water contents in the range of 20% to 0.32×10^{-9} m^2/s for membranes with water contents around 40%. These results are comparable to those found in Table 4.2.

The commercial anion exchange dialysis membrane Selemion DMT, manufactured by Asahi Glass, was tested by diffusion dialysis experiments using a 1 M HCl feed solution. The DMT was reported to have a D_{app} of 0.25×10^{-9} m^2/s and a water content of 35% [32], again comparable to values obtained for membranes of similar water content in Table 4.2.

Boyd and Soldano have conducted studies involving the self diffusion of cations in cation exchangers [133] and anions in anion exchangers [134]. The experiments were conducted by stirring spherical ion exchange particles containing radioactively labeled

ions in an electrolyte solution containing the same ion as the exchanger. The rate of isotopic redistribution was then determined by measuring the amounts of radioactivity in the solution at known periods after the start of the self-exchange reaction. In these studies, the self diffusion coefficients were on the order of 10^{-10} to 10^{-11} m^2/s for monovalent ions, similar to the values found for the self diffusion coefficients for acid in this work.

In order to compare the apparent acid diffusion coefficients of the protonated and alkylated membranes studied in this work, the relationship between the apparent acid diffusion coefficients and the water contents of the two series of membranes was examined. A plot of D_{app} versus percent weight water is shown in Fig. 4.5.

The diffusion coefficient of hydrochloric acid in water at infinite dilution is 3.33×10^{-9} m^2/s [35]. Extrapolation of the curves in Fig. 4.5 to 100% water content gives values for D_{app} of 2.9×10^{-9} m^2/s for the alkylated membrane series and 2.4×10^{-9} m^2/s for the protonated membrane series. These apparent acid diffusion coefficients at 100% water content approach the literature value of 3.33×10^{-9} m^2/s expected for diffusion in bulk water.

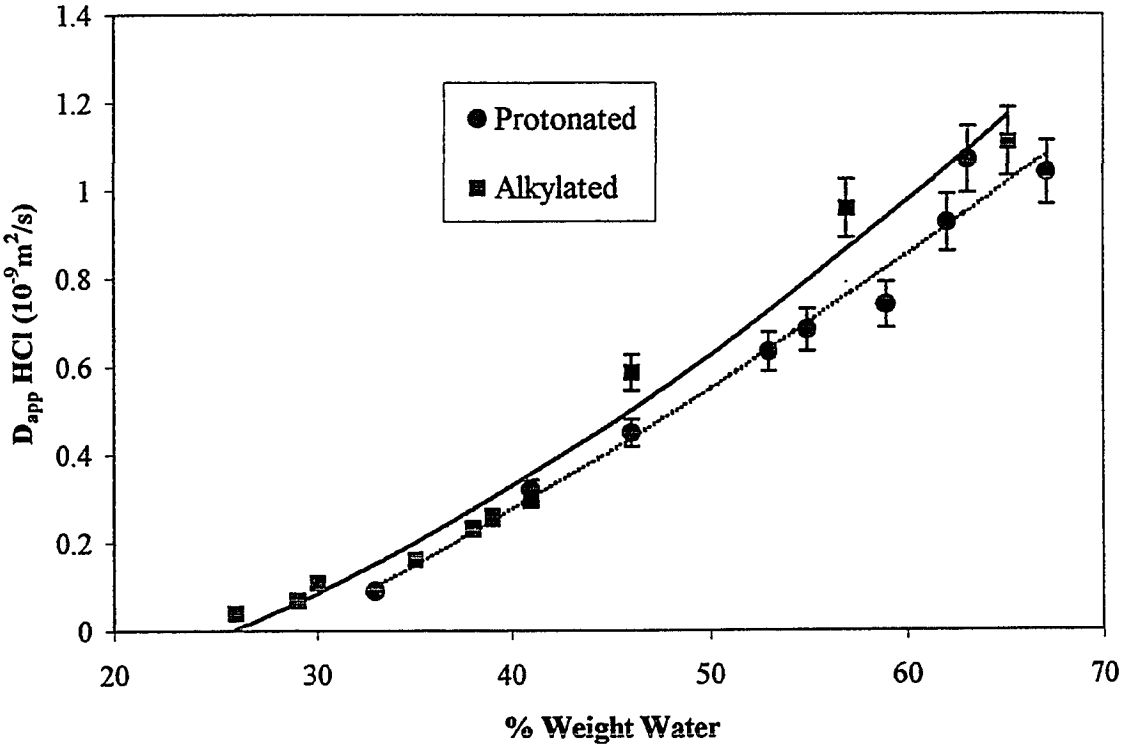

Fig 4.5. D_{app} vs Weight Percent Water for Protonated Membranes (Broken Line) and Alkylated Membranes (Solid Line)

As can be seen in Fig. 4.5, at a given water content, D_{app} for the alkylated membrane series is similar to, within experimental error, but consistently larger than D_{app} for the protonated membrane series. In Chapter 3 it was suggested that acid transport was dependent on total membrane water content and this current result seems to indicate that some other factor is influencing the acid transport to a small degree. The relationship between membrane fixed charge concentration and water content was investigated and is shown in Fig. 4.6.

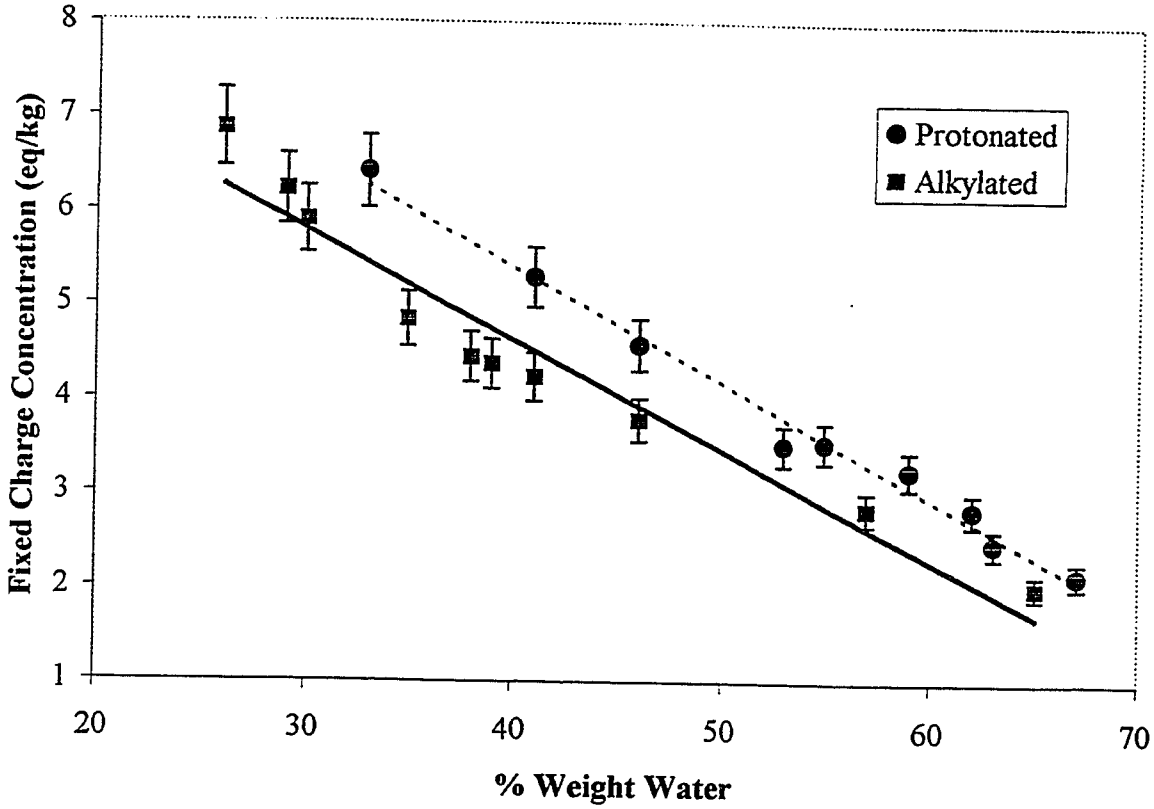

Fig. 4.6. Fixed Charge Concentration vs Weight Percent Water for Protonated Membranes (Broken Line) and Alkylated Membranes (Solid Line)

As can be seen in Fig. 4.6, at a given water content, the alkylated membranes have a lower fixed charge concentration than the protonated membranes. This is because the alkyl groups used to quaternize the pyridine nitrogen atoms effectively increase the mass associated with the fixed charge sites, thereby increasing the mass loading of the membranes without contributing to the fixed charge concentration.

The difference in fixed charge concentration at identical water contents has the following effect on acid diffusion, assuming that the transport of the counter ion, in this

case the chloride ion, is rate limiting. As the counter ion passes through the anion exchange membrane, it interacts with the fixed positive charges in the membrane, residing for a period of time in potential energy wells at each fixed charge site due to electrostatic interactions [136]. The higher the fixed charge concentration, the greater the number of interactions the counter ion will encounter as it passes through the membrane, thus slowing its diffusion through the membrane. Therefore, the lower fixed charge concentration of the alkylated membranes compared to the protonated membranes at a given percent weight water content results in the slightly higher D_{app} seen with the alkylated series.

Thus, acid transport appears to be generally dependent upon the total membrane water content, in agreement with the conclusions reached in Chapter 3, and is affected to a small degree by the fixed charge concentration of the membrane.

In the calculation of the apparent acid diffusion coefficients in this work, an assumption was made that the length of the acid diffusion path through a particular membrane was equal to the thickness of the membrane. This is an oversimplification of the process of diffusion through polyelectrolyte gels. The diffusion path of solutes through membranes is generally longer than the thickness of the membrane and leads to the concept of a "tortuosity factor", τ [137,138]. τ is defined as the ratio of diffusion path length to membrane thickness and can be calculated from equation 4.7 [137]:

$$\tau = D_o \times \varepsilon / D_{app} \qquad (4.7)$$

where D_o is the diffusion coefficient of the solute in pure water (3.33×10^{-9} m^2/s for HCl), ε is the weight fraction of water in the membrane and D_{app} is the apparent diffusion coefficient through the membrane.

The tortuosity factors with respect to the diffusion of HCl for the membranes studied in this work are given in Table 4.3 and plot of tortuosity versus percent weight water is shown in Fig. 4.7.

Table 4.3. Tortuosity Factors for the Diffusion of HCl Through the Membranes

Membrane	τ[1]	Membrane	τ
422	2.1	406me	2.0
406	2.0	426me	2.0
415	2.2	431me	2.6
412	2.7	513me	4.5
417	2.7	513et	5.0
428	2.8	513pr	5.5
431	3.4	513bu	7.2
432	4.3	513pe	9.2
PV19	12	513he	13
		513bz	22

[1] Tortuosity, ±7%

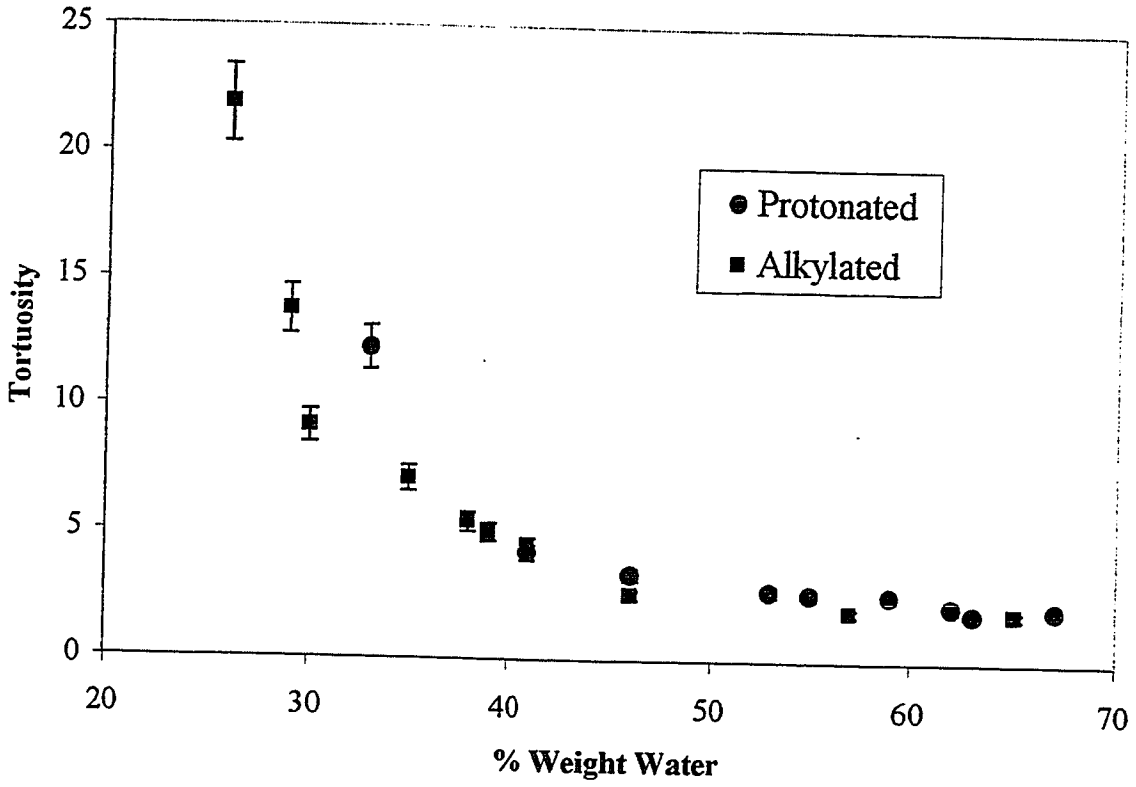

Fig. 4.7. Tortuosity vs Weight Percent Water for Protonated Membranes and Alkylated Membranes

As is apparent from the data in Table 4.3 and Fig. 4.7, the tortuosity decreases with increasing membrane water content in a similar manner for both series of membranes. These results are in agreement with those of Krajewska who studied diffusion through gel chitosan membranes [138].

4.5.3.2. Energy and Entropy of Activation For Acid Diffusion

Table 4.2 lists the activation energies of acid diffusion through the alkylated and protonated membranes as well as the term $d(\exp(\Delta S^{\ddagger}/R)^{1/2})$, an indicator of the entropy of

activation associated with the diffusion process. Comparison of the activation energies of the two series as a function of water content is given in Fig. 4.8.

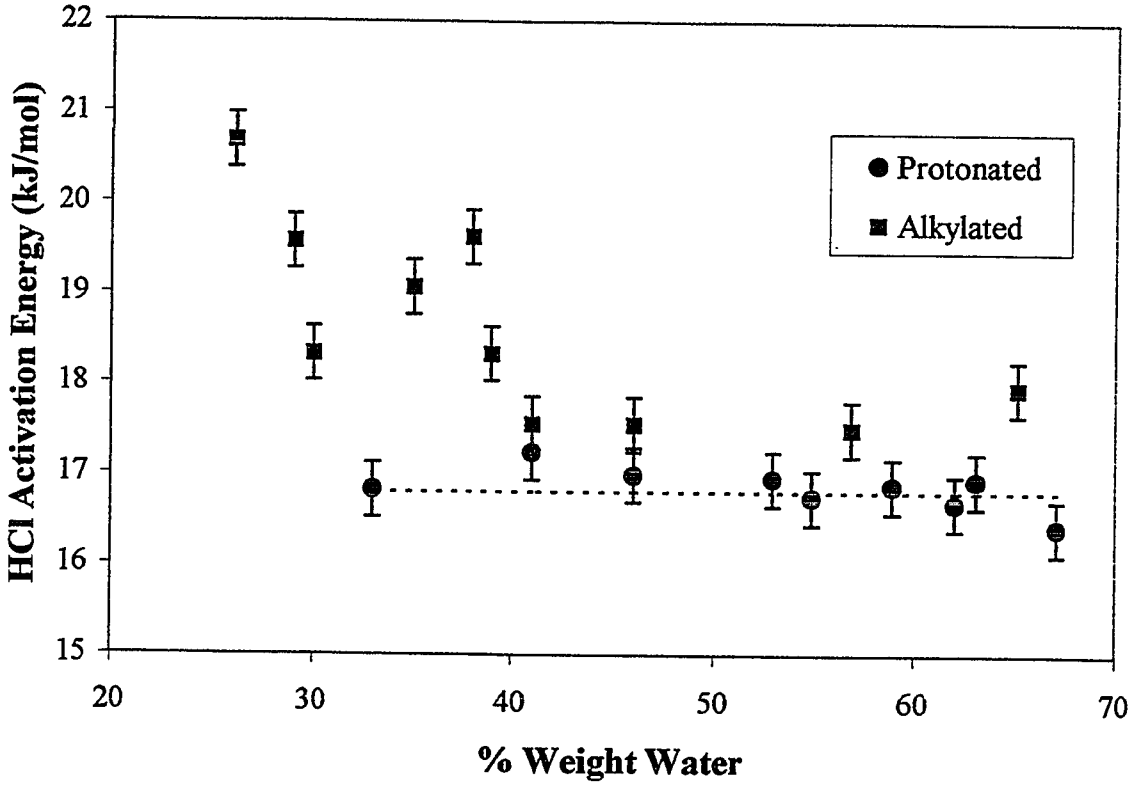

Fig. 4.8. Activation Energy of Diffusion vs Weight Percent Water for Protonated Membranes (Broken Line) and Alkylated Membranes

The activation energy for diffusion of acid through the protonated membrane series appears to be constant and independent of water content with a value of approximately 16.8 kJ/mol. The activation energies of the alkylated series are consistently higher than those of the protonated series at a given percent weight water content and range from approximately 17.5 kJ/mol to 20.7 kJ/mol, with the larger values found at lower membrane water contents.

The Selemion DMT membrane was found to have an activation energy for diffusion of acid of 21.8 kJ/mol [32], comparable to the values found for the low water content alkylated membranes in this study.

Boyd and Soldano found activation energies for the self diffusion of sodium ion in the range of 18 to 27 kJ/mol in cation exchange materials [133] and 28 kJ/mol for chloride ion in an anion exchanger [134]. Although Boyd's systems did not involve the diffusion of acid through a membrane, rather the self diffusion of a counter ion out of an ion exchanger, the process nevertheless involves migration of the counter ion from one ion exchange site to another. This mechanism is similar to the migration of the chloride ion, accompanied by proton transport, through the membranes discussed in this thesis. The values for activation energies of self diffusion found by Boyd are somewhat higher than the activation energies for acid diffusion found in this chapter.

It is interesting to note that Soldano found the activation energy for self diffusion of water in cation exchange resins to be independent of the degree of crosslinking, with a value of 20.9 kJ/mol [139]. As was noted earlier, the protonated membranes studied in this work had activation energies for acid diffusion that were independent of the degree of crosslinking and water content.

As is shown in Fig. 4.9, the values of the term $d(\exp(\Delta S^{\ddagger}/R)^{1/2})$ are consistently higher for the alkylated membranes than the protonated membranes at a given fixed charge concentration. The values range from 1.0×10^{-10} m to 3.0×10^{-10} m for the alkylated

membranes and 6.9×10^{-11} m to 2.4×10^{-10} m for the protonated membranes. The values increase with increasing water content for both series.

Values of $d(\exp(\Delta S^{\ddagger}/R)^{1/2})$ for the diffusion of sodium ion in cation exchangers have been reported to range from 1.9 to 5.7×10^{-10} m [133] and 1.3 to 7.4×10^{-10} m for bromide ion in anion exchangers [134]. The values increased with decreasing crosslinking of the ion exchanger in both cases [133,134]. A similar trend is seen in Fig. 4.9 for the protonated membrane series where membrane crosslinking decreases from left to right.

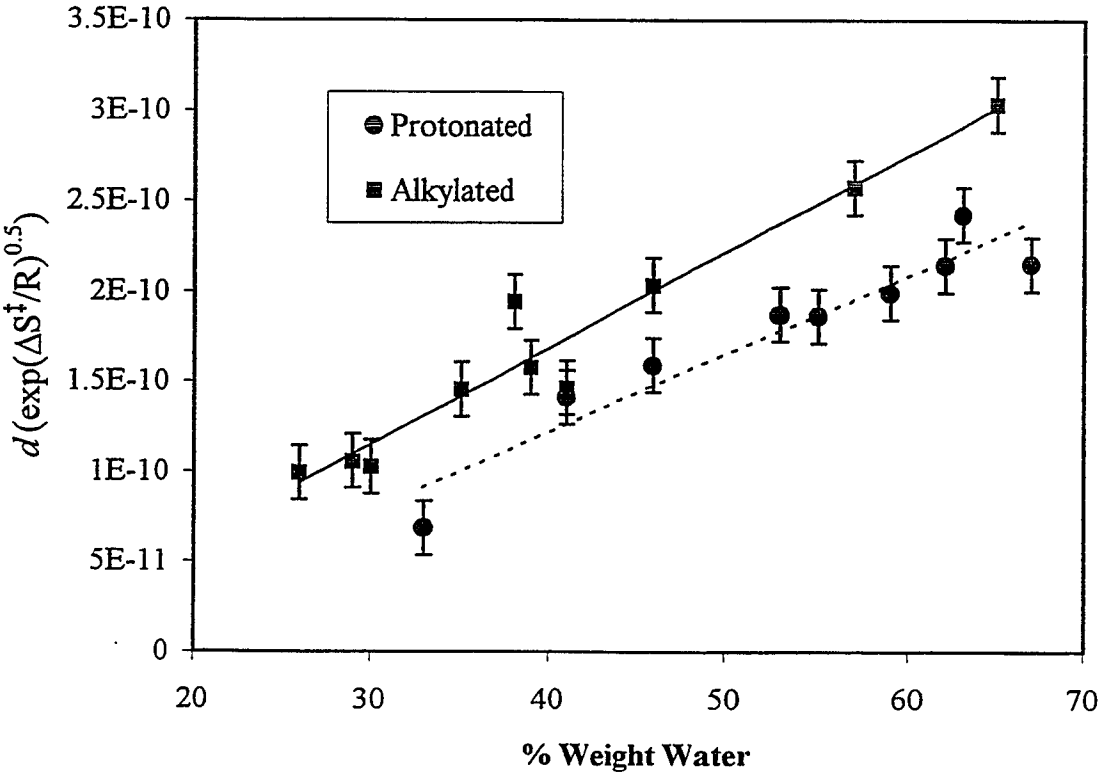

Fig. 4.9. $d(\exp(\Delta S^{\ddagger}/R)^{1/2})$ vs Weight Percent Water for Protonated Membranes (Broken Line) and Alkylated Membranes (Solid Line)

The differences in activation energies of diffusion and $d(\exp(\Delta S^{\ddagger}/R)^{1/2})$ between the alkylated and protonated membranes can be understood in terms of the structure of the membrane water. It was determined by differential scanning calorimetry and comparison with the literature that the structure of the water is greater in the alkylated membranes than in the protonated membranes.

It can be seen in the Eyring equation that D_{app} is dependent upon both the activation energy term and the $d(\exp(\Delta S^{\ddagger}/R)^{1/2})$ term. Chloride ion transport through the membrane can occur by two mechanisms, the first being transfer of the ion from one fixed charge site to the next, a hopping mechanism, and the second being simple diffusion [12]. In both mechanisms the chloride ion passes through the aqueous regions of the membrane and, therefore, disrupts the structure of the water as it diffuses through the medium [134]. The water in the alkylated membranes is more highly structured than the water in the protonated membranes in the form of hydrogen bonding. The disruption of the more extensively hydrogen bonded network in the alkylated series by the chloride ion as it diffuses results in a higher activation energy of diffusion than that which is seen for the protonated series.

Concomitantly, there is an increase in entropy that occurs with the disruption of the hydrogen bonded network of the alkylated membranes, resulting in the overall larger value of the term $d(\exp(\Delta S^{\ddagger}/R)^{1/2})$ for the alkylated series. Although the larger activation energy would cause a decrease in D_{app}, the increase in entropy offsets the increase in E_a, resulting in the slightly higher values of D_{app} seen for the alkylated membranes.

A similar argument can be presented for the effects of the membrane water structure on the transport of the proton. The Grotthus mechanism, as described earlier, involves the transfer of a proton by a series of proton exchanges along a hydrogen bonded chain of water molecules. Following the transfer of a proton from one end of the chain to the other, the water molecules must reorient in order to repeat the process. This reorientation involves breaking and reforming hydrogen bonds in the membrane water, a process which would involve a higher energy of activation in the alkylated membranes which possess a higher degree of hydrogen bonding in the water.

The presence of the extended hydrogen bonding in the alkylated membranes, however, may be considered to favour the transfer of protons from an entropic perspective. There is little loss in the entropy of the water in the alkylated membranes upon the formation of hydrogen bonded chains since the water is already highly structured. The protonated membranes, however, encounter a greater loss in entropy upon the organization of the membrane water to facilitate the Grotthus mechanism, therefore proton transport in favoured in the alkylated membranes.

In a similar manner to the diffusion of the chloride ion, although the diffusion of the proton in the alkylated membranes occurs with a higher activation energy, the greater entropy term associated with transport of a proton through the alkylated membranes results in the higher D_{app} values for the alkylated membranes.

Tasaka and coworkers have examined the thermoosmosis of water across poly(4-vinylpyridinium/styrene) membranes and determined that the entropy of the water in the

protonated membranes was greater than the entropy of the water in membranes quaternized with the methyl group [140], in agreement with the conclusions reached in this thesis.

4.5.4. Mobility of Water in Protonated and Alkylated Membranes by PGSE NMR

Since the transport of ionic species through membranes occurs through the water contained within the membranes, information about the diffusivity of the water in the membranes is crucial for understanding the transport properties.

Since its introduction in the 1960s, PGSE NMR has become a valuable tool in the study of molecular dynamics and mobility. It has been used to investigate diffusion rates in a large variety of polymer systems, for example the diffusion of plasticizers in PVC [141]. MacDonald and coworkers have studied the diffusion of hydrophobic ethoxylated urethane associating polymers in water [135], the self diffusion of water in microemulsions [126] and the self diffusion of water, methanol, t-butanol and other solvents in aqueous solutions of poly(vinylalcohol) [142,143]. More directly related to this work, the self diffusion of water and ethanol in cellulose membranes, polyacrylic acid-polysulfone composite membranes and sulfonated polyethylene membranes has been studied [144-146].

The PGSE NMR pulse sequence consists of two magnetic field gradient pulses interleaved with the two radio frequency pulses of a spin echo NMR sequence. The intensity of the NMR signal of the water at a time 2τ following the PGSE pulse sequence

is related to the diffusion coefficient of the water and the pulse program parameters according to Equation 4.1.

Five of the nine protonated membranes and seven of the ten alkylated membranes listed in Table 4.1 were subjected to PGSE NMR experiments to determine the self diffusion coefficients of the water in the membranes. The membrane samples were placed in standard 5mm NMR tubes and the experiments were performed once for each membrane, with the exceptions of membranes 422, 412, PV19 and 513et for which the experiment was performed in duplicate. The variation in the self diffusion coefficients of the duplicate measurements was less than ±2%. Further repeat measurements were not performed because of limited instrument availability.

A series of ^{1}H NMR spectra of the water in membrane PV19 for various durations of the field gradient pulse is shown in Fig. 4.10. This figure is representative of the spectra obtained for all the membranes tested. With increasing gradient pulse duration (increasing from left to right in Fig. 4.10), the NMR signal intensity from the water protons decreases exponentially.

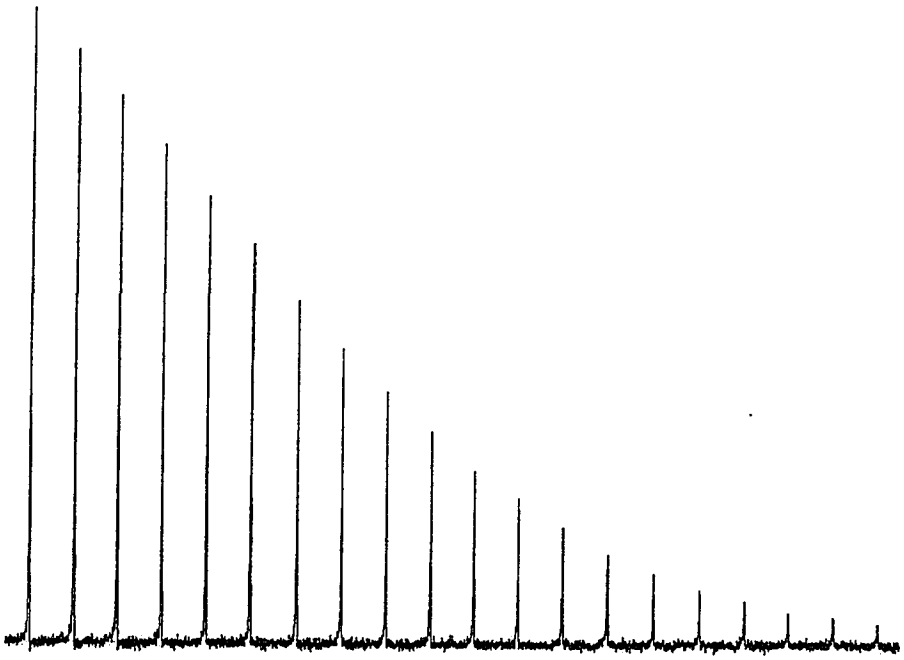

Fig. 4.10. A series of PGSE proton NMR spectra of the water in membrane PV19 at room temperature for different values of the gradient pulse duration, increasing from 1 ms to 5.75 ms by 0.25 ms increments from left to right.

Fig. 4.11 shows the manner in which the logarithm of the signal intensity ratio of the membrane water protons decreases as a function of the gradient pulse duration for two representative samples: protonated membrane PV19 and alkylated membrane 513he.

The NMR signal intensity of both membranes PV19 and 513he decreased in an approximately linear fashion with increasing gradient pulse duration, Fig. 4.11. The signal intensity of membrane 513he, however, decreased more slowly than that of membrane PV19, indicating a slower self diffusion of the membrane water in the former membrane. Similar linear decays were found for all membranes tested. The self diffusion coefficient of the membrane water for each membrane was determined from the negative

of the slope of the plot of $\ln(I/I_o)$ versus $(\gamma G\delta)^2(\Delta - \delta/3)$ and the values are shown in Table 4.4.

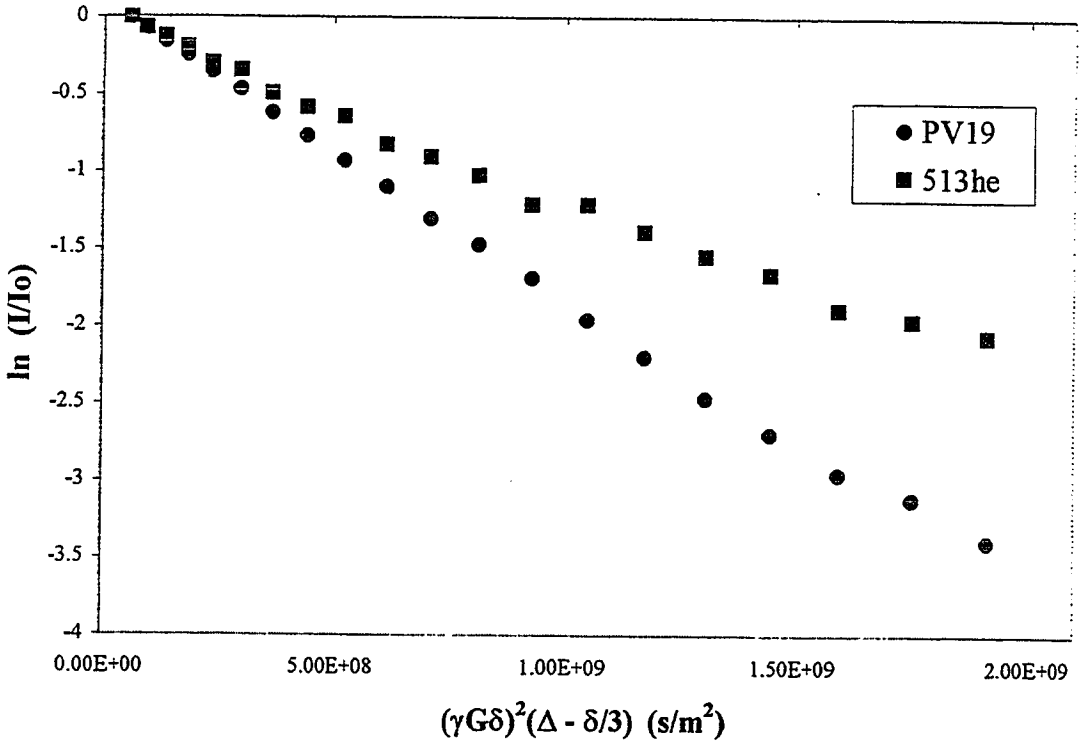

Fig. 4.11. Typical intensity decays of the membrane water signal in the PGSE NMR experiment as a function of $(\gamma G\delta)^2(\Delta - \delta/3)$ for protonated membrane PV19 (circles) and alkylated membrane 513he (squares).

The self diffusion coefficients of the membrane water from Table 4.4 are plotted as a function of percent weight water content of the membranes in Fig. 4.12 for both the protonated and alkylated membranes tested.

Table 4.4. Self Diffusion Coefficients of Water in Membranes

Protonated Membranes		Alkylated Membranes	
Membrane	D_{H2O}[1] (10^{-9} m^2/s)	Membrane	D_{H2O} (10^{-9} m^2/s)
422	1.9	406me	0.97
406	1.5	513me	1.2
412	1.6	513et	0.95
428	1.6	513bu	1.2
PV19	1.9	513pe	0.78
		513he	1.1
		513bz	0.91

As is apparent from the data in Table 4.4 and Fig. 4.12, the values of the self diffusion coefficients of water in the membranes studied in this work fall into two groups. All of the protonated membranes tested had similar values of the self diffusion coefficient of water compared to one another while all of the alkylated membranes tested had values similar to one another yet lower overall than the protonated membranes. The average self diffusion coefficient of water in the protonated membranes was $1.7 \pm 0.2 \times 10^{-9}$ m^2/s while that for the alkylated membranes was $1.0 \pm 0.2 \times 10^{-9}$ m^2/s. By comparison, the self diffusion coefficient of water in 2 vol% H_2O in D_2O is 1.902×10^{-9} m^2/s [135].

[1] Self diffusion coefficient of water at 25°C, ±10%

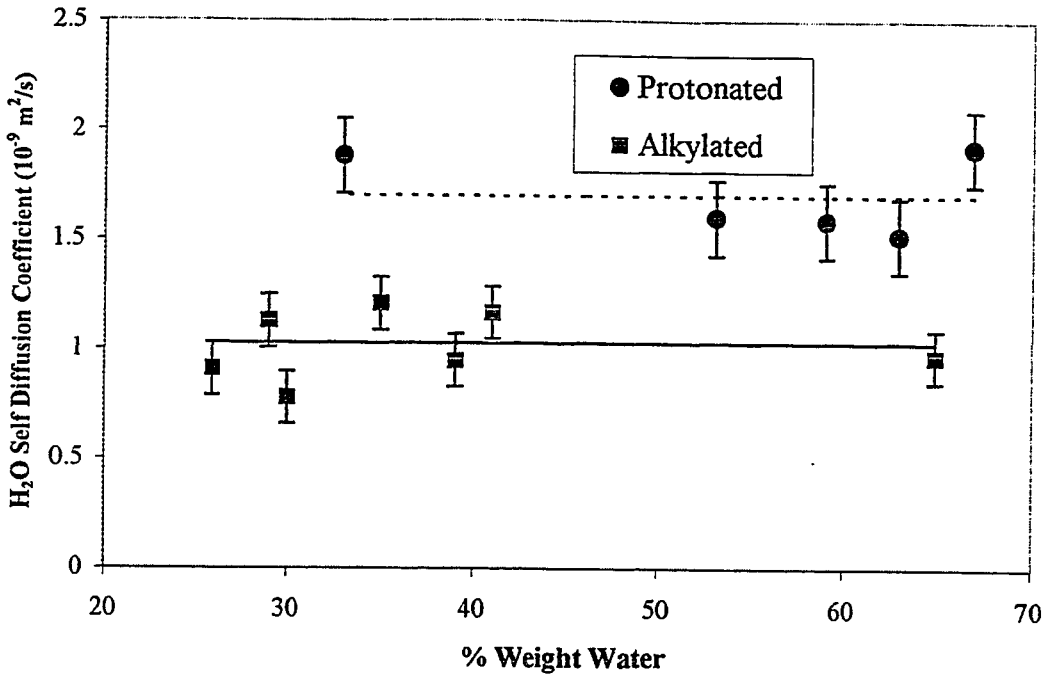

Fig. 4.12. D_{H2O} vs Weight Percent Water for Protonated Membranes (Broken Line) and Alkylated Membranes (Solid Line)

The grouping of the diffusion coefficients into two different average values, one for each series of membranes, is another indication of the difference in the structure of the water in the protonated membranes as compared to the alkylated membranes. The self diffusion coefficient of water in the alkylated membranes is fairly constant over the series, as is that for the protonated membranes, indicating that the mobility of the membrane water in each of these membrane series is similar throughout the membranes within each series. However, the lower average value of the diffusion coefficient in the alkylated membranes, compared to the protonated membranes, is consistent with an increase in structure of the membrane water of the alkylated membranes compared to the protonated membranes.

The decrease in the self diffusion coefficient of water in the alkylated membranes is also in agreement with the increase in activation energy for the diffusion of acid through the alkylated membranes, compared to the protonated membranes, as seen in section 4.5.3.2. The increase in the structure of the water in the alkylated membranes results both in an increase in activation energy of acid diffusion and, not surprisingly, in a decrease in the mobility of the membrane water, manifested in the lower self diffusion coefficient of water.

The activation energy of acid diffusion for the protonated membranes was found to be fairly constant throughout the series and lower than that for the alkylated membranes, section 4.5.3.2. The constant activation energy indicated that the mechanism of acid diffusion was the same throughout the protonated series. The similar values obtained for the self diffusion coefficient of water among protonated membranes indicates that the mobility of the membrane water is the same throughout the series and is consistent with the similar activation energies of acid diffusion.

Volkov and coworkers studied the self diffusion of water in cellulose derivative membranes using PGSE NMR [144]. These membranes were asymmetric, composed of a thin dense layer and a porous substrate. The PGSE NMR method allowed for the determination of diffusion characteristics in the dense layer and the support matrix separately. The self diffusion coefficient of water in the dense layer was in the range of 0.25×10^{-9} m^2/s to 0.45×10^{-9} m^2/s while that in the porous support was in the range of 1.0×10^{-9} m^2/s to 1.3×10^{-9} m^2/s. The water in the dense layer was found to be in the

form of bound water that did not freeze below 0° C, while the water in the porous support was determined to be similar to bulk water and did freeze below 0° C. The differences in the self diffusion coefficients of the water between the dense layer and the porous matrix was attributed to the presence of more bound, or nonfreezable, water in the dense layer which resulted in a lowering of the diffusion coefficient in the dense layer. This finding is similar to the results found for the pore-filled membranes studied in this work where the alkylated membranes have a higher degree of water structure than the protonated membranes, resulting in a lowering of the self diffusion coefficient of the water in the former membranes. The values for the self diffusion coefficients found by Volkov for the porous support are quite similar to those found for the pore-filled membranes studied in this work.

Volkov also studied the diffusion of water in poly(acrylic acid)-poly(sulfone) composite membranes and found values of 7.0×10^{-11} m^2/s and 1.8×10^{-9} m^2/s for the self diffusion coefficient of water in the polyacrylic acid layer and the polysulfone layer, respectively [145].

The self diffusion of water in Nafion 117 membranes has been investigated using PGSE NMR and diffusion coefficients of 0.6×10^{-10} m^2/s to 5.8×10^{-10} m^2/s were found for water contents ranging from 2 to 14 water molecules per sulfonate group [147].

As linear decays were found for all membranes tested, as shown in Fig. 4.11, this indicates that there was a single self diffusion coefficient for the water in each membrane [135]. A distribution of diffusion coefficients would have resulted in a nonlinear decay in

plots of the type shown in Fig. 4.11. The finding of a single diffusion coefficient for the membrane water in each membrane is not surprising since the membranes are symmetrically pore-filled and do not have a dense layer and a more porous layer.

The finding of only one diffusion coefficient for the water in each membrane may indicate that if there are portions of water that have different degrees of structure, they are not distinguishable by different rates of diffusion using this technique. This indicates, within experimental error, that there is only one average self diffusion coefficient for the water in each membrane as a result of the rapid exchange of water molecules. It is generally accepted that solvent exchange, such as that occurring between bulk water and water in the hydration shells of ions, is very fast and NMR spectroscopy is not able to distinguish individual resonances resulting from the two types of water [148,149].

Another explanation for the finding of only one self diffusion coefficient for the water in each membrane is the possibility that there may be only one type of water in the membranes. That is to say that perhaps there is no distinction between bound and free water within the membranes. This viewpoint is different than that of McBrierty and coworkers who have observed three distinguishably different types of water in hydrogels composed of poly(N-vinyl-2-pyrrolidone/methylmethacrylate) and poly(hydroxyethyl-methacrylate) [108,109]. It should be noted, however, that McBrierty used T_1 and T_2 NMR experiments to study the water in the hydrogels.

4.5.5. Diffusion of a Neutral Molecule Through Alkylated Membranes

In order to test the assumption made at the beginning of this chapter that the fixed charge concentration does not play a significant role in determining the rate of acid transport of the pore-filled membranes and that it is the water content of the membranes that is the major governing factor, it was necessary to study the diffusion of a molecule through the membranes in the absence of the effect of Donnan exclusion. This was accomplished by examining the rate of transport of a neutral molecule through the membranes and comparison with the rate of transport of hydrochloric acid.

The molecule used for diffusion testing as the neutral species was mesityl oxide (4-methyl-3-penten-2-one), the structure of this molecule is shown in Fig. 4.13.

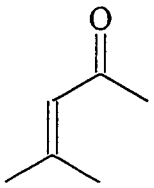

Fig. 4.13. Chemical structure of mesityl oxide.

Mesityl oxide was chosen as a representative molecule because it has good water solubility, it is a neutral molecule and is easily detected by UV spectrophotometry (λ_{max} at 244 nm, ε = 10,770 cm^{-1} M^{-1}).

Five alkylated membranes were tested by diffusion dialysis of mesityl oxide and the apparent diffusion coefficients were determined. The protonated membranes were not tested because the acidic solution required to introduce the positive charge into the membranes would protonate the mesityl oxide molecule. This would result in a charged

molecule which would be subject to Donnan exclusion from the membranes and therefore the experimental results would not give information as to the transport of a neutral molecule.

Table 4.5 shows the apparent diffusion coefficients of mesityl oxide (D_{MO}) determined for the five alkylated membranes tested.

Table 4.5. Apparent Mesityl Oxide Diffusion Coefficients

Membrane	D_{MO}[1] (10^{-10} m^2/s)
406me	2.1
426me	1.4
513me	0.24
513pe	0.18
513bz	0.033

Fig. 4.14 is a plot of the apparent diffusion coefficients of mesityl oxide (D_{MO}) from Table 4.5 as a function of membrane water content. Similar to the results seen for the diffusion of acid through the same membranes, the apparent diffusion coefficient of mesityl oxide is seen to increase dramatically with increasing membrane water content from 0.033×10^{-10} m^2/s at 26% water content for membrane 513bz to 2.13×10^{-10} m^2/s at 65% water content for membrane 406me.

[1] Apparent diffusion coefficient of mesityl oxide at 25°C, ±5%.

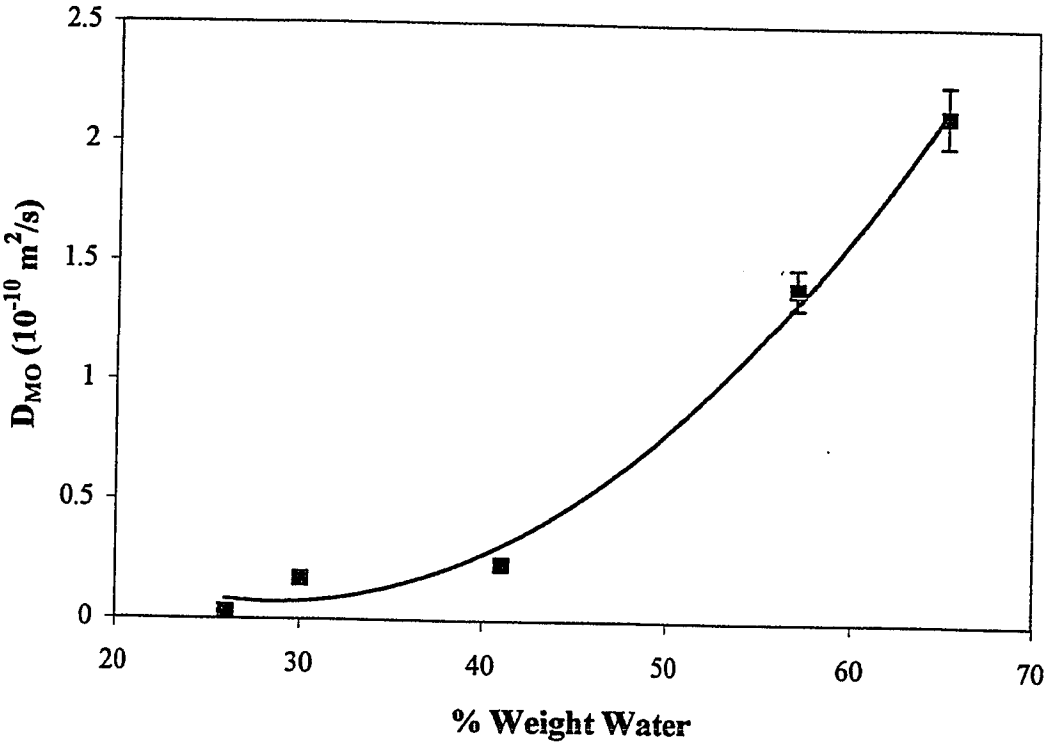

Fig. 4.14. D_{MO} vs Weight Percent Water Content for Alkylated Membranes.

The apparent diffusion coefficients for mesityl oxide seen in Table 4.5 are approximately one eighth the apparent acid diffusion coefficients for the same membranes as shown in Table 4.2. This is not surprising since mesityl oxide is considerably larger than a proton or chloride ion. The rate of diffusion of a molecule is inversely proportional to its size. The diffusion coefficient of mesityl oxide in water is not known. It can be estimated based upon the diffusion coefficients that have been determined for organic molecules of similar structure. For example, the diffusion coefficients of hexanol and hexanoic acid in water have been reported as 8.2×10^{-10} m^2/s and 7.8×10^{-10} m^2/s respectively [150]. The diffusion coefficient of mesityl oxide in water would be expected to be in the region of 8×10^{-10} m^2/s, a value which is

approximately one quarter of the diffusion coefficient of hydrochloric acid in water at infinite dilution.

As was mentioned in the previous paragraph, the apparent diffusion coefficients for mesityl oxide were approximately one eighth the apparent acid diffusion coefficients for the same membranes, whereas mesityl oxide in water is estimated to have a diffusion coefficient one quarter of that for acid in water. Krajewska studied the diffusion of solutes of varying size through gel membranes and found that, as the size of the solute increased, the ratio of the solute diffusivity in the membrane to the solute diffusivity in bulk solution decreased [138]. The results reported in this work are consistent with the findings of Krajewska. The membrane diffusivity of the larger mesityl oxide solute as compared to its diffusivity in bulk water was lower than that of HCl.

In order to compare the diffusion of mesityl oxide through the alkylated membranes with the diffusion of acid through the alkylated and protonated membranes, the apparent diffusion coefficients were normalized. This was done by dividing the diffusion coefficients of the particular species through a particular series of membrane by the diffusion coefficient found for the membrane of highest water content in that series of membranes. By normalizing the results in this way, an overall indication of the effect of percent membrane water content on the apparent diffusion coefficients of acid and mesityl oxide through the membranes can be compared.

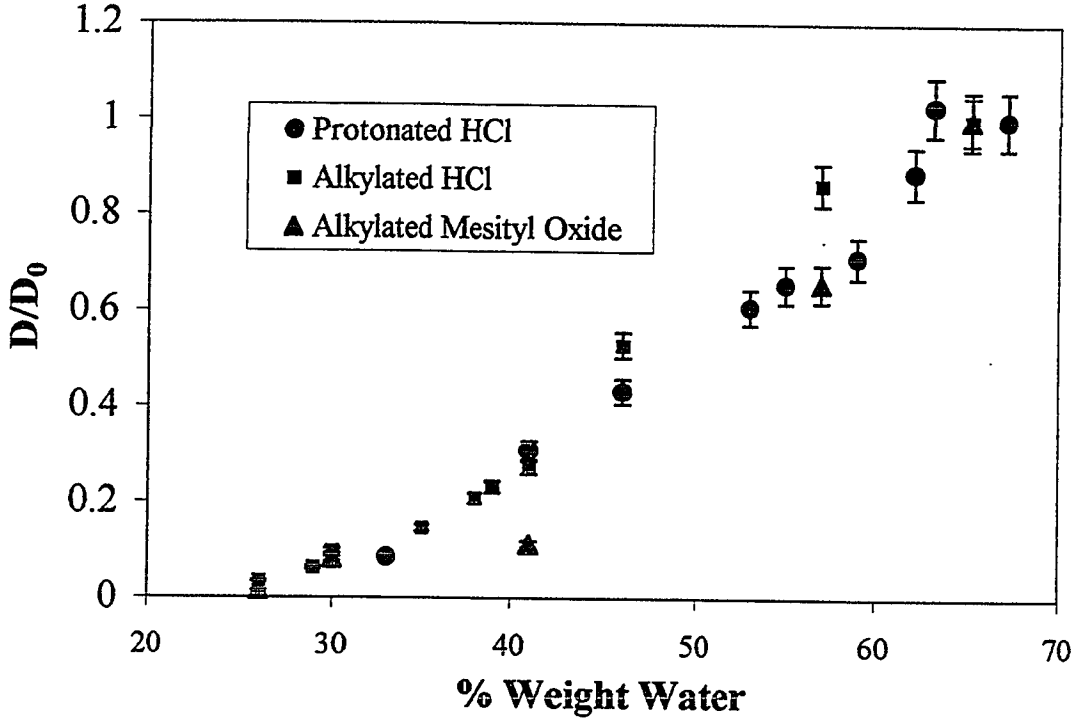

Fig. 4.15. Normalized apparent diffusion coefficients vs weight percent water content for acid through protonated membranes (circles), acid through alkylated membranes (squares) and mesityl oxide through alkylated membranes (triangles).

It can be seen in Fig. 4.15 that all of the points follow the same general trend and fall on approximately the same line. This indicates that the extent to which the membrane water content affects the apparent diffusion coefficient of acid through both the protonated and the alkylated membranes is the same as that for the apparent diffusion coefficient of mesityl oxide through the alkylated membranes. In other words, the rate of change in apparent diffusion coefficient of either acid or mesityl oxide as a result of a change in membrane water content is the same.

4.5.6. Impedance Spectroscopy of Protonated and Alkylated Membranes

The membranes studied in this work are ion exchange membranes, which are capable of conducting an electric current through the migration of counter ions. As such, apart from diffusion dialysis applications, they may be suitable for electrochemical applications such as electrodialysis and fuel cells. Therefore it would be prudent to determine some of the electrical properties of these membranes, such as their electrical resistance, to investigate their potential for use in these areas. In addition to providing information as to the suitability of the membranes for electrochemical applications, resistance measurements can also provide insight into understanding the membrane behaviour in diffusion dialysis applications, since the resistance parameter is a measure of resistance to the flow of ions through the membrane.

Impedance spectroscopy (IS) has become increasingly popular for the electrical characterization of materials because of the current availability of commercially made, high quality impedance bridges and automatic measuring equipment [128]. As a result, the experimental approach to IS has been improved over the last decade [151,152]. IS studies of membranes are abundant in the literature. Nafion and other perfluorinated ion exchange membranes, which find uses in areas such as chloralkali processes and fuel cells, have been extensively investigated [136,153-157]. The pore texture of a carbon membrane as determined by IS has been described [158] and bipolar membranes have been studied using IS [159,160]. The large number of publications on IS studies of

ultrafiltration membranes [161,162], reverse osmosis membranes [163] and others [123,152,164-168] is an indication of the popularity of this method.

Eight of the nine protonated membranes and six of the ten alkylated membranes from Table 4.1 were examined by IS. The samples were equilibrated in 1 M HCl and then clamped between two stainless steel electrodes. Their impedance was measured as a function of frequency from 0.5 Hz to 1 MHz and the bulk resistance of the sample was determined.

Fig. 4.16 is a normalized complex impedance plot of three different protonated membranes, 406, 432 and PV19. The resulting semicircles are representative of the results seen for all of the membranes tested, indicating that the membranes may be modeled as a resistor and capacitor in parallel. The intercept of the semicircle with the x axis in the complex impedance plot was determined before normalization using curve fitting software supplied with the impedance analyzer. The bulk resistance, R_b, of the membrane sample in the cell was taken as the value of the intercept. The resistances of the membranes were normalized to allow for comparison between membranes according to equation 4.8.;

$$R = R_b \bullet A/l \tag{4.8}$$

where R is the normalized resistance of the membrane, in Ω•cm, R_b is the bulk resistance obtained from the intercept of the semicircle with the real axis, in Ω, A is the surface area of the electrode, in cm^2 and l is the thickness of the membrane sample, in cm.

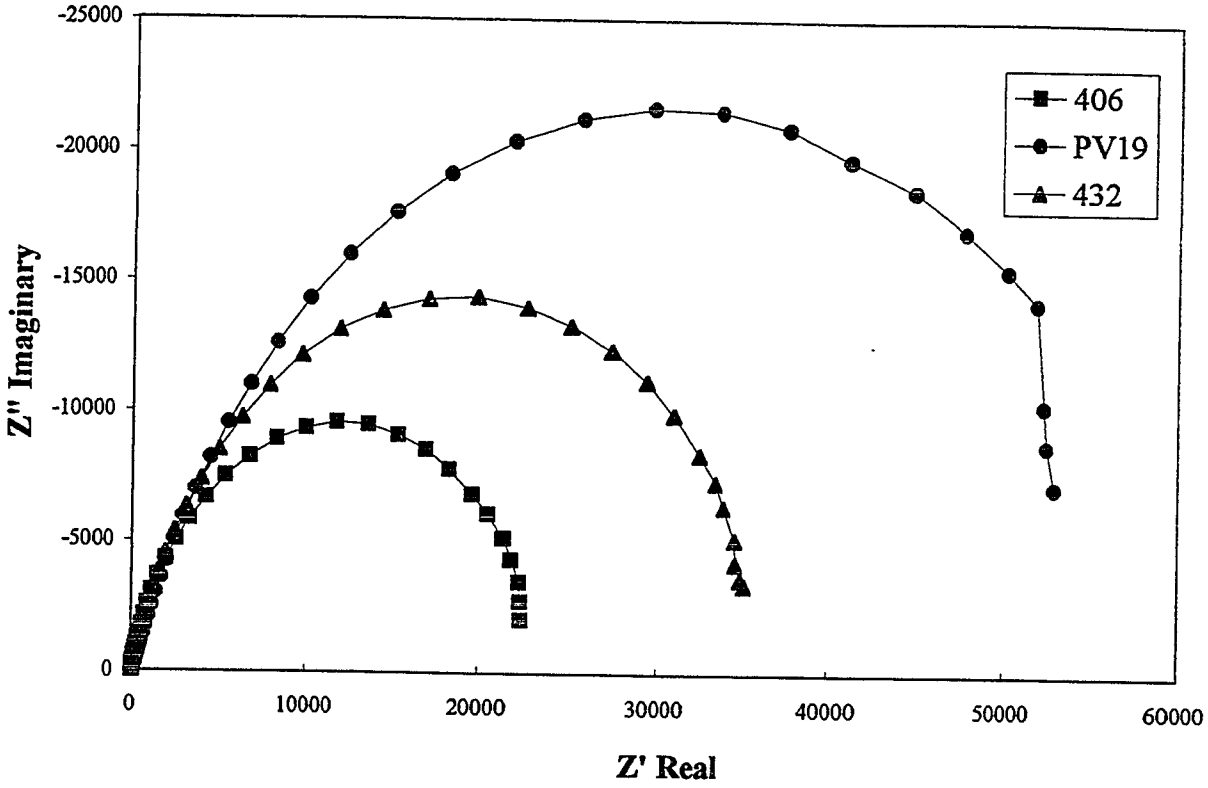

Fig 4.16. Complex impedance plot of three protonated membranes; 406 (squares), 432 (triangles) and PV19 (circles)

The resistances of the membranes tested are given in Table 4.6. To allow for a comparison between the protonated and alkylated membranes, the membrane resistance was plotted as a function of membrane water content for both the protonated and alkylated membranes in Fig. 4.17.

Table 4.6. Resistances of Membranes

Protonated Membranes		Alkylated Membranes	
Membrane	R[1] (kΩ•cm)	Membrane	R (kΩ•cm)
406	26	426me	2
415	31	431me	32
412	29	513et	41
417	33	513pr	38
428	35	513pe	51
431	37	513bz	47
432	40		
PV19	63		

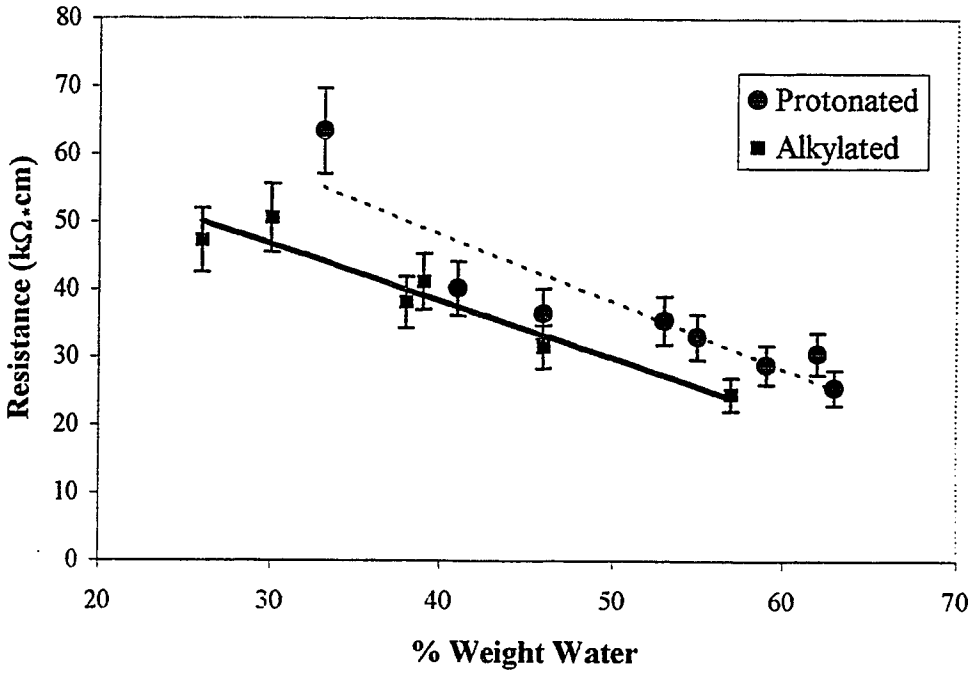

Fig. 4.17. Resistance vs percent weight water for protonated membranes (broken line) and alkylated membranes (solid line)

[1] Normalized membrane resistance, ±10%

As can be seen in Fig. 4.17, membrane resistance decreases with increasing water content of the membranes for both the protonated and alkylated series. Similar results were seen by Kim and coworkers who observed a decrease in the resistance of poly(acrylamidocaproic acid) membranes with an increase in water content [123]. Direct comparisons of the resistances found for Kim's membranes cannot be made with the resistances found for the membranes discussed in this chapter because the resistances of the former membranes were not normalized.

Pourcelly found that the resistance of the Nafion 117 perfluorosulfonic membrane also decreased with increasing membrane water content [136]. For monovalent counterions including H^+, Li^+, Na^+ and K^+ the resistance of Nafion was similar at a given water content, regardless of counterion. The membrane resistance decreased from approximately 200 kΩ•cm at 7 molecules of water per sulfonic acid group to approximately 300 Ω•cm at 14 molecules of water per sulfonic acid group, a decrease of three orders or magnitude.

The resistances of the membrane discussed in this thesis varied with water content by a factor of approximately 2.5 for the protonated series and approximately 2 for the alkylated series, Table 4.6, much less than the variation observed for Nafion. Care must be taken in comparing the resistance values of the pore-filled membranes to those mentioned above for Nafion. The results for the pore-filled membranes discussed in this thesis have been obtained from membranes that were equilibrated with the test solution prior to the experiment and therefore had achieved an equilibrium hydration of the

membrane. The Nafion membranes, however, were dried under vacuum in order to reduce their water content. Therefore the membrane preparation was markedly different between the pore-filled membranes and the Nafion membrane. Nafion is also known to have a phase separated morphology, as described in section 1.2.5.1, resulting in the formation of hydrophilic clusters connected by narrow channels through which ions can migrate. It is possible that the dehydration of the Nafion membrane may have dramatically affected the size and number of hydrophilic channels, thus causing the large increase in resistance upon drying.

No examples were found in the literature on impedance studies of anion exchange membranes similar to those discussed in this thesis. The vast majority of impedance studies are related to Nafion and similar perfluorosulfonic acid membranes because of their importance in fuel cell applications. Most of the membrane resistances that are reported in the literature are not the true bulk DC resistances of the membranes, as have been determined in this thesis, but rather the "resistance" that is reported is actually an impedance value determined at a frequency of 1 kHz. The impedance of a membrane at 1 kHz is much lower than the DC resistance, for example the pore-filled membranes examined by impedance spectroscopy in this thesis showed impedances in the range of 1Ω to 3Ω. For the reasons described in this paragraph, comparison of the membrane resistances found for the pore-filled membranes with the literature is difficult.

The decrease in membrane resistance with increasing water content that can be seen in Fig. 4.17 indicates that the conducting species, the chloride ion in this case,

migrates more rapidly under the influence of the electric field as the amount of water in the membranes increases. This is in agreement with the results seen in section 4.5.3 where the apparent acid diffusion coefficient through the membranes increased with increasing membrane water content.

Another apparent feature of Fig. 4.17 is the slightly lower resistance of the alkylated membranes compared to the protonated membranes at a given percent membrane water content. Again, these results are consistent with the results of section 4.5.3 where the alkylated membranes were seen to have a slightly higher apparent acid diffusion coefficient than the protonated membranes at a given membrane water content. As discussed in section 4.5.3, the lower fixed charge concentration of the alkylated membranes compared to the protonated membranes at a particular fixed charge concentration results in fewer interactions between the mobile chloride ion and the fixed charge sites as the ion moves through the membrane. This allows for more rapid migration under the influence of the electric field, resulting in a lower membrane resistance.

A comparison of the resistances of the pore-filled membranes studied in this work with two commercial ion exchange membranes was done in order to assess the suitability of the pore-filled membranes for electrochemical applications. Low membrane resistances are required for optimum membrane performance. High resistances cause heating of the membranes and lower the current efficiency of the process. The commercial membranes tested by IS were Selemion DSV and AMV, manufactured by Asahi Glass in Japan. Both

the DSV and AMV are strongly basic anion exchange membranes, while the DSV is produced for use in the diffusion dialysis recovery of acid and the AMV for electrodialysis applications.

When subjected to IS analysis under the same conditions as the pore-filled membranes, the DSV and AMV yielded bulk resistances of 29 kΩ•cm and 22 kΩ•cm respectively and resistances of 2Ω and 1.5Ω respectively at 1 kHz. Comparison of the Selemion membrane bulk resistance values with the pore-filled membrane values in Table 4.6 indicates that the commercial membranes have lower resistances than the pore-filled membranes. Of all the pore-filled membranes in Table 4.6, none had a lower resistance than the AMV and only one each of the protonated and alkylated membranes had lower resistances than the DSV and they were the membranes of the highest water content in each series.

It is not surprising that the AMV has quite low electrical resistance since this membrane was developed specifically for electrochemical applications, but the resistance of the DSV is also low, compared to pore-filled membranes with similar diffusion dialysis performance to the DSV. For example, membrane PV19 had the same acid dialysis coefficient as the DSV, as seen in chapters 2 and 3, but has a resistance value over twice that of the DSV. Membrane 513pe would be expected to show good diffusion dialysis performance and a somewhat higher acid dialysis coefficient than the DSV, based on the results of chapter 3, but 513pe has a resistance almost twice that of the DSV. Assuming that the bulk DC resistance of a membrane is important in electrochemical

applications, it appears that the pore-filled membranes may not be optimized with respect to their use in electrochemical applications, at the present time their resistance is too high.

4.6. Conclusions

The results of this chapter have shown that introducing alkyl groups has a major effect on the structure of the membrane water. It would seem that an increase in the structure of the membrane water is indeed occurring upon introduction of hydrophobic quaternizing groups, in agreement with the conclusions reached in Chapter 3.

The effects on the transport of acid through the membranes resulting from the increase in the membrane water structure from the protonated membrane series to the alkylated series have been determined. The increased water structure increases the energy of activation for the acid diffusion process but this effect is overpowered by a positive entropy contribution to give an overall slight increase in apparent acid diffusion coefficients for the alkylated membranes. The slightly lower electrical resistance of the alkylated membranes compared to the protonated membranes at a given water content is consistent with the slightly higher apparent acid diffusion coefficients of the alkylated membranes.

PGSE NMR studies have determined that the self diffusion coefficient of the membrane water in the alkylated membranes is lower than that in the protonated membranes, consistent both with the increase in water structure and the higher energy of activation for the diffusion of acid in the alkylated membranes.

4.6.1. Proposed Model of Membrane Water

In view of the results of this chapter and those of chapter three, an overall model of the pore-filled membranes may be presented. The DSC results of chapter three indicated the presence of more bound water in the alkylated membranes compared to the protonated membranes. It should be stressed that this interpretation assumes that the enthalpy of freezing of water is not changed by its incorporation into the membranes. It is now proposed that there is only one type of water in any given membrane, as opposed the two types of water that are distinguishable from each other. The DSC results can still be rationalized with respect to this new model. The decrease in the amount of free water in the alkylated membranes, as determined from the enthalpy of freezing of the membrane water, is simply a result of the overall increase in the total membrane water structure in the alkylated membranes. Since the alkylated membranes contain water which already has a higher degree of hydrogen bonding, there is less energy released as the membrane water freezes and the extensively hydrogen bonded ice structure is formed. The protonated membranes, having less structured water and less hydrogen bonding, show an overall higher free water content as there are a large number of hydrogen bonds formed upon freezing and a larger amount of energy released.

If the membrane water was present in two states in the membranes, it might have been expected that the activation energy for the diffusion of acid through the membranes would increase at lower water contents as the relative amount of bound water increased. This was not seen for the protonated series, which showed a constant activation energy

for acid diffusion. This indicates the presence of only one type of water with a similar degree of structure throughout the protonated series which supports the proposed new model. The activation energy for acid diffusion did increase somewhat for the alkylated series at low water contents but was fairly similar at moderate to high water contents. The increase in structure of the membrane water in the alkylated membranes accounts for the greater entropy term associated with the diffusion of acid through the alkylated membranes.

The PGSE NMR results indicated that there was only one self diffusion coefficient for the water in each membrane, as opposed to one diffusion coefficient for the bound water and one for the free water. The alkylated membranes were found to have similar water self diffusion coefficients throughout the series as did the protonated series, but the average diffusion coefficient for the alkylated series was lower than that for the protonated series. Therefore these results are also in agreement with the presence of only one type of water in each membrane and with the alkylated membranes containing water that is less mobile than the water in the protonated membranes as a result of the increase in water structure. The lower self diffusion coefficient for water in the alkylated membranes is in agreement with the higher activation energy for acid diffusion through the alkylated membranes.

The results of the investigation into varying monovalent ion size in section 3.4.6. of chapter 3 indicated that the hydrated ion size was the determining factor in the case of diffusion through the protonated membranes but the crystallographic ion size became a

controlling factor for diffusion through the alkylated membranes, even at high membrane water contents. This indicated that the alkylated membranes did indeed have more highly structure water, even at high water contents.

The proposal of this new model to describe the water in these anion exchange membranes gives rise to the question, can this model be extended to describe water containing membranes in general? It would be interesting to investigate membranes based on other functional groups and polymers to see if they would follow the model.

The selectivity of acid over salts shown by the membranes studied in this thesis has been determined to be an effect both of Donnan exclusion and the structure of the membrane water. The rate of acid transport through the membranes is strongly related to the total membrane water content and is largely independent of membrane water structure.

Comparison of the electrical resistances of the pore-filled membrane with those of commercial anion exchange membranes indicates that the McMaster membranes may require improvements if electrochemical applications are to be considered. Also, if these membranes are to be considered viable alternatives to the commercially available diffusion dialysis membranes or resin bed recovery systems, a dramatic improvement in the rate of acid transport is required.

Reducing membrane resistance by increasing water content is not a good solution to the problem because, although transport of acid through the membrane will be increased in diffusion dialysis applications, membrane selectivity will be lost. Since

membrane resistance is proportional to the thickness of the membrane, a thinner membrane would reduce the electrical resistance, while simultaneously increasing the acid transport. The major problem with this approach would be a loss of mechanical strength, rendering the membrane fragile and difficult to handle. This problem could be circumvented by producing a membrane with a dense, active layer, which provides the necessary selectivity for acid recovery, supported by a rigid porous substrate which provides the mechanical strength having a high rate of acid transport. The electrical resistance of such a membrane should also be quite low.

CHAPTER FIVE

CONCLUSIONS AND FUTURE WORK

This chapter summarizes the key results found in this thesis and attempts to describe their significance. Recommendations for future work are suggested and the results of some preliminary experiments in this direction are described.

5.1. Summary

The key findings in this thesis are:

- Poly(4-vinylpyridine)-filled microporous membranes cross-linked with divinylbenzene (DVB) have been produced by radical initiated copolymerization within the pores of a porous support. The mass loading of the pore-filling polymer can be controlled up to 200% by adjusting the polymerization time. These membranes can be converted to anion exchange membranes by either protonation or alkylation of the pyridine nitrogen atoms.
- The incorporated polyelectrolyte was found to be evenly distributed throughout the poly(propylene) substrate membrane.
- In their protonated form, the membrane thickness was found to increase with increasing mass loading and decrease with increasing DVB content.

Membrane water content was found to remain fairly constant with varying mass loading but decreased markedly with increasing DVB content. High mass loadings, in the range of 200% by weight, and high DVB contents, up to 44% by weight, produced membranes with low dialysis coefficients and high selectivities towards HCl relative to NaCl and $MgCl_2$ in diffusion dialysis testing.

- Quaternization of the pyridine nitrogen atom with alkyl bromides produces membranes with much improved performance compared to the protonated membranes. Acid over salt selectivities were found to exceed that found for a commercial diffusion dialysis membrane, the Selemion DSV.
- The changes in water structure caused by the introduction of alkyl quaternizing groups, as indicated by Differential Scanning Calorimetry experiments, has been found to be consistent with the increase in activation energy of acid diffusion as well as the increase in entropy of the diffusion process through the alkylated membranes. The overall result is a slightly higher apparent acid diffusion coefficient in the alkylated membranes compared to the protonated membranes.
- The mobility of the membrane water, as determined by PGSE NMR, is lower for the alkylated membranes, in comparison with the protonated membranes, consistent with the increase in water structure for these membranes. The self diffusion coefficients for the membrane water in the alkylated series were

found to be similar as were the self diffusion coefficients for the membrane water in the protonated series.

- As a result of the findings of similar activation energies for the diffusion of acid for the protonated series and similar self diffusion coefficients for the membrane water throughout each series, a new model has been proposed to describe the water contained in these anion exchange membranes. Instead of the water being present in the form of "bound" and "free" portions it is now proposed that the membrane water is of one type only in any particular membrane. The nature of the membrane water changes depending on the substituent on nitrogen but the water is not present in more than one state in any given membrane.
- The somewhat lower electrical resistance of the alkylated membranes compared to the protonated membranes, as determined by impedance spectroscopy, is consistent with the slightly higher apparent acid diffusion coefficients in the alkylated membranes.

The overall results of this work indicate that the poly(4-vinylpyridine)-filled membranes show promise for use in diffusion dialysis recovery of acid and may be suitable for electrodialysis applications with further optimization. It has been seen that quaternization of the pyridine nitrogen atoms with hydrophobic alkyl groups greatly enhances the performance of the membranes by increasing the structure of the membrane

water. This increase in water structure has been confirmed by a number of techniques, including DSC, Arrhenius experiments and PGSE NMR.

It has been found that the mass loadings of the membranes must be high, in the range of the maximum amount of 200%, based on initial void volume of the nascent substrate, in order for the pore-filled membranes to show any acid/salt selectivity in diffusion dialysis. Optimization of membrane performance with respect to acid permeability and selectivity can be achieved both by increasing the amount of DVB crosslinker and increasing the length of the alkyl group on the nitrogen atom, both of which increase membrane fixed charge concentration. Increasing the DVB content reduces the acid permeability and increases membrane selectivity while increasing the size of the alkyl group has a similar effect on acid permeability and produces a dramatic increase in selectivity.

This work contributes to the understanding of acid transport through an anion exchange membrane and the factors affecting acid/salt selectivity. It has been determined that acid transport is largely dependent on membrane water content and independent of the degree of structure of the membrane water. The acid/salt selectivity of the membranes was found to be a result of Donnan exclusion while the increased selectivity of the alkylated membranes compared to the protonated membranes was determined to be a result of the increase in membrane water structure in the former.

For these pore-filled membranes to be considered as serious alternatives to existing commercial diffusion dialysis membranes and resin bed technology, however, a

significant improvement in acid permeability must be achieved while retaining high acid selectivity. A reduction in electrical resistance of the pore-filled membranes may also required if electrodialysis applications are to be considered as these membranes showed considerably higher bulk resistances than the commercial membranes tested.

Another problem encountered with the pore-filled membranes studied in this work was that they became fragile after storage in 1 M HCl for over one year. A sample of nascent support membrane was also found to become brittle when stored in 1 M HCl. This raises questions as to the suitability of the support used in this work for diffusion dialysis membranes. It would be wise to explore alternative supports for future pore-filled membranes.

5.2. Future Work

As was noted in the conclusions to Chapter 4, one route to produce a diffusion dialysis membrane with high acid permeability and high selectivity would be to fabricate an asymmetric membrane composed of a very dense top layer with a thickness of a few microns or less supported by a porous sublayer with a thickness of approximately 100 μm which would provide the mechanical strength needed. This type of membrane would combine the high selectivity of a dense membrane with the high permeability of a very thin membrane. The introduction of an asymmetric poly(sulfone) ultrafiltration membrane presented a breakthrough to industrial applications [34] but no examples of asymmetric membranes applied to diffusion dialysis have been found.

The concept of an asymmetric membrane is based upon maintaining the active layer, which has a high fixed charge concentration, as thin as possible. While a dense pore-filled layer with a high fixed charge concentration provides the Donnan exclusion necessary for high acid/salt selectivity, the low water content of this layer reduces the acid transport rate. By keeping the active layer thin, the reduction in acid transport is minimized. The porous support has a high water content to provide high acid transport while also providing the mechanical strength. The porous support layer need not have a high fixed charge concentration since the acid/salt selectivity is provided by the active layer, which is positioned facing the feed solution for acid recovery by diffusion dialysis.

In order to produce an asymmetric membrane using a porous host, two basic approaches may be considered. The first involves filling only part of the thickness of the porous support with the active pore-filling polyelectrolyte. The second approach, and the one that is proposed here, makes use of the results found in this thesis by taking advantage of the difference in membrane performance that results from using different alkyl groups to quaternize the pyridine nitrogen atoms. In this approach, the porous substrate is symmetrically filled with the crosslinked poly(4-vinylpyridine) copolymer and the asymmetry is then introduced by alkylation of the incorporated polymer to a certain depth inwards from both surfaces of the membrane using two different quaternizing groups. The methyl group, for example, would provide the high acid permeability but relatively low selectivity required for the support layer while the benzyl group would form the active layer, providing the high selectivity required and reducing

the acid permeability to only a small extent if the benzylated layer is kept thin. Figure 5.1 illustrates the concept of an asymmetrically alkylated pore-filled membrane.

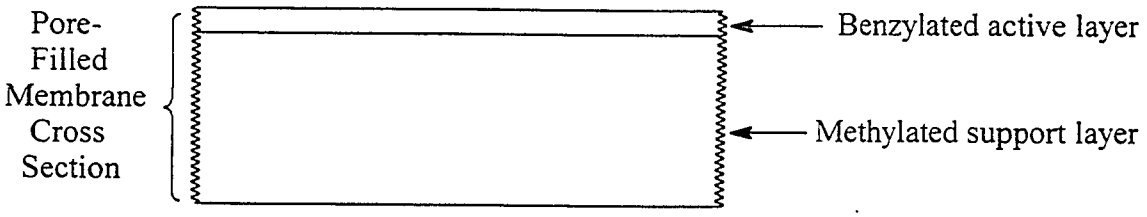

Fig. 5.1. Asymmetrically Alkylated Pore-Filled Membrane

5.2.1. Fabrication and Characterization of an Asymmetric Membrane

To determine if it would be possible to asymmetrically alkylate a thin layer near the surfaces of a pore-filled membrane, a preliminary experiment was done to test the proposal. In this test, samples of a dried pore-filled membrane in free base form were submerged in two different alkylating agents with no additional solvents, namely 1-bromopropane and benzyl bromide. The use of a solvent would swell the membrane and allow the alkylating agents to penetrate the entire thickness of the membrane, thus producing a symmetrically alkylated membrane. It was hoped that, by using dry membrane samples and neat alkylating agents, the penetration of the alkylating agents into the membrane would be minimized and surface alkylation would result. In the case of the submerged samples, alkylation would be observed on both surfaces of the sample.

Based upon the results of the test described in the previous paragraph, alkylation of only one surface of the membrane could be done by simply introducing the neat alkylating agent to one side of the membrane only. By using benzyl bromide as the

alkylating agent, this would produce the thin active layer that is required. The remainder of the membrane could then be alkylated with the methyl group to form the high water content support.

5.2.1.1. Experimental

5.2.1.1.1 Surface Alkylation On Both Sides of the Membrane

A sample of a poly(4-vinylpyridine)-filled membrane (membrane 503) with a mass gain of 173% and a DVB content of 25% was placed in freebase form, dried and cut into eight identical discs 1 cm in diameter. The mass of each piece was recorded and found to be the same, within ±3%. Four pieces were placed in neat 1-bromopropane and four were placed in neat benzyl bromide, all at room temperature. The samples were then withdrawn from the alkylating agents at specific time intervals, soaked in methanol, dried and weighed and then placed in 0.5 M Na_2SO_4 to convert the membranes into sulfate form followed by three rinses in deionized water to remove any sulfate not associated with fixed charge sites in the membrane sample. Sulfur analysis of the membrane cross sections was performed by EDX analysis using ESEM.

5.2.1.1.2 Surface Alkylation On One Side of the Membrane

A sample of a poly(4-vinylpyridine)-filled membrane (membrane 503) with a mass gain of 173% and a DVB content of 25% was placed in freebase form, dried and cut

into a disc 4.4 cm in diameter. The sample was then glued to the bottom of a glass tube which had a diameter slightly less than that of the sample using epoxy adhesive. Benzyl bromide was poured into the glass tube in a thin layer to cover one side of the membrane sample and the tube was covered and kept at room temperature. After a reaction time of 6.5h the membrane was cut from the bottom of the tube, rinsed with methanol, dried and weighed. A small piece of the membrane (noted as 503bz) was cut from the sample for EDX analysis and the remaining larger portion of the sample (noted as 503bzme) was placed in a 20 vol% solution of dimethylsulfate in DMF. Sample 503bz was placed in 0.5 M Na_2SO_4 to prepare for sulfur analysis by EDX and then rinsed three times in deionized water to remove excess Na_2SO_4. Sample 503bzme was removed from the methylating solution after five days, and stored in 1 M HCl. A small piece of 503bzme was cut from the larger sample for EDX analysis and converted into sulfate form in a similar manner to 503bz. 503bzme was tested by diffusion dialysis using a solution of 1 M HCl, 0.5 M NaCl and 0.5 M $MgCl_2$, as described in Chapters 2 and 3.

5.2.1.2. Results and Discussion

5.2.1.2.1 Surface Alkylation On Both Sides of the Membrane

Four membrane samples in freebase form were immersed in 1-bromopropane and four more in benzyl bromide to determine if the alkylation reaction would proceed from the outer surface of the membranes and, over time, penetrate deeper into the membranes.

A solvent, such as DMF, was not used in order to prevent membrane swelling which would allow the alkylating agents to penetrate the membrane and cause alkylation to occur symmetrically. The results would indicate if asymmetric alkylation is a feasible technique to produce asymmetric membranes. One of the four samples was removed from each of the two alkylating agents at the same time over a period of two days in order to monitor the reaction progress. The theoretical mass gain that would be achieved if alkylation proceeded to 100% was calculated for each sample and the measured mass gain was compared to the theoretical maximum. The results are shown in Table 5.1.

Table 5.1. Results of Alkylation Reactions

Membrane[1]	Time (h)	% Alkylation[2]	Membrane	Time (h)	% Alkylation
Pr1	1	0	Bz1	1	0
Pr2	4	28	Bz2	4	10
Pr3	22	43	Bz3	22	31
Pr4	50	58	Bz4	50	36

As is shown in Table 5.1, the degree of quaternization increased with immersion time, up to 58% for the 1-bromopropane samples and up to 36% for the benzyl bromide samples after 50 h.

In order to determine the location of the alkylation in the membrane samples, the counterion was changed from bromide to sulfate and the cross section of each sample was analyzed for sulfur content by EDX analysis in the ESEM instrument. The intensity of the

[1] Pr = 1-bromopropane, Bz = benzyl bromide

[2] Based on theoretical mass gain of 100% quaternization

EDX signal due to sulfur at any location across the membrane cross section is proportional to the quantity of sulfur at that point. Sulfur will be present only in areas where the quaternization reaction has occurred, thus providing information as to the location of the alkyl groups. The sulfur EDX profiles of the membrane samples containing the propyl group are shown in Fig. 5.2 and those containing the benzyl group in Fig. 5.3. The membrane samples were oriented so that the edges of the membrane cross sections were clearly visible in the viewing screen of the ESEM. Therefore, in Figs. 5.2 and 5.3, the membrane cross sections extended over the range of approximately 0.5 mils to 3.0 mils in the EDX plots.

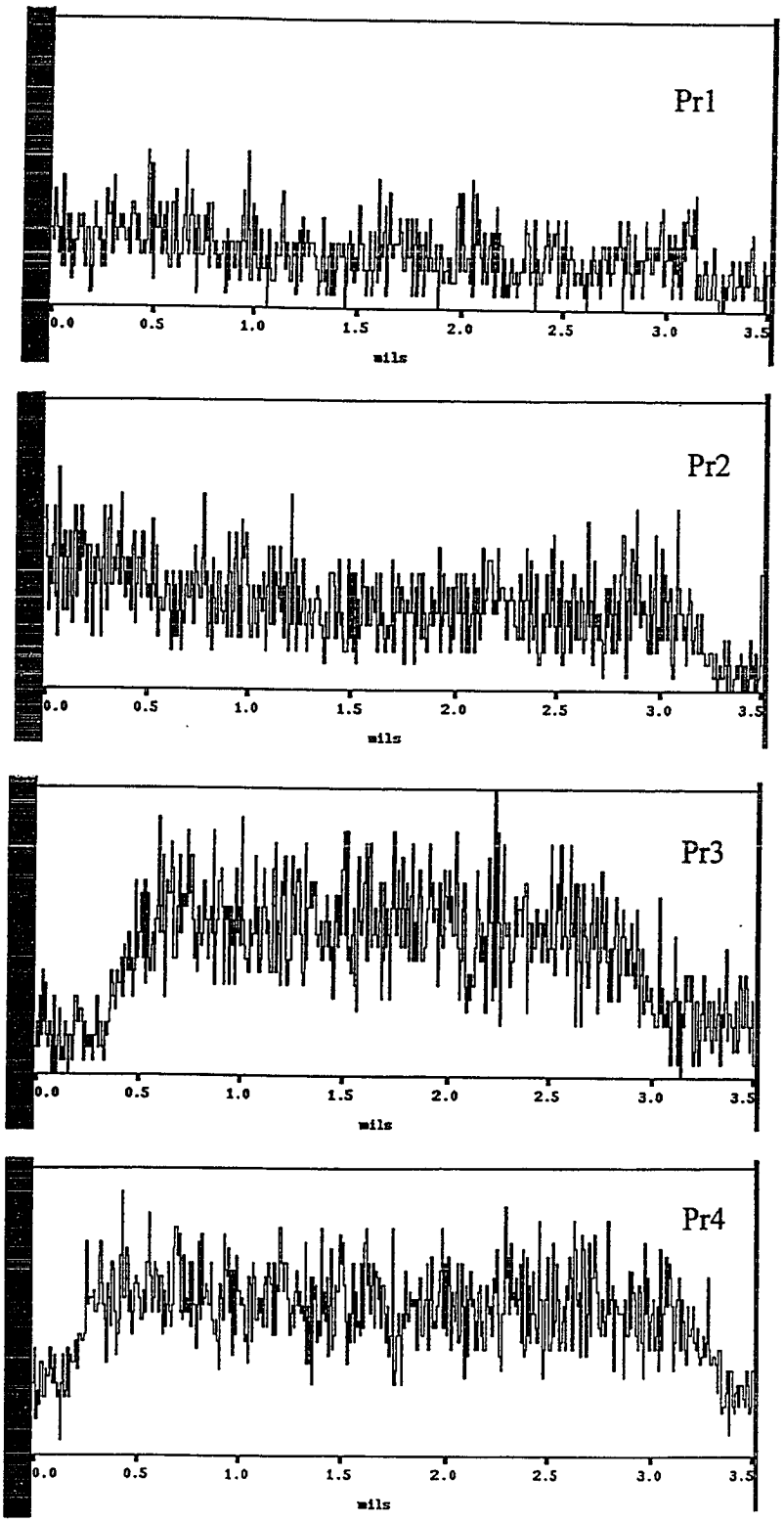

Fig. 5.2. Sulfur EDX profiles of cross sections of membranes Pr1, Pr2, Pr3 and Pr4

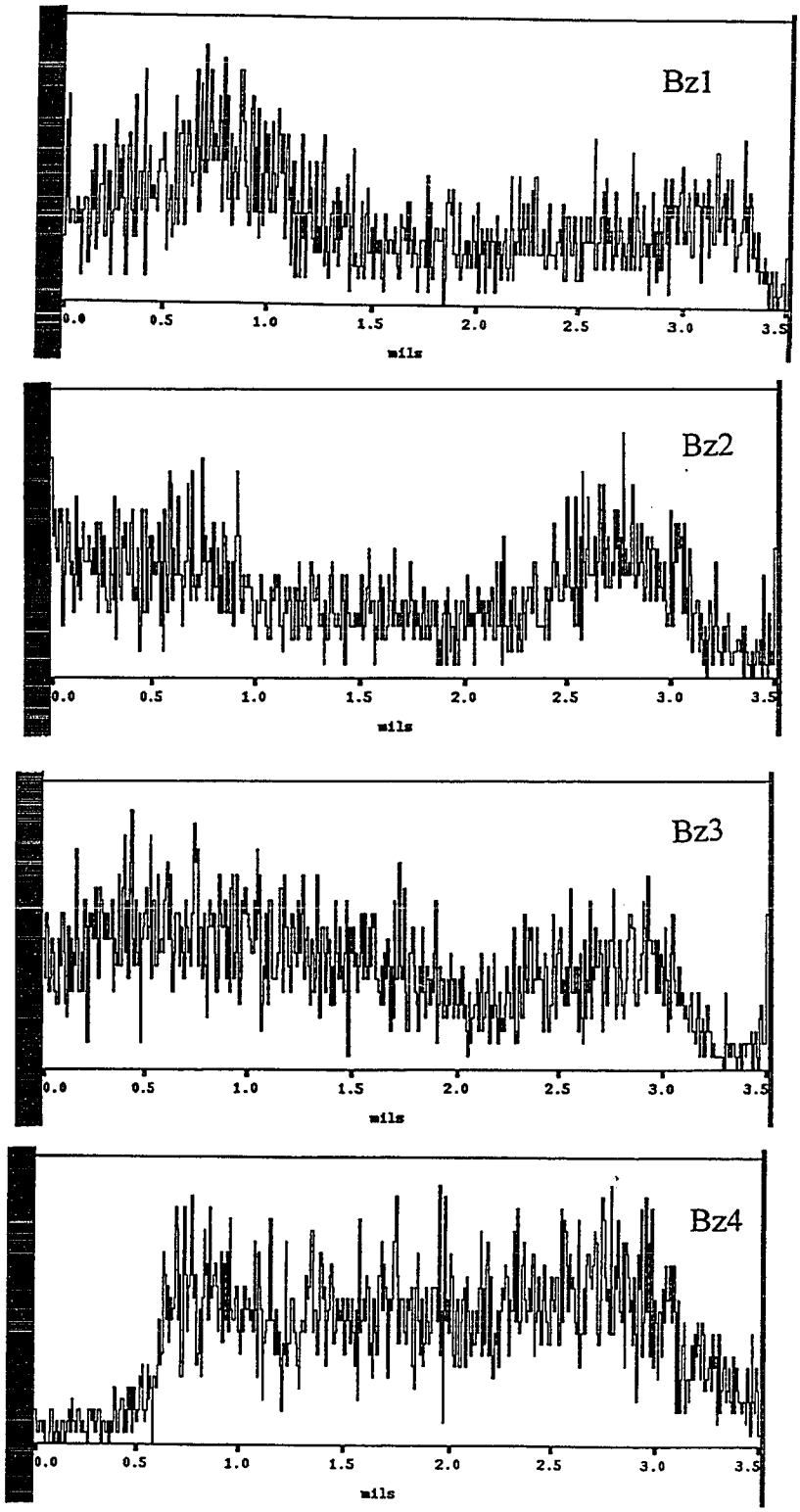

Fig. 5.3. Sulfur EDX profiles of cross sections of membranes Bz1, Bz2, Bz3 and Bz4

The results shown in Table 5.1 and Figs. 5.2 and 5.3 yield some interesting results. The membrane samples alkylated with the propyl group achieved higher percent mass gains than those alkylated with the benzyl group at reaction times over 1 h, Table 5.1. The cause of the higher mass gains in the case of the propyl group can be seen by comparing Figs. 5.2 and 5.3. Alkylation with the propyl group appeared to occur fairly evenly throughout the thickness of the membrane samples, Fig. 5.2. The intensity of the sulfur EDX signal is similar across the membrane cross section for each propyl sample and increases with increasing time of the alkylation reaction. The results of the reaction with benzyl bromide, however, show striking differences, Fig. 5.3. For samples Bz1, Bz2 and Bz3 the sulfur EDX signal is not constant in intensity across the membrane cross sections. It is highest close to each surface, increasing in intensity with reaction time, and diminishing towards the center of the membrane. Sample Bz4 gave a fairly constant sulfur signal of high intensity across the membrane cross section.

The 1-bromopropane penetrated the membranes more readily, even in the absence of any solvent, thus reaching more reactive sites and yielding an overall greater extent of reaction than the benzyl bromide samples. The ease of penetration also resulted in a fairly uniform degree of alkylation across the entire membrane thickness, indicating that 1-bromopropane is not a good choice for asymmetric alkylation reactions.

Benzyl bromide appears to perform relatively well for asymmetric alkylation. It has a low solubility in the membrane so that penetration is not rapid. This is apparent in Fig. 5.3 for the three samples with immersion times of 1, 4 and 22h, Bz1, Bz2 and Bz3

respectively. Sample Bz4 had an immersion time of 50h and the benzyl bromide was able to penetrate through the entire thickness of the membrane, as indicated by the constant sulfur signal in the EDX profile, Fig. 5.3.

A point of concern is the fact that the alkylation reactions for both 1-bromopropane and benzyl bromide did not proceed to their maximum degree, which would be approximately 80% based upon alkylation reactions performed in DMF, Chapters 3 and 4, even after 50h and penetration of the reagent throughout the entire membrane sample. The same reaction carried out in DMF with benzyl bromide was seen to reach ~80% of the theoretical value after 2 to 3 days. In the case of Bz4, the extent of reaction was only 36% after 50h and 58% for Pr4. A polar aprotic solvent such as DMF would promote the S_N2 reaction, which indicates that if high degrees of quaternization are to be achieved, even in a thin asymmetric layer on one side of a membrane, a solvent may be required. The problem would be achieving a high degree of reaction in a thin layer without penetration of the solvent and reagent deeper into the membrane, which would result in an increase in the thickness of the active layer and a decrease in its fixed charge concentration.

5.2.1.2.2. Surface Alkylation On One Side of the Membrane

In order to test the potential of the proposed asymmetric quaternization technique further it was necessary to alkylate a membrane sample asymmetrically, using different quaternizing groups on each side of the membrane. Based upon the results described in

section 5.2.1.2.1., it was determined to use the benzyl group as the active layer quaternizing agent and the methyl group as the quaternizing group for the other side of the membrane.

The membrane sample was benzylated on one side only and the extent of alkylation was determined to be approximately 11%, based on the mass gain of the sample after benzylation and the expected mass gain if 100% of the pyridine nitrogen atoms were quaternized. After cutting a small sample for EDX analysis (503bz), the remaining pyridine nitrogen atoms were methylated using a solution of dimethylsulfate in DMF. It was assumed that full methylation (~80% maximum) was achieved after five days since it has been shown in the past that the reaction is complete after only 3 days, Chapter 2. A sample was taken from the fully quaternized membrane (503bzme) for EDX analysis.

The sulfur EDX profiles of 503bz and 503bzme are seen in Fig. 5.4. It is seen in this figure that the benzylation occurred on one side of the membrane, as indicated by the relatively narrow band in the sulfur line profile for 503bz. The sulfur intensity was greatest at the surface of the membrane, 0.5 mils, and decreased to zero intensity at 1.0 mils, which is equivalent to a depth of 13 μm into the membrane, or one fifth of the thickness of the membrane. Similar to the results from section 5.2.1.2.1, the alkylation reaction did not proceed to its maximum in this layer of the membrane. A rough estimation based on a benzylated layer one fifth the thickness of the membrane should

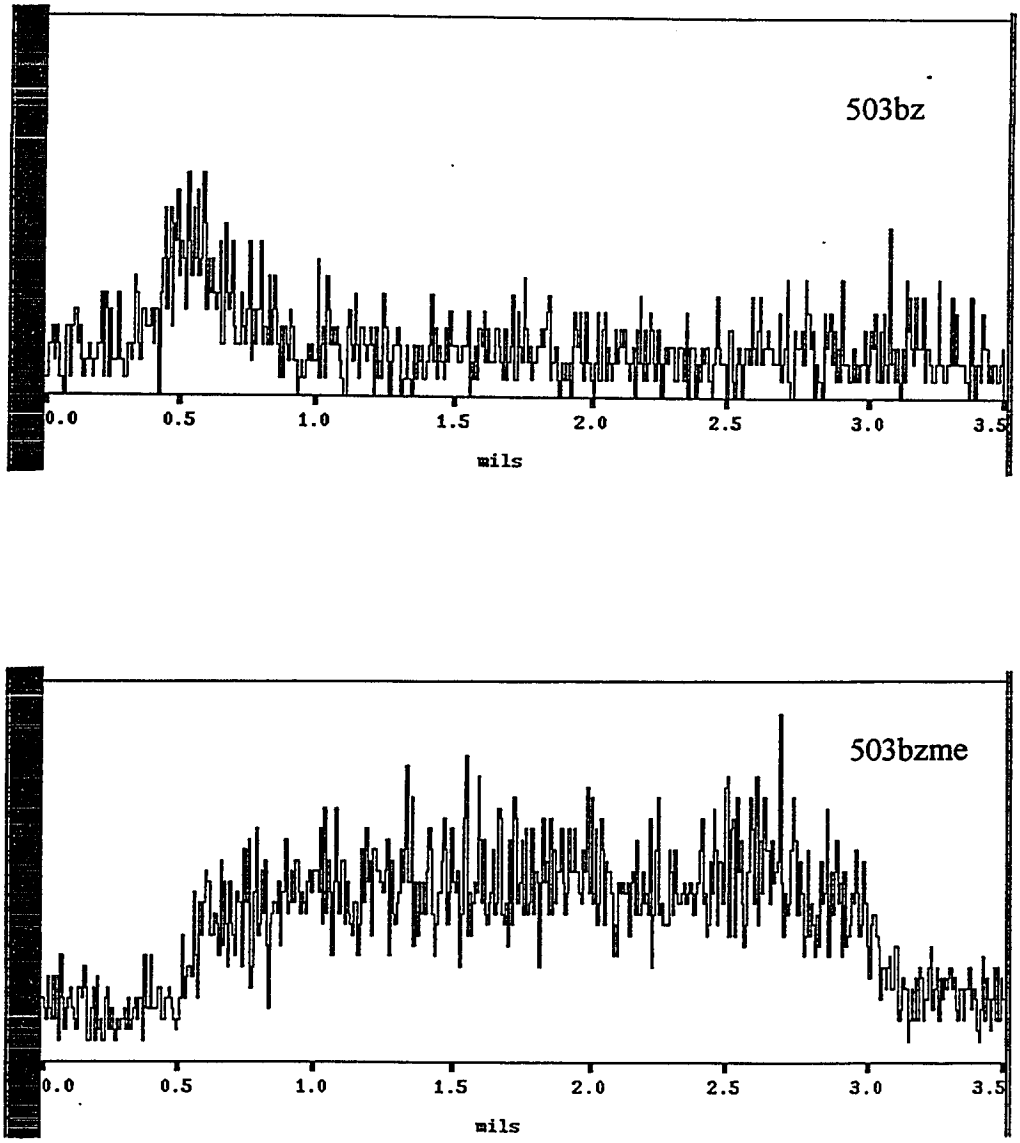

Fig. 5.4. Sulfur EDX profiles of cross sections of membranes 503bz and 503bzme.

have given a degree of alkylation close to 20%, instead of the approximately 11% degree of alkylation found for 503bz.

After methylation, it can be seen in Fig. 5.4 that the intensity of the sulfur EDX line profile for 503bzme is high and fairly constant throughout the thickness of the membrane. This indicates that the sample is fully alkylated, the remainder of the pyridine nitrogen atoms that were not benzylated are now methylated.

Diffusion dialysis testing of 503bzme was conducted with the benzylated side of the membrane facing the feed solution. The resulting acid dialysis coefficient was found to be 21.1 mol/h•m^2•ΔC with selectivities of acid over sodium and magnesium chlorides of 73 and 440 respectively. These results are not particularly good when compared to the performance of the symmetrically quaternized membranes discussed in Chapter 3. Table 5.2 compares the diffusion dialysis results of 503bzme with membranes 432et and 432pr, similar membranes to 503bzme but symmetrically alkylated with ethyl and propyl groups (data taken from Table 3.3).

Table 5.2. Diffusion Dialysis Results

Membrane	U (HCl)	$\frac{U\ (HCl)}{U\ (NaCl)}$	$\frac{U\ (HCl)}{U\ (MgCl_2)}$
503bzme	21.1	73	440
432et	31	78	430
432pr	20	110	800

As can be seen from the data in Table 5.2, membrane 503bzme has a lower acid dialysis coefficient than membrane 432et but similar selectivities, whereas membrane 432pr has a similar acid dialysis coefficient to 503bzme but significantly higher selectivities. Membrane 503bzme, therefore, does not perform as well as the symmetrically alkylated membranes from Chapter 3.

It is apparent that the asymmetric membrane prepared here has not been optimized for acid recovery by diffusion dialysis. The degree of quaternization in the active layer, the benzylated layer of membrane 503bzme, should be much closer to the maximum, ~80%. It is most likely that the pyridine nitrogen atoms located in the active layer that were not benzylated were subsequently methylated by the dimethylsulfate/DMF solution. This would produce an active layer composed of a mixture of benzylated and methylated pyridine groups, thus increasing the water content and reducing the fixed charge concentration of the active layer and resulting in membrane selectivity that is less than would be obtained by an active layer composed only of benzylated sites. This may be the cause of the poor performance of membrane 503bzme since the acid permeability and selectivities were similar to membranes quaternized with ethyl or propyl groups, more or less an average of the permeability and selectivities of membranes quaternized with methyl and benzyl groups.

5.3. Recommendations

The poly(4-vinylpyridine)-filled membranes discussed in this thesis have been fully characterized and the transport of acid through the membranes has been described. The membranes are classed as symmetric and have been optimized for acid recovery by diffusion dialysis. The performance of these membranes is comparable to the commercial membrane, Selemion DSV, and the selectivities of the DSV can be exceeded by utilizing alkyl groups such as pentyl, hexyl and benzyl as quaternizing groups. For these membranes to be considered as a significant improvement on the existing technology, however, dramatic increases in performance are required. It is therefore recommended that further research should focus on the formation of asymmetric membranes.

Improvement of the asymmetric technique described in this chapter should result in an membrane which would have acid permeabilities a factor of five to ten greater than those of the DSV while still maintaining high selectivity. The degree of benzylation of the active layer must be increased to near 80% to achieve the required selectivity while maintaining the active layer as thin as possible. The use of a small amount of solvent to facilitate the alkylation reaction may be required.

It would also be prudent to investigate the potential of these membranes in the area of electrodialysis applications. A small reduction in the electrical resistance of the membranes may make them competitive with the existing technology. Preliminary work has been done in this area and the McMaster membranes show promise. The potential of

these membranes has only just been tapped and the future appears bright for these pore-filled ion exchange membranes.

References

1. L. Cecille and J.C. Toussaint, Future industrial prospects of membrane processes, New York, Elsevier Science Publishers, (1989).

2. T.A. Davis, J.D. Genders and D. Pletcher, Ion Permeable Membranes, Hants, Eng. The Electrochemical Consultancy, (1997).

3. R. Mosdale, G. Gebel and M. Pineri, Water profile determination in a running proton exchange membrane fuel cell using small-angle neutron scattering, J. Membrane Sci, 118(1996)269-277.

4. H.F. Oetjen, V.M. Schmidt, U. Stimming et al, Performance data of a proton exchange membrane fuel cell using H_2/CO as fuel gas, J. Electrochem. Soc., 143(1996)3838-3842.

5. A. McDougall, Fuel Cells, New York, John Wiley & Sons, (1976).

6. R.D. Hoak, Industrial Wastes: Treatment and Disposal of Spent Pickling Liquors, Sewage Works J., 17(1945)940-951.

7. C.J. Brown, Process and Apparatus for Purification of Contaminated Acids, US Patent #5,547,579(1996).

8. D.J. Lewis and F.L. Tye, Treatment of Spent Pickle Liquors by Electrodialysis, J. Appl. Chem., 9(1959)279-292.

9. C. Horner, A.G. Winger, B.W. Bodamer et al, Electrolytic Treatment of Waste Sulfate Pickle Liquor Using Anion Exchange Membranes, Ind. Eng. Chem., 47(1955)1121-1129.

10. F.J. Bartholomew, Sulfuric Acid Recovery from Waste Liquors, Ind. Eng. Chem., 44(1952)541-545.

11. B.J. Robbins, R.W. Field, S.T. Kolaczkowski et al, Rationalisation of the relationship between proton leakage and water flux through anion exchange membranes, J. Membrane Sci., 118(1996)101-110.

12. I. Tugas, G. Pourcelly and C. Gavach, Electrotransport of protons and chloride ions in anion exchange membranes for the recovery of acids. Part I. Equilibrium properties, J. Membrane Sci., 85(1993)183-194.

13. Y. Lorrain, G. Pourcelly and C. Gavach, Influence of cations on the proton leakage through anion -exchange membranes, J. Membrane Sci., 110(1996)181-190.

14. H.G. Hertz, B.M. Braun, K.J. Muller et al, What is the physical significance of the pictures representing the Grotthus H+ conductance mechanism?, J. Chem. Ed., 64(1987)777-784.

15. D.M. Stachera, R.F. Childs, A.M. Mika et al, Acid recovery using diffusion dialysis with poly(4-vinylpyridine)-filled microporous membranes, J. Membrane Sci., 148(1998)119-127.

16. Y. Kobuchi, H. Motomura, Y. Noma et al, Application of ion exchange membranes to the recovery of acids by diffusion dialysis, J. Membrane Sci., 27(1986)173-179.

17. A. Elmidaoui. J. Molenat and C. Gavach, Competitive diffusion of hydrochloric acid and sodium chloride through an acid dialysis membrane, J. Membrane Sci., 55(1991)79-98.

18. Nippon Stainless Steel Co. and Tokuyama Soda Co., Pickling acid-recovery process by diffusion dialysis, Trans. Iron Steel Inst Jap., 27(1987)386.

19. P. Sridhar and G. Subramaniam, Recovery of acid from cation exchange resin regeneration waste by diffusion dialysis, J. Membrane Sci., 45(1989)273-280.

20. Z. Palaty and A. Zakova, Diffusion dialysis of sulfuric acid in a batch cell, Collect. Czech. Commun., 59(1994)1971-1982.

21. B. Chakravorty, R.N. Mukherjee and S. Basu, Synthesis of ion exchange membranes for electrodialytic treatment of indutrial effluents, Desalination, 46(1983)353-360.

22. M. Boudet-Dumy, A. Lindheimer and C. Gavach, Transport properties of anion exchange membranes in contact with hydrochloric acid solutions. Membranes for acid recovery by electrodialysis, J. Membrane Sci., 57(1991)57-68.

23. Tokuyama Soda Co. Ltd., Recovery of nitric acid and hydrofluoric acid by diffusion dialysis process, Company Report (1985)1-8.

24. N.S. Chamberlain and B.H. Vromen, Make Dialysis Part of Your Unit Operations With New Acid-Resistant Membranes, Chem. Eng., (1959)117-122.

25. B.H. Vromen, Dialysis a Sleeper?, Ind. Eng. Chem, 54(1962)20-28.

26. N.N. Li, R.B. Long and E.J. Henley, Membrane Separation Processes, Ind. Eng. Chem., 57(1965)18-29.

27. A. Narebska and A. Warszawski, Diffusion Dialysis. Effect of Membrane Composition on Acid/Salt Separation, Sep. Sci. Tech., 27(1992)703-715.

28. E.K. Spirin, N.M. Smirnova and V.G. Litvinenko, Separation of Nitric Acid From Aqueous Solution of Alkali Metals by Dialysis, J. Appl. Chem. USSR, 57(1984)1297-1299.

29. J.D. Edwards and M.M. Benjamin, Diffusion Dialysis for Recovery of Acid from Concentrated Process Solutions: The Importance of Chemical Speciation, Environ. Sci. Technol., 24(1990)880-885.

30. M. Lesko and E. Nahlik, Separation of an Acid and its Salt by Dialysis Through Ionic Epoxide Membranes, J. Membrane Sci., 31(1987)177-194.

31. A. Elmidaoui, A.T. Cherif, J. Brunea et al, Preparation of perfluorinated ion exchange membranes and their application in acid recovery, J. Membrane Sci., 67(1992)263-271.

32. Y. Oda, A. Nishihara, H. Hani et al, New Dialysis Membrane, Ind. Eng. Chem. Prod. Res. Dev., 3(1964)244-249.

33. F. Helfferich, Ion exchange,Toronto, McGraw-Hill Book Co. Inc. (1962).

34. M. Mulder, Basic principles of membrane technology, Kluwer Acad. Pub. (1991).

35. E.L. Cussler, Diffusion: Mass Transfer in Fluid Systems, New York, Cambridge University Press, (1984).

36. H.G. Hertz, Diffusion and conductance in ionic liquids, a linear response treatment, Z. Phys. Chemie, Neue Folge, Suppl. 1,(1982)7.

37. T. Sata and Y. Yamamoto, Modification of transport properties of ion-exchange membranes VIII. Changes in properties of anion exchange membranes on introduction of hydrophobic groups, J. Polymer Sci., Polym. Phys., 27(1989)2229-2241.

38. K. Takata, F. Hanada, Y. Kagiyama et al, Preparation and properties of monovalent anion permselective anion exchange membranes, Bull. Chem. Soc. Jpn., 69(1996)1443-1448.

39. Y.C. Chiao, F.P. Chlanda and K.N. Mani, Bipolar membranes for purification of acids and bases, J. Membrane Sci., 61(1991)239-252.

40. W.Y. Hsu and T.D. Gierke, Elastic theory for ionic clustering in perfluorinated ionomers, Macromolecules, 15(1982)101-105.

41. M. Fujimura, T. Hashimoto and H. Kawai, Small-angle X-ray scattering study of perfluorinated ionomer membranes. 1. Origin of two scattering maxima, Macromolecules, 14(1981)1309-1315.

42. H.L. Yeager and A. Steck, Cation and water diffusion in Nafion ion exchange membranes: Influence of polymer structure, J. Electrochem Soc., 128(1981)1880-1884.

43. T. Imato, H. Yabu, S. Morooka et al, Evaluation of permselectivity of a liquid anion exchange membrane by diffusion dialysis, J. Membrane Sci., 10(1982)21-33.

44. J.T. Kim and J.L. Anderson, Diffusion and Flow through Polymer-Lined Micropores, Ind. Eng. Chem. Res., 30(1991)1008-1016.

45. Y. Uyama, K. Kato and Y. Ikada, Surface modification of polymers by grafting, Adv. Polym. Sci, 137(1998)1-39.

46. G. Xu and S. Lin, Functional modification of polypropylene, J.M.S.-Rev. Macromol. Chem. Phys., C34(1994)555-606.

47. A.S. Hoffman, Surface modification of polymers: Physical, Chemical, Mechanical and Biological Methods, Macromol. Symp., 101(1996)443-454.

48. C.M. Chan, Polymer Surface Modification and Characterization, New York, Hanser Publ. (1994).

49. F. Garbassi, M. Morra and E. Occhiello, Polymer Surfaces, New York, John Wiley & Sons, (1994).

50. Y. Mir, P. Auroy and L. Avray, Density profile of polyelectrolyte brushes, Phys. Rev. Letters, 75(1995)2863-2866.

51. K.N. Jayachandran and P.R. Chatterji, Grafted polymeric microspheres: a synthetic approach to structurally well-defined brush polymers, J.M.S.-Pure Appl. Chem., A35(1998)1971-1986.

52. V. Thom, K. Jankova, M. Ulbricht et al, Synthesis of photoreactive 4-azidobenzoyl-w-methoxy-poly(ethyleneglycol)s and their end-on photo-grafting onto polysulfone ultrafiltration membranes, Macromol. Chem. Phys., 199(1998)2723-2729.

53. C. Freij-Larsson and B. Wesslen, Grafting of polyurethane surfaces with poly(ethyleneglycol), J. Appl. Polym. Sci., 50(1993)345-352.

54. G. Chen, Y. Ito and Y. Imanishi, Micropattern immobilization of a pH-sensitive polymer, Macromolecules, 30(1997)7001-7003.

55. Matsuda and T. Sugawara, Photochemical protein fixation on polymer surfaces via derivatized phenyl azido group, Langmuir, 11(1995)2272-2276.

56. T. Matsuda and T. Sugawara, Development of a novel protein fixation method with micron-order precision, Langmuir, 11(1995)2267-2271.

57. I.R. Bellobono, E. Selli, B. Marcandalli et al, Photosynthetic membranes III: Influence of photo-cross-linking on permeation and diffusion coefficients of hydrogen and carbon momoxide through asymmetric membranes prepared by photografting of 1,6 hexanediol diacrylate onto cellulose, J. Photochem., 35(1986)231-237.

58. M. Casolaro and R. Barbucci, Protonation thermodynamics of membranes grafted with polyelectrolytes controlling solute permeability, Colloids and Surfaces, 77(1993)81-89.

59. M. Imaizumi, H. Kubota and Y. Hata, Comparative examination of acrylic acid and 4-vinylpyridine monomers in liquid-phase photografting on polyethylene film, Eur. Polym. J., 30(1994)979-983.

60. E.A. Hegazy, A.M. Dessouki, M.M. El-Dessouky et al, Crosslinked grafted PVC obtained by indirect radiation grafting, Radiat. Phys. Chem., 26(1985)143-149.

61. A.M. Dessouki, E.A. Hegazy, M.M. El-Dessouky et al, Anionic membranes obtained by radiation grafting of 4-vinylpyridine onto poly(vinyl chloride), Radiat. Phys. Chem., 26(1985)157-163.

62. M.M. El-Dessouky, E.A. Hegazy, A.M. Dessouki et al, Electrical conductivity of anionic graft copolymers obtained by radiation grafting of 4-vinylpyridine onto poly(vinyl chloride), Radiat. Phys. Chem., 27(1986)443-446.

63. E.A. Hegazy and A.M. Dessouki, Preparation and selected properties of ion-containing reverse osmosis membranes, Radiat. Phys. Chem., 28(1986)273-279.

64. I. Kaur, B.N. Misra and R. Barsola, Graft copolymerization of 4-vinylpyridine onto isotactic polypropylene hydroperoxide by mutual irradiation method, J. Appl. Polym. Sci., 48(1993)575-581.

65. R. Simons, J. Zuccon, M.R. Dickson et al, Pervaporation and evaporation characteristics of a new type of ion exchange membrane, J. Membrane Sci., 78(1993)63-67.

66. Y. Okahata, K. Ozaki and T. Seki, pH-Sensitive permeability control of polymer-grafted nylon capsule membranes, J. Chem. Soc., Chem. Commun.,(1984)519-521.

67. B. Khakimdzhanov, U.N. Musayev, A. Kurbanov et al, Spontaneous graft polymerization of alkylated 4-vinylpyridine in polyethylene, Polymer Sci. USSR, 29(1987)973-979.

68. A.M. Mika, R.F. Childs, J.M. Dickson et al, A new class of polyelectrolyte-filled microfiltration membranes with environmentally controlled porosity, J. Membrane Sci., 108(1995)37-56.

69. A.M. Mika, R.F. Childs, M. West et al, Poly(4-Vinylpyridine)-Filled Microfiltration Membranes: Physicochemical Properties and Morphology, J. Membrane Sci., 136(1997)221.

70. A.M. Mika and R.F. Childs, Acid/base properties of poly(4-vinylpyridine) anchored within microporous membranes, J. Membrane Sci., 152(1999)129-140.

71. A.M. Mika, R.F. Childs and J.M. Dickson, Ultra-low pressure water softening: a new approach to membrane construction, Desalination, 121(1999)149-158.

72. Y. Makino, K. Hamada and T. Iijima, Mobility of spin probes in quaternized poly(4-vinylpyridine) membranes, Polymer Journal, 19(1987)737-745.

73. T. Nakanishi, Y. Usuda, T. Tak et al, Reverse osmosis salt rejection with quaternized poly(4-vinylpyridine) membranes. Polymer Commun., 26(1985)300-303.

74. A.K. Pandey, R.F. Childs, M. West et al, Formation of pore-filled ion-exchange membranes using in-situ cross-linking: poly(vinylbenzyl ammonium salt) filled membranes, J. Polymer Sci.: Part A: Polym. Chem., In press(2000).

75. S.P. Rowland, Water in Polymers, Washington D.C., American Chemical Society, (1980).

76. D.W. Urry, S. Peng, J. Xu et al, Characterization of Waters of Hydrophobic Hydration by Microwave Dielectric Relaxation, J. Am. Chem. Soc., 119(1997)1161-1162.

77. F. Muller-Plathe, Different States of Water in Hydrogels?, Macromolecules, 31(1998)6721-6723.

78. P.M. Wiggins, High and low density water in gels, Prog. Polym. Sci., 20(1995)1121-1163.

79. B.E. Conway, Ionic Hydration in Chemistry and Biophysics, Amsterdam, Elsevier Scientific Publishing Company, (1981).

80. A. Russer, Membrane processes for acid/metal ion recovery. A workshop sponsored by the Ontario Centre for Materials Research, Mississauga, Ontario(1996).

81. M. Kovacs, Diffusion dialysis testing, (1995)(Report).

82. A.M. Mika, R.F. Childs, J.M. Dickson et al, Porous, Polyelectrolyte-Filled Membranes: Effect of Crosslinking on Flux and Separation, J. Membrane Sci., 135(1997)81-92.

83. M. Mika, R.F. Childs and J.M. Dickson, Pore-filled membranes- a new class of robust membranes, 15th Annual Membrane Technology/Separations Planning Conference, Newton, MA, Oct. 27-29(1997).

84. K.J. John and V.N. Pillai, Functionalization of crosslinked poly(4-vinylpyridine) and poly(4-vinylpyridine-co-styrene) with permanganate species: Preparation of poly(4-vinylpyridinium permanganate)s and their use as oxidizing reagents, J. Polymer Sci., Polym. Chem., 27(1989)2897-2906.

85. T. Kawahara, H. Ihara and Y. Mizutani, Anion exchange membranes prepared from chloromethylstyrene and 2-methyl-5-vinylpyridine, J. Appl. Polym. Sci., 33(1987)1343-1357.

86. D.L. Kurdikar and N.A. Peppas, Method of determination of initiator efficiency: Application to UV polymerizations using 2,2-dimethoxy-2-phenylacetophenone, Macromolecules, 27(1994)733-738.

87. P. Molyneux, Water Soluble Synthetic Polymers: Properties and Behaviour, Vol. II, CRC Press, (1983).

88. S.B. Tuwiner, L.P. Miller and W.E. Brown, Diffusion and membrane technology, New York, Reinhold Pub.Corp. (1962).

89. M. Yoshida, Solution properties of poly(vinylpyridine) in acid-II. Solution properties of poly(4-vinylpyridine) in aqueous solution of hydrochloric acid, Eur. Polym. J., 33(1997)943-948.

90. W. Jiang, Preparation and Characterization of Pore-Filled Cation-Exchange Membranes, Ph.D. Thesis, McMaster University (1999).

91. P.A. Dworjanyn and J.L. Garnett, Synergistic effect of urea with polyfunctional acrylates for enhancing the photografting of styrene to polypropylene, J. Polym. Sci., Polym. Lett., 26(1988)135.

92. T. Sata and Y. Yamamoto, Hydrophobic anion exchange membrane, Makromol. Chem., Rapid Commun., 8(1987)611-614.

93. T. Sata, S. Ogura and F. Kishimoto, Properties of composite membranes from ion exchange membranes and conducting polymers. III. Changes in acid transport, J. Membrane Sci., 84(1993)259-269.

94. T. Sata, F. Kishimoto and S. Ogura, High acid retention properties of composite membranes prepared from anion exchange membranes and poly(pyrrole), J. Chem. Soc.,Chem. Commun.,(1993)1159-1160.

95. T. Sata, Y. Yamane and K. Matsusaki, Preparation and properties of anion exchange membranes having pyridinium or pyridinium derivatives as anion exchange groups, J.Polymer Sci.: Part A: Polym. Chem., 36(1998)49-58.

96. T. Sata, Y. Yamane and K. Matsusaki, Relationship of permselectivity between two anions to water content of anion exchange membranes with pyridinium groups, Electrochimica Acta, 42(1997)2427-2431.

97. T. Sata, T. Yamaguchi and K. Matsusaki, Effect of hydrophobicity of ion exchange groups of anion exchange membranes on permselectivity between two anions, J. Phys. Chem., 99(1995)12875-12882.

98. T. Sata, T. Yamaguchi, K. Kawamura et al, Transport numbers of various anions relative to chloride ions in modified anion-exchange membranes during electrodialysis, J, Chem, Soc., Faraday Trans., 93(1997)457-462.

99. T. Sata, K. Teshima and T. Yamaguchi, Permselectivity between two anions in anion exchange membranes crosslinked with various diamines in electrodialysis, J. Polymer Sci.: Part A: Polym. Chem., 34(1996)1475-1482.

100. E.A. Boucher and C.C. Mollett, Kinetics and mechanism of the quaternization of poly(4-vinylpyridine) with 1-bromopropane, J. Polymer Sci., Polym. Phys., 15(1977)283-289.

101. E.A. Boucher, J.A. Groves, C.C. Mollett et al, Kinetics and mechanism of the quaternization of poly(4-vinylpyridine)with ethyl, n-propyl, n-butyl, n-hexyl and benzyl bromide in sulpholane, J. Chem. Soc., Faraday Trans., 73(1977)1629-1635.

102. E.A. Boucher, E.K. Babadi and C.C. Mollett, Quaternization of poly(4-vinylpyridine), J. Chem. Soc.,Faraday Trans., 75(1979)1728-1735.

103. Y. Frere and P. Gramain, Reaction kinetics of polymer substituents. Macromolecular steric hindrance effect in quaternization of poly(vinylpyridines), Macromolecules, 25(1992)3184-3189.

104. D. Navarro-Rodriguez, Y. Frere and P. Gramain, Kinetics and steric limitation of quaternization of poly(4-vinylpyridine) with mesogenic w-(4'-methoxy-4-biphenylyloxy) alkyl bromides, J. Polymer Sci.: Part A: Polym. Chem., 30(1992)2587-2594.

105. A.R. Khare and N.A. Peppas, Investigation of hydrogel water in polyelectrolyte gels using differential scanning calorimetry, Polymer, 34(1993)4736-4739.

106. J. Rault, R. Gref, Z.H. Ping et al, Glass transition temperature regulation effect in a poly(vinyl alcohol)-water system, Polymer, 36(1995)1655-1661.

107. T. Ponomariova, Y. Melnichenko, P.A. Albouy et al, Influence of the Crosslink Density on the Crystallization of Water in PAA Gels, Polymer, 38(1997)3561-3564.

108. F.X. Quinn, E. Kampff, G. Smyth et al, Water in Hydrogels. 1. A Study of Water in Poly(N-vinyl-2-pyrrolidone/methyl methacrylate) Copolymer, Macromolecules, 21(1988)3191-3198.

109. G. Smyth, F.X. Quinn and V.J. McBrierty, Water in Hydrogels. 2. A Study of Water in Poly(hydroxyethyl methacrylate), Macromolecules, 21(1988)3198-3204.

110. B. Vazquez, J.S. Roman, C. Peniche et al, Polymeric hydropohilic hydrogels with flexible hydrophobic chains. Control of the hydration and interactions with water molecules, Macromolecules, 30(1997)8440-8446.

111. M. Pontie and D. Lemordant, Water characterization in composite organic membranes by thermal analysis, J. Membrane Sci., 141(1998)13-17.

112. C. Tanford, The Hydrophobic Effect: Formation of Micelles and Biological Membranes, New York, John Wiley & Sons, (1980).

113. J.R. Grigera, S.G. Kalko and J. Fischbarg, Wall-water interface. A molecular dynamics study, Langmuir, 12(1996)154-158.

114. K. Hallenga, J.R. Grigera and H.J.C. Berendsen, Influence of hydrophobic solutes on the dynamic behavior of water, J. Phys. Chem., 84(1980)2381-2390.

115. J.D. Worley and I.M. Klotz, Near-infrared spectra of H_2O-D_2O solutions, J. Chem. Phys., 45(1966)2868-2871.

116. C. Jolicoeur, N.D. The and A. Cabana, Near infrared spectra of water in aqueous solutions of organic salts. A solvation study of Bu_4NBr, Ph_4AsCl and $NaBPh_4$, Can. J. Chem., 49(1971)2008-2013.

117. P.R. Philip and C. Jolicoeur, Near-infrared study of the state of water in aqueous solutions of tetraalkylammonium and phosphonium bromides and alkali halides at 10, 25 and 40 degrees, J. Phys. Chem., 77(1973)3071-3077.

118. T. Head-Gordon, J.M. Sorenson, A. Pertsemlidis et al, Differences in hydration structure near hydrophobic and hydrophilic amino acids, Biophys. J., 73(1997)2106-2115.

119. N.A.M. Besseling and J. Lyklema, Molecular thermodynamics of hydrophobic hydration, J. Phys. Chem. B, 101(1997)7604-7611.

120. N.A.M. Besseling and J. Lyklema, Hydrophobic hydration of small apolar molecules and extended surfaces: A molecular model, Pure & Appl. Chem., 67(1995)881-888.

121. R.L. Mancera, Hydrogen-bonding behaviour in the hydrophobic hydration of simple hydrocarbons in water, J. Chem. Soc., Faraday Trans., 92(1996)2547-2554.

122. A. Eisenberg, Clustering of ions in organic polymers. A theoretical approach, Macromolecules, 3(1970)147-154.

123. H. Kim, J. Park and K. Lee, Impedance spectroscopic study on ionic transport in a pH sensitive membrane, J. Membrane Sci., 115(1996)207-215.

124. G.E. Zaikov, A.L. Iordanskii and V.S. Markin, Diffusion of Electrolytes in Polymers, Utrecht, VSP, (1988).

125. W.S. Price, Gradient NMR, Ann. Rep. NMR Spectroscopy, 32(1996)51-142.

126. C.H. Chew, L.M. Gan, L.H. Ong et al, Bicontinuous structures of polymerized microemulsions: 1H NMR self-diffusion and conductivity studies, Langmuir, 13(1997)2917-2921.

127. E.O. Stejskal and J.E. Tanner, Spin diffusion measurements: spin echoes in the presence of a time-dependent field gradient, J. Chem. Phys., 42(1965)288.

128. J.R. Macdonald, Impedance Spectroscopy, Toronto, John Wiley & Sons, (1987).

129. I. Rubenstein, Physical Electrochemistry Principles, Methods and Applications, New York, Marcel Dekker Inc. (1995).

130. W.S. Tait, An introduction to electrochemical corrosion testing for practicing engineers and scientists, Racine, PairODocs Publications, (1994).

131. P.G. Bruce, Polymer Electrolyte Reviews, New York, Elsevier Applied Science, (1987).

132. S. Glasstone, K.J. Laidler and H. Eyring, The Theory of Rate Processes, New York, McGraw Hill, (1941).

133. G.E. Boyd and B.A. Soldano, Self-diffusion of cations in and through sulfonated polystyrene cation-exchange polymers, J. Am. Chem. Soc., 75(1954)6091-6099.

134. B.A. Soldano and G.E. Boyd, Self-diffusion of anions in strong-base anion exchangers, J. Am. Chem. Soc., 75(1954)6099-6104.

135. Y. Uemura and P.M. Macdonald, NMR diffusion and relaxation time studies of HEUR associating polymer binding to polystyrene latex, Macromolecules, 29(1996)63-69.

136. G. Pourcelly, A. Oikonomou and C. Gavach, Influence of the water content on the kinetics of counter-ion transport in perfluorosulphonic membranes, J. Electroanal. Chem., 287(1990)43-59.

137. V. Kapur, J.C. Charkoudian, S.B. Kessler et al, Hydrodynamic permeability of hydrogels stabilized within porous membranes, Ind. Eng. Chem. Res., 35(1996)3179-3185.

138. B. Krajewska and A. Olech, Pore structure of gel chitosan membranes. I. Solute diffusion measurements, Polym. Gels and Networks, 4(1996)33-43.

139. B.A. Soldano, The kinetics of ion exchange processes, Ann. N.Y. Acad. Sci., 57(1953)116-124.

140. M. Tasaka, T. Suzuki, R. Kiyono et al, Thermoosmosis and transported entropy of water across poly(4-vinylpyridine/styrene) and poly(N-vinyl-2-methylimidazole/styrene) type membranes in electrolyte solutions, J. Phys. Chem., 100(1996)16361-16364.

141. E.D. VonMeerwall, Diffusion in polymer systems, measured with the pulsed-gradient NMR method, J. Non-Cryst. Sol., 131-133(1991)735-741.

142. M. Petit, X.X. Zhu and P.M. Macdonald, Solute probe diffusion in aqueous solutions of poly(vinylalcohol) as studied by pulsed-gradient spin-echo NMR spectroscopy, Macromolecules, 29(1996)70-76.

143. J.M. Petit, B. Roux, X.X. Zhu et al, A new physical model for the diffusion of solvents and solute probes in polymer solutions, Macromolecules, 29(1996)6031-6036.

144. V.I. Volkov, S.A. Korotchkova, I.A. Nesterov et al, The self-diffusion of water and ethanol in cellulose derivative membranes and particles with the pulsed field gradient NMR data, J. Membrane Sci., 110(1996)1-11.

145. V.I. Volkov, S.A. Korotchkova, H. Ohya et al, Self-diffusion of Water-Ethanol Mixtures in Polyacrylic acid-polysulfone Composite Membranes Obtained by Pulsed-Field Gradient NMR Spectroscopy, J. Membrane Sci., 100(1995)273-286.

146. V. Freger, E. Korin, J. Wisniak et al, Diffusion of water and ethanol in ion-exchange membranes: limits of the geometric approach, J. Membrane Sci., 160(1999)213-224.

147. T.A. Zawodzinski, M. Neeman, L.O. Sillerud et al, Determination of water diffusion coefficients in perfluorosulfonate ionomeric membranes, J. Phys. Chem., 95(1991)6040-6044.

148. J.O. Bockris and P.P.S. Saluja, Approximate calculations of heats and entropies of hydration according to various models, J. Phys. Chem., 76(1972)2298-2310.

149. J. Burgess, Metal Ions in Solution, Chichester, Ellis Horwood, (1978).

150. E.H. Oelkers, Calculation of diffusion coefficients for aqueous organic species at temperatures from 0 to 350°C, Geochim. et Cosmochim. Acta, 55(1991)3515-3529.

151. G. Chiodelli and P. Lupotto, Experimental approach to the impedance spectroscopy technique, J. Electrochem. Soc., 138(1991)2703-2711.

152. H.G.L. Coster, T.C. Chilcott and A.C.F. Coster, Impedance spectroscopy of interfaces, membranes and ultrastructures, Bioelectrochem. Bioenerg., 40(1996)79-98.

153. K.A. Mauritz, Dielectric relaxation studies of ion motions in electrolyte-containing perfluorosulfonate ionomers. 4. Long-range ion transport, Macromolecules, 22(1989)4483-4488.

154. Z.D. Deng and K.A. Mauritz, Dielectric relaxation studies of acid-containing short-side-chain perfluorosulfonate ionomer membranes, Macromolecules, 25(1992)2369-2380.

155. G. Xu and Y.S. Pak, Dielectric relaxation and conductivity study of polytetrafluorene-ethyl ionomers, J. Electrochem. Soc., 139(1992)2871-2874.

156. J.J. Fontanella, M.G. McLin, M.C. Wintersgill et al, Electrical impedance studies of acid form NAFION membranes, Solid State Ionics, 66(1993)1-4.

157. C. Gavach, G. Pamboutzoglou, M. Nedyalkov et al, AC impedance investigation of the kinetics of ion transport in NAFION perfluorosulfonic membranes, J. Membrane Sci., 45(1989)37-53.

158. P. Fievet, M. Mullet and J. Pagetti, Impedance measurements for determination of pore texture of a carbon membrane, J. Membrane Sci., 149(1998)143-150.

159. H. Holdik, A. Alcaraz, P. Ramirez et al, Electric field enhanced water dissociation at the bipolar membrane junction from ac impedance spectra measurements, J. Electroanal. Chem., 442(1998)13-18.

160. A. Alcaraz, H. Holdik, T. Ruffing et al, AC impedance spectra of bipolar membranes: an experimental study, J. Membrane Sci., 150(1998)43-56.

161. H.G.L. Coster, K.J. Kim, K. Dahlan et al, Characterisation of ultrafiltration membranes by impedance spectroscopy. I. Determination of the separate electrical parameters and porosity of the skin and sublayers, J. Membrane Sci., 66(1992)19-26.

162. H.M. Tolwinska, A. Wencel and Z. Figaszewski, Impedance of polypropylene membranes hydrophelized with ethyl alcohol, J.M.S.-Pure Appl. Chem., A34(1997)1413-1427.

163. D.J. Lee, Y.K. Choi, S.B. Lee et al, The analysis of electric properties of thin film composite reverse osmosis membrane with wet impedance method, J. Membrane Sci., 150(1998)9-21.

164. L. Canet, P. Vanel, N. Aouad et al, Impedance and electrical potential across supported liquid membranes: role of interfacial potentials on the active transport of a metal cation, J. Membrane Sci., 163(1999)109-121.

165. B.M. Hansen, T.S. Sorensen, J.B. Jensen et al, Electric impedance of cellulose acetate membranes and a composite membrane at different salt concentrations, J. Colloid Interface Sci., 130(1989)359-385.

166. J. Benavente, M. Oleinikova, M. Munoz et al, Characterization of novel activated composite membranes by impedance spectroscopy, J. Electroanal. Chem., 451(1998)173-180.

167. K. Roberg and L. Dunsch, Electrochemical impedance spectroscopy on conducting polymer membranes, Electrochimica Acta, 44(1999)2061-2071.

168. L.E. Bromberg, Electrical impedance of composite membranes based on complexes, J. Membrane Sci., 62(1991)145-154.